Ben-Gurion University of the Negev
Jacob Blaustein Institutes for Desert Research
Albert Katz International School for Desert Studies

Dynamics of floodwater infiltration and groundwater recharge along ephemeral channels in arid regions, Southwest Africa

Thesis submitted in partial fulfillment of the requirements for the degree of "Master of Science"

By Boaz Tatarsky

November 2007

Abstract

Groundwater in arid regions can be found in various types of aquifers, of different depths and qualities. Shallow alluvial aquifers often present the most accessible reservoirs of the finest water quality. Increases in population, industry and standard of living have resulted in a constant increase in water demands. Overexploitation in excess of the natural replenishment rates has caused progressive lowering of groundwater levels followed by a severe deterioration in water quality.

The main source of replenishment of alluvial aquifers in arid regions is floodwater infiltration through stream beds. Accordingly, investigation of floodwater infiltration and groundwater recharge beneath ephemeral channels is fundamental for the development of sustainable water-resource management schemes. In addition, percolation fluxes are one of the main controlling factors of contaminant transport from the surface to the groundwater. Hence, knowledge and quantification of infiltration rates and flow mechanisms are highly relevant for remediation plans of contaminated sites and for the location of potential new waste-disposal facilities.

This study focuses on the dynamics of floodwater infiltration along ephemeral channels and the replenishment of underlying alluvial aquifers associated with this process. Monitoring was conducted for two years at three different arid sites: (1) the Gobabeb station, lower Kuiseb River, Namibia; (2) the Buffelsrivier station, lower Buffels River, South Africa and (3) the Rooifontein station, upper Buffels River, South Africa. Special emphasis was given to the interrelations between the surface, vadose zone and groundwater.

The specifically designed monitoring setup enabled simultaneous monitoring in real time of the three domains participating in the recharge process: (a) the flood, (b) the vadose zone, (c) the groundwater. High temporal and spatial resolution of moisture

variations along the unsaturated sediment profile was achieved using multi-level flexible time-domain reflectometry (FTDR) probes. Floodwater and groundwater levels, as well as electrical conductivity, were also monitored on site.

During the study period, between five and seven flood events were monitored at each station. Each flood initiated infiltration that was followed later by an increase in groundwater storage. All sites exhibited a direct linkage between surface flow and recharge of the alluvial aquifers. No recharge was recorded during periods of no flow. Data obtained in this study reveal the entire infiltration-recharge process step by step, from the arrival of the flood in the channel through the propagation of a wetting front from the surface to the water table, followed by groundwater mounding and eventually, water table relaxation. During all infiltration events at all sites, the vadose zone remained unsaturated even though the rivers were flowing 'bank-to-bank' for days. Saturation of the subsurface took place from the bottom of the vadose zone upward and was governed by water table fluctuations. Following the recharge, the water table at all sites rose all the way to the surface and the aquifers were fully replenished. This stage represented the maximum storage capacity of the aquifers into which no more water could infiltrate. As a result, surface flow continued for long periods and the flood traveled further downstream.

The average wetting front propagation velocity was calculated per event for each site and was found to be directly related to the initial water content along the sediment profile. Percolation fluxes at Gobabeb were calculated by three independent methods, which all yielded very similar values. Although the floods varied widely in their magnitude and duration, average recharge fluxes for all events were very similar (~1.0 cm/h). This was attributed to a natural regulating mechanism related to the stratified structure of the alluvial deposits and inter-layering of fine grains along the profile. Two of the calculation methods could be applied at the Buffels River, where average fluxes were one order of magnitude higher than those at Gobabeb, ranging between 0.36 and 52 cm/h. This was related to the coarser sediments that comprise the alluvium in the Buffels River in comparison with the Kuiseb River. Results from the Buffels River indicated the presence of preferential flow pathways which are active together with the diffuse infiltration.

Total groundwater recharge at Gobabeb for the study period averaged around 210,000 m^3 per 1 km of stream reach. Recharge at Rooifontein varied between 41,000 and 81,000 m^3/km whereas the minimum value calculated at Buffelsrivier was ~200,000 m^3/km. These estimations are appropriate only for stream sections that present geomorphic characteristics and aquifer dimensions similar to those at the monitoring stations. All sites presented a direct relationship between the duration of flow in the active channel and total recharge. The results also demonstrated the important role of floodwater recharge in improving groundwater quality by lowering salinity.

Acknowledgments

I would like to express my deep gratitude to my supervisor, Dr. Ofer Dahan, who made this period not only educational from an academic standpoint, but also enjoyable and constructive in many other ways. Special thanks go to Michael Kugel and Yuval Shani, who were my technical mentors and superb companions during the many hours of field work in Israel and Africa.

I am grateful to my fellow student friends: Mark Stanton, Yaara Rimon, Ruti Talby and Shachar Baram, for joining me on many of the trips to the Arava and for their willingness to help at any time. I thank Prof. Yehouda Enzel (Hebrew University) who helped me find Ofer in the first place and who was thoroughly involved in this project all along the way. I also thank Dr. Yossi Yechieli (Israel Geological Survey) for his constructive advice at the early stages of my research and his willingness to assist whenever needed.

I deeply appreciate the collaboration with the Desert Research Foundation of Namibia and the Gobabeb Training and Research Center. I thank Dr. Mary Seely and Dr. Joh Henschel who led these groups and coordinated the installations in Namibia. Special thanks to Hartmut and Helen Kolb, Julia Bradley-Cook, Veronica Siteketa, John Guittar, Daniel Shapi, Calvin Sisamu and to all of the others who lent a hand, for the data collection and station maintenance in the Kuiseb River. None of this could have happened without you.

I am grateful to Simon Todd (University of Cape Town) for coordinating the installations of the stations in South Africa and for the endless journeys from Cape Town to the Buffels River for data collection and station maintenance. I thank Klaudia Schachtschneider (University of Cape Town) for coordinating the soil analysis, and Dr. Tamir Grodek (Hebrew University) for sharing the geomorphic data from the Kuiseb

River with me. I also thank Dr. Gerardo Benito (Centro de Ciencias Medioambientales, Spain) for assisting with data regarding the Buffels River, and Dr. Shai Arnon for his technical support with some of the graphic (and other) software.

Special thanks to Efrat for bearing with me (or more accurately without me) in the last intensive writing period, and for her important remarks before every presentation and to this final draft.

And last but not least, my dear family—thank you for supporting and encouraging me all along the way.

This study was funded by the sixth framework of the European Commission (WADE project, GOCE-CT-2003-506680), and by the U.S.-Israel Cooperative Development Research Program, Bureau for Economic Growth, Agriculture, and Trade, U.S. Agency for International Development (Grant No. C24-26).

Table of contents

Abstract .... **I**

Acknowledgments .... **I**

List of figures .... **IX**

List of tables .... **XI**

1. Introduction **1**

1.1 Groundwater recharge in arid lands 2

1.2 Percolation processes beneath ephemeral rivers 4

1.2.1 Basic theory 4

1.2.2 Vadose zone techniques for measurements of water content and potential 7

1.2.3 Parameters controlling infiltration in ephemeral channels 10

1.2.3.1 Climate 10

1.2.3.2 Surface conditions 10

1.2.3.3 Vadose zone controls 11

1.3 Recharge from ephemeral streams – review of works and methods 13

1.3.1 Water budget 14

1.3.2 Direct Methods 15

1.3.3 Tracer Techniques 16

1.3.4 Numerical modeling 17

1.4 Study objectives 18

2. Methods **19**

2.1 Methodological concept 19

2.2 Flood monitoring 20

2.3 Vadose zone monitoring 22

2.4 Groundwater monitoring 24

2.5 Data acquisition 25

2.6 Soil analysis 26

3. Study sites **27**

3.1 Kuiseb River, Namibia 27

3.1.1 Geography 27

3.1.2 Climate 28

3.1.3 Geology 28

3.1.4 Hydrology 28

3.1.5 Vegetation 29
3.1.6 Population and water supply 30
3.1.7 Previous studies..30
3.1.8 Gobabeb monitoring station 31
3.2 Buffels River, South Africa..33
3.2.1 Geography 33
3.2.2 Climate 34
3.2.3 Geology 34
3.2.4 Hydrology 35
3.2.5 Vegetation 36
3.2.6 Population and water supply 36
3.2.7 Previous studies..36
3.2.8 Monitoring stations description...37
3.2.8.1 Rooifontein station 37
3.2.8.2 Buffelsrivier station..39
4. Results 42
4.1 Gobabeb station, Kuiseb River, Namibia..43
4.1.1 Floods summary 43
4.1.2 1st flood event..44
4.1.2.1 Infiltration dynamics 44
4.1.2.2 Groundwater level fluctuations 45
4.1.3 Second flood event...46
4.1.3.1 Infiltration dynamics 46
4.1.4 Fifth flood event..48
4.1.5 Vadose zone summary 49
4.1.6 Groundwater levels summary 49
4.1.7 Groundwater salinity summary...50
4.2 Buffelsrivier station, Lower Buffels River, South Africa 53
4.2.1 Floods number 1, 2 and 3 53
4.2.2 Groundwater EC response to the 1st and 2nd floods 54
4.2.3 The forth flood event..55
4.2.4 The 5th flood event 57
4.2.5 The 6th flood event 57
4.2.6 Groundwater levels summary 58

4.2.7 Groundwater salinity summary 59
4.3 Rooifontein station, Upper Buffels River, South Africa 60
4.3.1 Floods summary 60
4.3.2 Infiltration dynamics 60
4.3.3 Groundwater levels summary 62
4.3.4 Groundwater salinity summary 63
4.4 The conceptual model of the infiltration-recharge process 65
4.5 Flow velocities and fluxes 68
4.5.1 Analytical method 68
4.5.1.1 Wetting front propagation velocity (WFPV) 68
4.5.1.2 Percolation fluxes 68
4.5.2 Gobabeb station, Kuiseb River, Namibia 73
4.5.3 Buffelsrivier station, Lower Buffels River, South Africa 76
4.5.4 Rooifontein station, Upper Buffels River, South Africa 78
4.6 Total recharge estimations 80
4.6.1 Calculation method 80
4.6.2 Gobabeb station, Kuiseb River, Namibia 81
4.6.3 Buffelsrivier station, Lower Buffels River, South Africa 82
4.6.4 Rooifontein station, Upper Buffels River, South Africa 84
5. Discussion 85
5.1 Infiltration dynamics 85
5.1.1 Percolation mechanism 85
5.1.2 Percolation rates 87
5.2 Recharge processes beneath ephemeral channels 93
5.2.1 The effect of evapotranspiration 93
5.2.2 Total recharge quantities 95
5.3 Groundwater recharge mechanism 97
5.4 Aquifer storage and recharge potential 101
5.5 Aspects of water quality and groundwater recharge 102
5.6 Practical implications for wise groundwater management 104
6. Summary 108
7. References 108

List of figures

Figure 2.1 Schematic illustration of the monitoring set up 21
Figure 2.2 (A) The monitoring station from the outside. (B) FTDR probe attached to the PVC sleeve……………………………………………………… 21
Figure 2.3 The PVC sleeve is inserted into the slanted borehole 25
Figure 2.4 The data control system and the access to the piezometer 26

Figure 3.1 Satellite image of the middle and lower Kuiseb River with the location of the Gobabeb study site 27
Figure 3.2 Dense woody vegetation along the Kuiseb Valley 29
Figure 3.3 The active channel of the Kuiseb River with the monitoring stations 32
Figure 3.4 Location of FTDR probes at the Gobabeb stations (boreholes 200, 300, 400) in relation to the sedimentary sequence 32
Figure 3.5 A topographic presentation of the Buffels River catchment area with the location of the two study sites at Buffelsrivier and Rooifontein 34
Figure 3.6 Location of the Rooifontein Station 38
Figure 3.7 Location of FTDR probes at the Rooifontein station (boreholes 300, 400) in relation to the sedimentary sequence 39
Figure 3.8 Location of the Buffelsrivier station 40
Figure 3.9 Location of FTDR probes at the Buffelsrivier station (in boreholes 100, 200) in relation to the sedimentary sequence 41

Figure 4.1 The Kuiseb hydrograph at the Gobabeb station 43
Figure 4.2 The 1st flood event as recorded at: (a) the stream (b) the vadose zone and (c) the groundwater at Gobabeb (borehole 200) 45
Figure 4.3 Water content variation in the vadose zone during the second flood 46
Figure 4.4 A safari truck that got bogged in the riverbed 48
Figure 4.5 Water content variations at various depths during Dec' 2005 – May 2007 49
Figure 4.6 Groundwater levels at Gobabeb between July 2005 and June 2007 50
Figure 4.7 EC values at the stream and groundwater and groundwater levels during the first four floods 51

Figure 4.8 Groundwater EC and levels at the Gobabeb monitoring station between December 2005 and June 2007 52

Figure 4.9 (a) flood stage (b) vadose zone water content (c) groundwater level fluctuations as measured between September 2005 and August 2007 at the Buffelsrivier station 54

Figure 4.10 EC measurements of the floodwater and the groundwater with groundwater levels 55

Figure 4.11 (A) Water content variations in the unsaturated zone and groundwater levels during and after the 4th flood event (B) enlargement of the first 4 days........ 56

Figure 4.12 Water content variations at various depths and groundwater levels as recorded during the 5th flood event 57

Figure 4.13 Flood stage and groundwater levels during the 6th flood event 58

Figure 4.14 Groundwater levels fluctuations in response to the flood events 58

Figure 4.15 Groundwater EC and groundwater levels........ 59

Figure 4.16 (a) flood hydrograph, (b) water content variations in the vadose zone and (c) groundwater levels at the Rooifontein station, September 2005 and July 2007........ 61

Figure 4.17 Groundwater and flood levels during the 5th flood, Rooifontein station 62

Figure 4.18 Groundwater levels and flood height during July 2005 – July 2007........ 63

Figure 4.19 Groundwater EC, groundwater levels and floodwater EC between July 2005 and July 2007 at the Rooifontein station........ 64

Figure 4.20 The downward propagation of a wetting front is recorded by the FTDR probes in the vadose zone 66

Figure 4.21 Groundwater response to the recharge event 67

Figure 4.22 Water content in different parts of the local hydrological system........ 72

Figure 5.1 Water content and flood stage during the 2nd flood event at Gobabeb........ 87

Figure 5.2 Depth of the wetting front vs. time as measured for floods 1-4 at the Gobabeb station........ 88

Figure 5.3 Water content and flood height during the 2nd flood at Buffelsrivier........ 90

Figure 5.4 Average percolation fluxes vs. flood height 91

Figure 5.5 (a) Fine grain layers in the Kuiseb alluvial cross section (b) alternating fine and coarse layers along the Rooifontein site alluvial cross section 92

Figure 5.6 Drainage rate vs. depth according to FTDR probes at Gobabeb 95
Figure 5.7 Storage increase vs. flood duration in all study sites 96
Figure 5.8 Rainfall and flood height at the Buffelsrivier station 99
Figure 5.9 Rainfall vs. flood height at the Rooifontein station 100
Figure 5.10 EC values of the floods in the Buffelsrivier and Rooifontein stations 104

List of tables

Table 1. Vadose zone techniques for measuring water content and water potential........ 9
Table 2. Grain size distribution along the soil profile at GOB 1 33
Table 3. Grain size distribution along the soil profile at GOB 2 33
Table 4. Grain size distribution along the soil profile at Rooifontein station 38
Table 5. Grain size distribution along the soil profile at Buffelsrivier station 40
Table 6. WFPV and fluxes as calculated for the 1st flood at Gobabeb 69
Table 7. Average WFPV and fluxes at the Gobabeb station (borehole 200) 74
Table 8. Average WFPV and fluxes at the Buffelsrivier station (borehole 100) 77
Table 9. Average WFPV and fluxes at the Rooifontein station (borehole 300)............. 79
Table 10. Groundwater recharge estimations for the Gobabeb station 81
Table 11. Groundwater recharge estimations for the Buffelsrivier station 83
Table 12. Groundwater recharge estimations for the Rooifontein station...................... 84
Table 13. Groundwater EC values range for each site (mS/cm) 104

1. Introduction

Groundwater recharge has been the focus of many studies due to its critical role in replenishment of aquifers and contaminant transport from the surface to underground reservoirs. In arid and semi-arid areas high radiation together with irregular and little rainfall, cause potential evaporation values to exceed average rainfall quantities, making surface-water scarce and intermittent. Therefore, the only reliable water source in arid environments is the one lying beneath the surface, often in the form of shallow alluvial aquifers (de Vries and Simmers, 2002).

One third of the world's terrestrial surface area is considered as semiarid or arid while this value is constantly increasing (Dregne, 1991). The growing water demand in arid regions in the last few decades resulting from the fast growing population and development of these areas caused major depletion in groundwater quantities and qualities. This in turn, may lead to loss of water supply, land subsidence, intrusion of saline water, increased pumping costs and irreversible damage to the local ecological environment (Stephens, 1995). Haimerl (2004) reported a decline rate of 2 m/year at the coastal aquifer in northern Oman. According to Gelt et al. (1999), water table drop of nearly 60 m over 50 years was recorded in central Tucson, USA due to over exploitation. In the Arava valley, Israel, groundwater levels dropped by 16 m over a period of 30 years while Cl^- concentrations rose by ~200 mg/l toward the end of this period (Flischer et al., 1997). The understanding of recent years that in order to maintain a sustainable groundwater management, pumping should never exceed natural recharge rates, emphasizes the need of a better understanding of recharge mechanisms, rates and the factors that control it. Moreover, quantifying infiltration-recharge fluxes is of great importance for predicting contaminant transport from the surface to the groundwater for assessing remediation plans of contaminated sites as well as for planning and locating new waste disposal sites (Scanlon et al., 1997).

1.1 Groundwater recharge in arid lands

Recharge mechanisms might vary widely throughout the basin. Factors such as climate, geology, morphology, vegetation and soil type will determine the recharge pattern. Lerner et al. (1990) divided the different sources of recharge into three main groups: **(1) Direct recharge** – direct vertical percolation of precipitation that escapes soil storage and evapotranspiration to reach the groundwater (also named 'diffuse recharge'), **(2) Indirect recharge** – percolation to the groundwater following runoff mainly through the beds of surface-water courses (transmission loss), **(3) localized recharge** – a form of indirect recharge resulting from the concentration of (near-) surface-water in topographic lows and depressions in the absence of well-defined channels. Feth (1964) defined another form of **hidden recharge,** the recharge of an aquifer by subsurface inflow from an adjacent aquifer.

Many studies state that the contribution of direct recharge in comparison to indirect processes decreases with increasing aridity (Wright, 1980; Gee and Hillel, 1988; Walvoord and Scanlon, 2004). The weather and soil characteristics of desert environments (high intensity rain events of short duration and relatively limited infiltration capacity), promotes overland flow and surface runoff which sometimes develop into floods along ephemeral channels. It is suggested that in those dry regions, recharge occurs in only small portions of the basin, where flow of water is concentrated such as depressions and channels (Goodrich et al., 2004). Therefore, floodwater infiltration through the beds of ephemeral streams is often the main source of replenishment of shallow alluvial aquifers, though it is seldom more than 5% of the annual precipitation (Besbes et al., 1978; Sorman and Abdulrazzak, 1993; Scanlon et al., 2006). In the Southwest US, many perennial reaches of streams turned ephemeral as a result of increasing water demands. Thus, the fraction of recharge attributed to ephemeral stream channels is increasing (Anderson et al., 1992).

Nevertheless, representation of recharge rates and mechanisms in arid regions presents serious challenges that arise due to the extremely small fluxes which are highly variable in time and in space. Moreover, recharge mechanisms vary widely throughout the basin and require different evaluation techniques (Phillips et al., 2004). These difficulties are exacerbated when trying to monitor infiltration-recharge processes below ephemeral channels during floods. The irregular and unknown occurrence interval, the short duration of flow and the forceful pattern of flash floods in desert environments make it almost impossible to directly monitor the natural process in real time. For this reason most methods applied in studies of ephemeral channel recharge are indirect and monitor only some aspects of the process either in the surface flow, groundwater or vadose zone.

Two main mechanisms of recharge associated with ephemeral flow are mountain front and channel recharge. In arid regions both types can occur in the same basin and are hard to differentiate between in practice (Lerner et al., 1990). Ephemeral streams vary widely in their hydrogeological features and depend greatly on the basin topographic, geologic, climatic and geomorphic settings. Precipitation frequency, distribution and intensity along with spring discharge and basin runoff characteristics will determine the frequency, duration and magnitudes of floods along the channel (Enzel, 1990; Reid and Frostick, 1997). The connectivity between the channel and the aquifer has major consequences on the recharge potential. Two main classifications of stream-aquifer relationship are generally used (Fetter, 1988): (1) by the connectivity of the stream and aquifer: the stream can be connected to the underlying aquifer (usually found in humid areas), or disconnected from the underlying aquifer (common in arid regions); (2) by the pattern of water exchange between the two reservoirs: in a **losing stream** streamflow will infiltrate to feed the underlying aquifer whereas in a **gaining stream**, the regional water table will be higher then the channel bed and groundwater will discharge into the surface to maintain a constant baseflow. In general, in (semi-) arid regions the stream will usually be ephemeral and disconnected from the aquifer. Any intermittent flow will infiltrate rapidly through the channel bed sediments to feed the groundwater. However, in the case of shallow aquifers, both losing and gaining types can be found in the same channel at different reaches or even at a given reach in different times. The dominant recharge mechanism in the basin will determine the type of relationship between the channel and groundwater.

1.2 Percolation processes beneath ephemeral rivers

1.2.1 Basic theory

Infiltration is defined as the flow of water through the soil surface into the vadose zone (Chow, 1964). Percolation refers to the deeper downward movement of water, below the root zone, whereas redistribution relates to the movement of water in the subsurface after infiltration ceased i.e. termination of the surficial source (rain, flood). The process of water flow in porous media has been the focus of numerous works in the last ~100 years and is reviewed in many papers and text books (Zimmermann et al., 1967; Childs and Bybordi, 1969; Philip, 1971; Bear, 1972; Hillel, 1980; Raats, 2001). Infiltration processes are directly related to groundwater recharge, contaminant transport from surface to the groundwater, and surface erosion processes. Lorenzo A. Richards (1931) modified the Buckingham-Darcy equation (1907) for describing transient flow at the unsaturated zone. In the vadose zone the water content and pressure head are two dependent variables and can both change in time (t) and in space (z). For one dimensional vertical flow:

$$\frac{\partial \theta}{\partial t} = \frac{\partial}{\partial z}\left[K(h)\left(\frac{\partial h}{\partial z} + 1\right)\right] + s \tag{1.1}$$

Where θ is the soil moisture content, t is time, z is elevation above a reference level, $K(h)$ is the unsaturated hydraulic conductivity, h is the pressure head and s is a source/sink term for water per unit time. The solution of the equation requires knowledge of the soil water retention curve and the unsaturated hydraulic conductivity curve which are difficult to obtain, especially in natural subsurface conditions. In many cases numerical methods are applied to solve this flow equation (Marshall et al., 1996). Two of the frequently used solutions are those of Brooks & Corey (1966) and Van Genuchten (1980).

According to Freyberg et al. (1980) during a flood, the stream surface is quickly saturated and a positive pressure head (equal to the flood stage) is exerted upon the channel bed. The infiltration flux, q, across the ground surface can be expressed by:

$$q = -K_s \frac{\psi_f - \psi_0 - Z_f}{Z_f} \tag{1.2}$$

Where Ks is the saturated hydraulic conductivity, Z_f is the depth of the wetting front, ψ_f is the pressure head at the wetting front, ψ_o is the pressure head applied at the ground surface. The velocity of the wetting front, V_f, will be:

$$V_f = \frac{q}{\theta_s - \theta_a} = -K_s \frac{\psi_f - \psi_0 - Z_f}{Z_f(\theta_s - \theta_a)} \tag{1.3}$$

Where θs is the saturated water content and θa is the antecedent water content. According to this equation, the wetting front propagation velocity (V_f) will increase with increase in the initial water content. V_f is also directly proportional to Ks. Because the hydraulic conductivity is expected to increase with increasing water content, the percolation rate would be expected to increase also. However, V_f is also inversely proportional to the distance of the wetting front from the surface i.e. the velocity will be highest initially as Z_f is smallest and the overall head gradient is highest. As the wetting front propagates downward, the pressure gradient decreases and the movement is governed mainly by gravity (Warrick, 2002). Eventually the propagation of the wetting front is slowed to a constant minimum value of:

$$V_f = K_s / (\theta_s - \theta_a) \tag{1.4}$$

This corresponds well with Horton's equation (1940) which predicts a steep decline with time of the infiltration rate (v) down to a minimum constant value:

$$v = v_f + (v_i - v_f) e^{-\beta t} \tag{1.5}$$

Where v_f and v_i are the final and initial infiltration rates, respectively, t is time and β is an empirical constant. The final infiltration rate should in theory be equal to the saturated hydraulic conductivity but is actually smaller in natural field conditions due to the effect of entrapped air, clogging and swelling in the case of loess soils.

Integrating equation 1.3 gives an equation for the time (t) at which the wetting front will advance to a depth Z_f, which is very similar to the equation developed by Green and Ampt (1911) for describing the infiltration phenomena:

$$t = \frac{(\theta_s - \theta_a)}{K_s} \left\{ Z_f + (\psi_f - \psi_s) \ln\left[1 + \frac{Z_f}{(\psi_s - \psi_f)} \right] \right\} \tag{1.6}$$

If for a given water table at depth Z, the time calculated by the equation is less than the duration of flow in the channel, then recharge will take place during stream flow (Blasch et al., 2004).

The infiltration theories of Green and Ampt and of Philip (1957) refer to sharp, stable wetting fronts in dry homogenous soils. These theories lie in the basis of numerous soil physics studies and were validated by many column experiments.

However other studies, mainly larger scale field observations, reported different phenomena (such as finger flow and macropore flow) which the classical theories do not account for (Hendrickx and Walker, 1997). Thus, these approaches should be used as general guidelines but their suitability should be examined with relation to the specific problem in question. According to the classical theories during infiltration, a wetting front of higher water content moves down through the unsaturated zone driven by the potential and gravitational heads. The potential head is combined of the pressure head exerted by the height of water column at the surface and the matric potential at the wetting front. The abruptness of the wetting front is a function of the pore size distribution and the shape of the $K(h)$ function and will probably be more sharp for coarse textured soils with a narrow distribution of particle sizes. After the termination of the water source at the surface, redistribution takes place in which water is subject to one of three forces (Warrick, 2002): (a) evaporation or evapotranspiration, (b) free drainage governed by gravity (which may lead to recharge if the water table is shallow) and (c) lateral movement driven by matric gradient. In coarse-textured soils drainage will be relatively fast and short in duration while in fine-textured soils, redistribution will be slower and longer lasting. The water content when redistribution becomes negligible is called field capacity. Few different models of redistribution are available in the literature among are those of Gardner et al. (1970) and Bruce et al. (1985).

1.2.2 Vadose zone techniques for measurements of water content and potential

Changes in the soil water content and soil water potential in space and in time can reveal the dynamics of water flow (direction and flux) in the subsurface. Thus, measurement of water content and potential in the vadose zone is of great importance for groundwater recharge estimations and monitoring of contaminant migration from waste sites to the groundwater (Stephens, 1995). Numerous methods are available commercially and are being constantly developed and modified to fit more applications. Table 1 summarizes advantages and disadvantages of the main physical methods. Many considerations when choosing an appropriate tool should be taken into account: whether water content or potential is a better criterion for the purpose, whether field or laboratory conditions are targeted, the required resolution, the scale of interest, the necessary precision, the labor involved, budget, reliability and robustness of the equipment and the skills required for operating the system and analyzing results (Marshall et al., 1996).

***Table 1**: Vadose zone techniques for measuring water content and water potential*

	Method	Physical principle	Advantages	Disadvantages	References
Water content					
A. Subsurface methods					
1	Gravimetric method	Mass weight	Direct, simple, low cost (used as standard for calibrating indirect methods)	Destructive (not repeatable for the same sample). Time consuming and labor intensive	Gardner (1986) Marshall et al. (1996)
2	Neutron Probe	Thermalization of neutrons	Repeatable, averages relatively large sample volume, accuracy	Radiation hazard, not suitable for near surface, soil specific calibration required, automation not possible.	Stephens (1995) Warrick (2002)
3	Gamma Ray Attenuation	Attenuation of gamma rays	Nondestructive, high resolution, very suitable for laboratory experiments	Radiation hazard, necessity of 2 boreholes in the field at constant spacing with depth, accurate bulk density required.	Marshall et al. (1996) Gurr (1962) Hillel (2004)
4	Time Domain Reflectometry (TDR)	Dielectric properties	High accuracy (1-2%), no specific calibration required, continuous automated reading possible.	Limited applicability in highly saline and clay soils. High equipment expense.	Jones et al. (2002) Topp et al. (1980)
5	Frequency Domain Reflectometry (FDR)	Dielectric properties	High accuracy (0.2% by volume), accurate vertical resolution, instantaneous reading	specific calibration required for saline soils >2dS/m, Not applicable in salinities over 10 g/L	Bell et al. (1987) Cook et al. (1992)
6	Capacitance methods	Dielectric properties	Lower expense relative to TDR, no health hazard.	errors associated with air gaps around sensors utilizing access tubes	Whalley et al. (1992) Chanzy et al. (1998)
B. Surface methods (non-invasive)					
1	Electromagnetic Induction (EMI)	Electric conductivity	Non invasive, no disturbance of natural conditions, covers large area	Low spatial resolution, low accuracy, usually used for qualitative estimates	Stephens (1995) Scanlon et al. (1997)
2	Ground Penetrating Radar (GPR)	Dielectric properties	Efficient tool for large area subsurface mapping	Low spatial resolution, complex data analysis, clay strongly limits effective depths	Stephens (1995) Huisman et al. (2003)
3	Remote sensing (aircraft / satellite)	Photography / Infrared	Efficient tool for regional subsurface mapping. Long term repetitive coverage.	High cost, low spatial resolution, shallow depth, limited to daytime and clear skies (no clouds)	Jackson (2002) Ulaby et al. (1996) Mattikalli et al. (1998) Owe et al. (1992)
		Microwave	Large area mapping, long term repetitive coverage. Applicable to cloudy conditions and at night time	High cost, low spatial resolution, shallow depth, Low monitoring frequency. Vegetation and surface roughness correction are required	
4	Tomography	X-Ray Gamma Ray	Highly suitable for detecting macropore structures and finger/preferential flows.	Low resolution, expensive Some application may take considerable time, hazard radiation (X-Ray)	Amin et al. (1998) Duliu (1999)
		MRI (Magnetic Resonance Imaging)	Highly suitable for detecting macropore structures and finger/preferential flows. High resolution	Applicable only to small scale samples in the lab, high technical demands. Practical experience required for interpretation, distortion by magnetic background within the sample, very expensive.	Amin et al. (1998) Bellon-maurel et al. (2003) Amin et al. (1996)
Water potential					
A. Direct methods					
1	Tensiometers	Matric equilibrium	Accurate Simple	Useful range < 85 kPa, slow response (problematic monitoring of rapid changes), temperature dependent , small influence volume, good contact with the soil is vital	Marshall et al. (1996) Warrick (2002) Stephens (1995)
2	Psychrometers	Relative humidity	Simple and accurate under controlled conditions (lab) Can be applied at large depths	Fine equilibrium required Difficulty maintaining undisturbed conditions Short lifetime in field, mainly lab applications	Marshall et al. (1996) Warrick (2002) Stephens (1995)
B. Indirect methods					
1	Electrical Resistance Blocks	Electric conductivity (Gypsum, nylon, fiberglass)	Inexpensive In-situ long term measurements Applicable for drier conditions then tensiometers, easy to operate	Low accuracy, deterioration under prolonged wet conditions, temp' measurement needed for calibration, insensitive to salinity (mainly nylon, fiber glass), hysteretic calibration curve	Marshall et al. (1996) Stephens (1995)
2	Heat Dissipation Sensors	Thermal conductivity	Wide range of applicability: -0.01 to -12.0 MPa, low expense Insensitive to soil salinity.	Specific calibration per sensor required. Field lifetime ~2 years. Sensitive to Temp' and pressure	Flint et al. (2002a) Warrick (2002) Scanlon et al. (1997)
3	Filter Paper Method	Matric equilibrium between soil and filter paper	Simplest and least expensive method for measuring matric potential. Wider range than tensiometers	Time consuming method (equilibrium is a prerequisite), not applicable for transient conditions, error associated with temp' gradient, labor intensive.	Stephens (1995) Scanlon et al. (1997)
4	Electro-Optical Method	Infrared transmission through nylon filter	Low cost, reliability, rapid response Less destructible then paper filters	Applicable only at lab conditions Possible development of microbial growth and rust might introduce errors.	Cary et al. (1991) Scanlon et al. (2002)
5	Water Activity Meter / Dew point Potentiameter		Relative short measurement time, Larger capacity then psychrometer,	Destructive method, less accurate then psycrhometer, lab application only, Temp' control is vital (may lead to significant error)	Scanlon et al. (1997) Cancela et al. (2006) Gee et al. (1992a)

1.2.3 Parameters controlling infiltration-recharge processes in ephemeral channels

Infiltration fluxes and patterns vary widely in arid regions both from one site to another and within the same site. This is a result of many variables that affect the infiltration process at different stages and domains. Together they create a complex process of interrelated controlling factors (Scanlon et al., 1997). Although there is a direct relationship between infiltration and recharge, it is important to remember that this relationship is not straight forward and high infiltration rates will not necessarily lead to high recharge fluxes.

1.2.3.1 Climate

Rainfall – the rainfall pattern (mainly the intensity and duration) together with the surface characteristics will determine if and when flooding will take place and thus, the amount and form of water available for infiltration (Bull and Kirkby, 2002).

Evaporation – average annual evaporation rates in arid region might reach few thousands of mm. This might have little effect on short duration flooding but considerably influence redistribution patterns at shallow depths (Haimerl, 2004).

1.2.3.2 Surface conditions

Channel characteristics – (a) the wetted perimeter – braided or wide channels will generally lead to more infiltration in relation to primary narrow channels, but will also result in lower water stage i.e. lower pressure head at the surface, (b) slope of the stream bed will effect the propagation velocity of the flood wave and the distance it travels downstream (Guzman et al., 1989).

Flood characteristics – among the important factors are the velocity of flow, the inflow discharge, duration of flow, flood stage, floodwater temperature, and amount of suspended sediments. In general, total infiltration will increase with increase in flow duration (Issar and Passchier, 1990; Parissopoulos and Wheater, 1991). Infiltration rates increase with increase in water and bed sediments temperature (Constantz et al., 1994). Rates also increase with increase in the water depth at the surface, but mainly at low flow stages. As stages increase, this dependency decreases (Mudd, 2006). Infiltration rates will decrease with increase in suspended sediments input, which may clog the surface layer, mainly in the downstream direction (more load, lower water energy) (Knighton and Nanson, 1994; Kruseman, 1997).

Vegetation - evapotranspiration plays a major role in controlling soil water fluxes. Phillips (1994) attributed the uniformity in chloride profiles in southwest United States to water uptake by the local vegetation (although rainfall and soil type varied widely among the sites). On the other hand, increased infiltration was reported in other studies due to preferential flow associated with root tunnels (Wang et al., 2007).

Surface layer – processes and characteristics associated with the surface layer such as low permeability, swelling, clogging by fine particles and/or organic matter, deposition of fine suspended material towards the end of the flow and microbial crust (in the case of return flow from effluent) might reduce dramatically flow rates into the subsurface (Abdulrazzak and Morel-seytoux, 1983; Blasch et al., 2004). Modeling of two sequential stream flow events by Bailey (2002) showed a reduction by four orders of magnitude in the hydraulic conductivity of the surface layer between events, due to redistribution of sediments.

1.2.3.3 Vadose zone controls

Sediment texture – parameters such as permeability, water repellency, hydraulic conductivity and grain size distribution can greatly affect water movement in the vadose zone (Scanlon et al., 1999). The lithology of the source area for channel sediments will determine the type of material comprising the alluvium and thus might affect the above parameters. In general, fine-grained soils provide large water storage capacity and decrease infiltration while coarse-grained sediments enhance deep quick percolation (Scanlon et al., 1997). Bailey (2002) demonstrated that infiltration rate during stream flow is more sensitive to K(h) than to the water stage at the surface.

Soil structure – layering of sediments reduces percolation rates. A fine-grained layer underlying a coarse-grained layer will promote perched water conditions that might significantly reduce average percolation fluxes. Where fine-grained sediments overlie coarse material, capillary barriers may form at the interface between layers and water flow into the coarse layer will be delayed until the potential at the wetting front increases to the water entry value for the coarse layer (Warrick, 2002). In places where interfaces between layers are sloped, lateral flow may occur (Scanlon et al., 1997).

Antecedent soil moisture – initial water content can act both to increase and decrease infiltration rates. One aspect is the direct relationship between water content and the unsaturated hydraulic conductivity. This suggests that higher initial water content will result higher percolation fluxes (Freyberg et al., 1980; Blasch et al., 2004). However, the inverse relationship between soil moisture and tension suggests that high antecedent water content will result in a lower initial infiltration rate due to a diminished potential gradient (Hendrickx and Walker, 1997; Warrick, 2002).

Entrapped air – entrapped air can be divided into mobile and immobile pockets of air. The immobile air is entrapped in dead-end pores and can be removed only by dissolution. The mobile air might migrate from the smaller to the larger voids, having a disproportional effect in reducing infiltration (Faybishenko, 1995). When entrapped air can not dissolve nor migrate during ponded infiltration it might be compressed by the hydrostatic forces and pushed down in front of the wetting front, reducing further the vertical fluxes.

1.3 Recharge from ephemeral streams – review of works and methods

The associated difficulties when trying to explore infiltration-recharge processes in arid regions led to the development of numerous methods and approaches. The different techniques usually apply either chemical or physical methods to obtain representative data from the field. These can be later integrated into numerical, analytical or empirical methods which use field data to calibrate theoretical models for defining water fluxes or sources of recharge. Many through reviews of the different methods can be found in the literature including the advantages and limitations associated with each method and the guidelines for choosing the appropriate technique in relation to the study requirements and site characteristics (Lerner et al., 1990; Allison et al., 1994; Enzel and Wells, 1997; Kruseman, 1997; de Vries and Simmers, 2002; Scanlon and Cook, 2002; Goodrich et al., 2004; Cataldo et al., 2004). While all approaches are well acknowledged and applied, it is important to emphasize that techniques based on surface-water and vadose zone data only, provide estimates of potential recharge, whereas those based on groundwater data generally provide estimates of the actual recharge (Scanlon et al., 2002). Because of the low fluxes associated with arid and semi-arid regions, the high variability in time and in space and the uncertainties in each method, it is recommended to apply few techniques in order to increase reliability of the study results (Lerner et al., 1990). Flint et al. (2002b) and Goodrich et al. (2004) are two good examples of studies that applied multiple approaches (almost all) at the same site, where results represent the realistic full range of recharge rates at the basin. Any model of a recharge system involves decisions about the likely flow mechanism (Kruseman, 1997). The ability to analyze correctly the hydrological system lies in identifying the dominant features influencing recharge at the study site and choosing the appropriate method for measuring the water fluxes. The chosen model must represent essential features of the flow mechanism and finally, the results should support the mechanism that was chosen to describe the local hydrological system. The aim of this section is to elaborate on the various methods and to review some of the works done in this field.

1.3.1 Water budget

Water-budget is one of the most common methods found in the literature and can be applied to all hydrological domains. The water budget equation is often the basis for many other approaches. It is based on a realistic representation of all inflows and outflows of water into the system, while the recharge is set equal to the residual. The main advantage of the method is its applicability over a wide range of space and time scales. The main limitation is the dependency of the recharge estimate on the accuracy of measurements of all variables in the equation. This is even more pronounced in cases where the recharge fluxes are in the range of measurement error of the other components, which is the case in most arid regions (Scanlon and Cook, 2002). **Surface-water budget** will usually represent the transmission losses into the channel bed between two gauging stations at the channel. Many examples are found in the literature, among are studies of Hughes and Sami (1992), Sharma and Murthy (1994), Sorman et al. (1997), Shentsis et al. (1999). **Vadose zone water-budget** is based on measurements of water content, potential energy or temperatures for estimating water flow in the subsurface (methods are reviewed in section 1.2.2). **Water table fluctuation method** (WTF) is based on measurements of groundwater rise and estimation of the specific yield (Healy and Cook, 2002). Abdulrazzak (1994) estimated transmission losses through a mass balance approach that accounted for the influence of tributary runoff and evaporation in the Tabalah basin in southwestern Saudi Arabia. Estimated losses from 27 rain events during 2 years were between 0.05-0.96 Mm^3. Osterkamp et al. (1994) used a water balance approach and a distributed transmission loss model for estimating groundwater recharge at 17 basins in the area of Al Ain on the border of Oman and Abu Dhabi. Average annual recharged volumes ranged from 0.23 to 10.1 Mm^3/y. The WTF method was adopted both by Abdulrazzak, et al. (1989) which estimated a recharge rate of 5 mm/year in the Tabalah Basin, Saudi Arabia and by Allemoz and Olive, (1978) which estimated a recharge volume of 2.25 to 4.5 Mm^3 from a single flood at Wadi El Hira, Libya. Rushton et al. (2006) developed a model for estimating recharge from precipitation based on soil moisture balance at a semi-arid study site in northeast Niger. Precipitation, evapotranspiration and runoff were either calculated or measured to provide an annual recharge estimate of 65 mm.

1.3.2 Direct Methods

Direct measurements are few and include mainly lysimeter studies and seepage meters (infiltrometers). **Seepage meters** are simple cylinders designed to measure infiltration rates at the surface. The cylinder is pushed into the upper soil and filled with water. Infiltration is determined by the rate of change in the water volume. The meters are inexpensive and simple but provide only point measurements. **Lysimeters** consist of containers filled with soil for the purpose of measuring the components of the water balance in the subsurface. The lysimeters are hydrologically isolated from the surrounding soil but regarded as representative of the local environment. In order to minimize edge effect and to average local variations in soil and vegetation that are unavoidable, large diameters (up to 10 m) are recommended. Soil matrix parameters such as water content, water composition, water potential and drainage can be readily retrieved by in-situ measurements, sampling or highly accurate weighing. Disadvantages include high cost, high maintenance requirements and difficulties associated with insuring undisturbed conditions and modification of the bottom boundary conditions. Advantages include a wide range of detectable fluxes and variety of measurable components (Gee and Hillel, 1988). Gee et al. (1992b) used a 18 m deep lysimeter to predict the arrival time of contaminants to the groundwater at Hanford site, Washington, USA. Recharge rates varied from 0 up to >100 mm/year.

1.3.3 Tracer Techniques

Two main advantages of tracer techniques over physical methods are: (1) ability to precisely measure very small fluxes (2) while the physical approach measures current processes, the chemical approach provides information on current and long term cumulative net water flux (Edmunds, 1998).

Applied tracers are introduced as a pulse at the surface and can be identified later at the vadose zone or at the saturated zone, either visually (dyes) or by specific analytical methods. By the depth of propagation and time, the recharge rates can be calculated. It is important to take into account any transport process that may affect the movement of the tracer such as: retardation, anion exclusion, sorption, uptake by plants etc. (Gee and Hillel, 1988).

Historical tracers are related to human activities which generated a large quantity of a certain tracer into the environment at a known point of time. These include ^{3}H and ^{36}Cl from the atmospheric nuclear testing in the 50's and 60's or local incidental contaminant spills (Scanlon et al., 2002; Dahan et al., 2003).

Environmental tracers in common use are (a) Meteoric chloride - mass balance equation is applied to calculate recharge fluxes based on the inverse relationship between drainage and Cl^- concentration in the vadose zone (b) ^{36}Cl, ^{14}C and others – based on radioactive decay or variations in cosmogenic production, known as age dating techniques (Phillips, 1995).

Stable isotopes such as ^{18}O and ^{2}H are used for identifying sources and processes of recharge based on isotopic characteristics of different water bodies as well as fractionation processes caused by evaporation. Though these methods are widely used they are less suitable for quantitative estimates (Gat and Issar, 1974; Adar and Nativ, 2003). Allison et al. (1983) used few different tracer approaches to study soil water movement in a desert in southern Australia. Cl^- profiles showed an increase from <0.1 mm/year to 3 mm/year in deep percolation rates, following clearing of the vegetation. Tritium profiles indicate preferential flow pathways along root channels.

Heat tracer - continuous measurements of the soil temperature at the subsurface might provide estimates of the soil water flux and recharge. The temperature gradient along the soil profile depends on the atmospheric temperature, the geothermal gradient, the thermal properties of the vadose zone and the soil water flux. Inverse modeling is generally used to estimate hydraulic conductivity of the soil based on measured spatial and temporal changes in temperature. Subsurface temperatures can be monitored accurately and inexpensively however, data analysis is complex. Constantz et al. (1994) studied the effect of stream bed temperature on infiltration rates and recorded rates of 0.7-2.0 m/d at the Tijeras Arroyo River, New Mexico based on temperature monitoring at the surface and vadose zone.

1.3.4 Numerical modeling

The basic concept of hydrological modeling is to simulate flow processes and to assess the sensitivity of the results to different variables of the model. All models require field data for calibration and validation but use different approaches (Sanford, 2002). **Surface models** use codes for rainfall/runoff models or channel routing scheme. **Unsaturated models** may use numerical solution to the Richard's equation such as HYDRUS, UNSATH, while codes as MODFLOW, FLOWPATH can be used to simulate flow in the **saturated zone** based on solutions to the continuity equation. A crucial requirement for all models is to define the initial and boundary conditions in a way that will represent the natural conditions (Sanford, 2002). El Hames and Richard (1998) integrated three physically based techniques into one model for prediction of floods and transmission loss in ephemeral wadis. They utilized the kinematic wave theory and the St Venant equation for flood routing over slopes and down channels, respectively. The Crank-Nicholson numerical scheme was applied to solve Richard's equation for infiltration estimates. The results suggest that up to 88% of the rainfall volume might be lost into the alluvial beds due to transmission loss.

1.4 Study objectives

This study focused on floodwater infiltration and groundwater recharge of alluvial aquifers along ephemeral rivers in arid lands. By implementing an innovative monitoring setup, the study was aimed at gaining better insight into the dynamics of water percolation through the subsurface during natural flood events and the factors that control this process. The study was conducted along two large ephemeral rivers flowing through the arid regions of southwest Africa: 1) the Kuiseb River, Namibia and 2) the Buffels River, South Africa. Aside from the qualitative objectives, the overall goal was to quantitatively estimate recharge fluxes and evaluate total groundwater recharge at a given study site. The research was carried out with the assistance of the local communities living around the studied channels in the hope that it would contribute to the development of sustainable water-resource management strategies.

2. Methods

2.1 Methodological concept

The process of groundwater recharge involves three different hydrological domains: (a) the surface (b) the vadose zone and (c) the groundwater. While each of the domains presents totally different hydrological characteristics, they are all closely related one to another and greatly influenced by the conditions prevailing at the adjacent domains. Each zone encompasses different controls on the infiltration and recharge processes, while together they form the local hydrological environment. The interrelations between all domains and the characteristics of the local hydrological system will determine water availability at the area and thus has a major affect on the local ecological environment and any form of living around it. Accordingly, understanding the infiltration dynamics and the recharge component requires monitoring of all three hydrological zones. In order to obtain meaningful data regarding flow dynamics beneath ephemeral channels in arid regions a few requirements must be met: (1) high resolution of measurements in time and in space due to the high variability in both dimensions (2) high accuracy of the measuring technique due to the low values of water content and fluxes (3) minimum disturbance of the local settings (4) ability to monitor preferential flows as it might potentially account for a significant portion of the total recharge (5) continuous readings of the water content in real time are necessary because the hydraulic parameters in the vadose zone change significantly following small variations in water content, (6) robustness of the monitoring system to endure the destructive nature of flash floods. Most of the techniques described in table 1 (section 1.2.2) have limited application in ephemeral rivers for various reasons (not applicable at the field, can not be automated, destructive, require equilibrium or long measurement time, depth measurement limitation, low resolution and low accuracy).

The monitoring set up in this study attempts to track the complete hydrological pathway of water from land surface to groundwater with special attention to the interrelationship between the three domains. This is done by simultaneous measurements of the conditions at the surface and groundwater together with continuous measurements of soil moisture variations at multiple depths along the unsaturated profile, from surface down to the water table (fig. 2.1). The innovative system allows for the first time, in situ automated continuous measurements of floods and the percolation and recharge events that follow, in real time with minimum disturbance of the local environment. The system was also described in details by Shani (2006), Dahan et al. (2006), Rimon et al. (2007), Dahan et al. (2007b).

2.2 Flood monitoring

Monitoring of the floods' characteristics at the surface was done using a pressure transducer of type Levelogger M5 model 3001 by *Solinst* and a CS547A Conductivity and Temperature Probe by *Campbell Scientific Inc.* (*CSI*). Both instruments were placed inside a protective metal mesh connected to the piezometer tower, leveled with the channel bed surface (fig. 2.2A). The M5 Levelogger effective range is 0 – 500 cm water head and its accuracy is 0.05% of reading. Readings were later compensated for barometric pressure using a separate Levelogger functioning as a barologger. Effective range of the EC probe is ~0.005 – 7.0 mS/cm and 0° – 50°C with accuracy of ±5% of reading. All instruments took measurements once every 15 minutes. Data retrieved from the Levelogger and EC probe include: arrival time of flood, end time of flow in the channel (flood duration), water levels during the flood and floodwater EC.

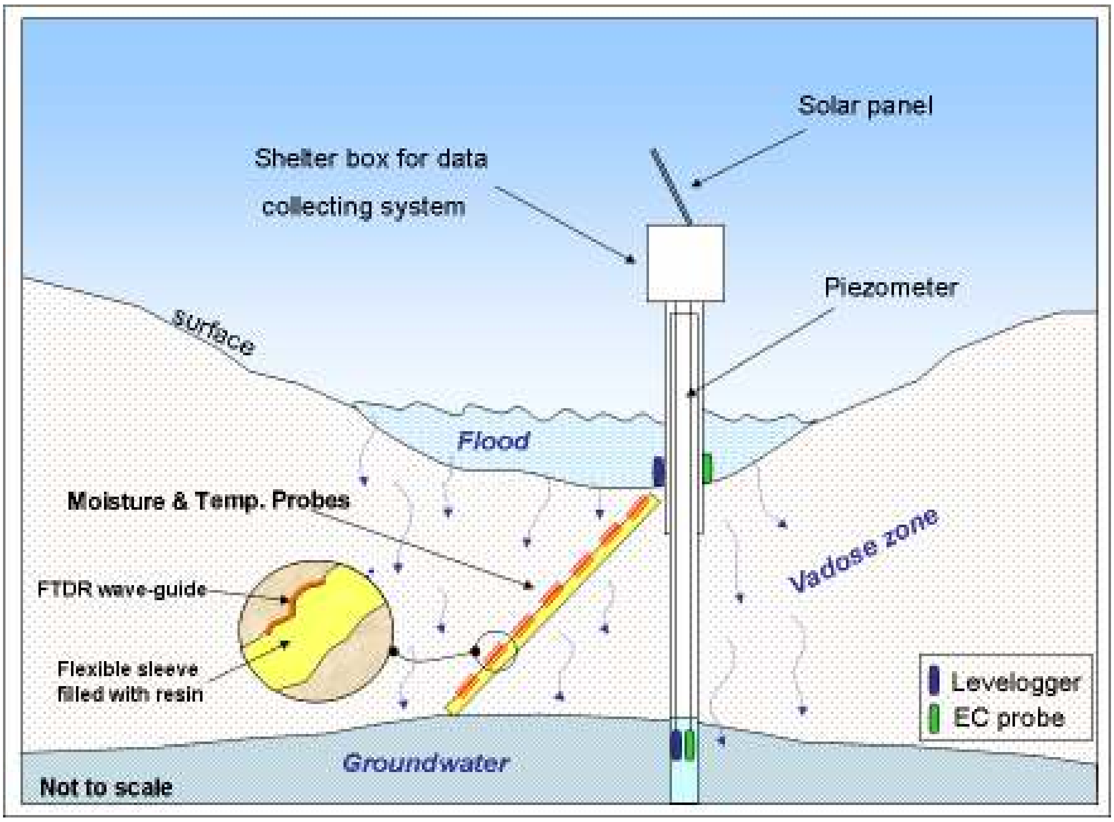

__Figure 2.1__ Schematic illustration of the monitoring set up.

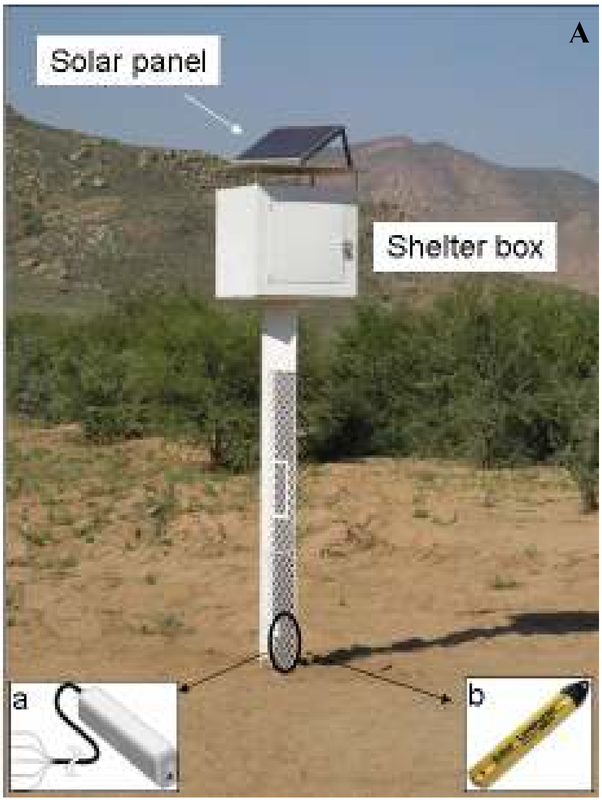

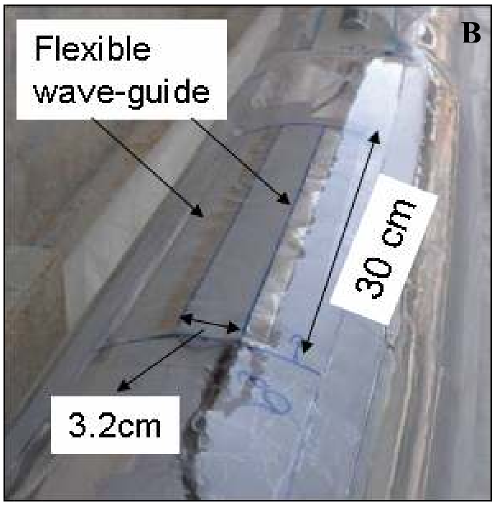

__Figure 2.2 (A)__ The monitoring station. Location of EC probe (a) and Levelogger (b) for monitoring the flood parameters __(B)__ FTDR probe attached to the PVC sleeve.

2.3 Vadose zone monitoring

Monitoring spatial and temporal variations in water content in the vadose zone was done using Time Domain Reflectometry (TDR) probes. The TDR method is widely applied and acknowledged for measuring soil moisture since the early 80's and was reviewed to date in many papers (Topp et al., 1980; Dalton and Van Genuchten, 1986; Ledieu et al., 1986; Heimovaara, 1994; Ferre et al., 1998; Logsdon, 2000; Robinson et al., 2003). The fundamental principle that lies in the basics of the TDR technique is the significantly higher dielectric constant of water (80) compared to that of air (~1) or any type of dry soil (2 – 5). Thus, even very small amounts of water present in a soil matrix will affect its dielectric properties. The system actually measures the travel time of an electromagnetic wave along a known length of a TDR probe. The travel time is directly related to the dielectric properties of the medium through which the electromagnetic signal travels and thus, directly related also to the water content of the medium. Eventually a calibration equation is applied to the TDR readings in order to obtain the volumetric water content. The method allows point measurement of soil moisture content with high accuracy.

However, the standard TDR probes are limited only to shallow depths. An innovative monitoring set up developed by Dahan et al. (2003) of flexible TDR (FTDR) probes attached to a PVC sleeve, enables in situ field measurements of water contents at large depths with minimal disturbance of the local settings. The sleeve is prepared in advance in the lab according to the thickness of the unsaturated zone. The FTDR probes are made of two 30 cm long flexible flat stainless steel wave guides; distance between the conductors is 3.2cm (fig. 2.2B). The number of probes attached to the sleeve and distance between the probes can be constructed according to the resolution requirements. Next to each probe a T type thermocouple (by *Omega*) is attached to the sleeve. The PVC sleeve (10") with the FTDR probes facing up towards the surface is inserted into an uncased slanted borehole (6", 35°–45°) and then filled with a double component poly-urethane resin featuring high density of 1.6 g/cm^3 (fig. 2.3). Drilling method should be chosen according to sedimentological characteristics of the study site. Methods applied successfully during this study include flight-auger, rock bit and air-lift. The resin fills the entire volume of the sleeve, supporting the borehole walls and forcing the probes against the borehole upper side wall, ensuring full contact of the probes with the local alluvial material. Soon after (~45 min) the resin fully solidifies and the probes, as well as the whole sleeve are tightly secured in their position. The slanted angle creates a set up where every probe is located at the bottom of an undisturbed soil column which is being monitored by it. Assuming the flow of water in the subsurface is primarily vertical, this set up provides minimal disturbance to the natural percolation process. The upper end of the sleeve is usually sealed and buried between 0.5 and 1 m below the stream bed to reduce impact of the active layer during strong stream flow on the sleeve. The final outcome of this installation technique is the ability to measure temporal variations in water content at various depths of the vadose zone from land surface to the water table, with minimum interference to the natural processes. Measurement frequency of the water content and temperature in the vadose zone was once every 10-15 minutes.

Specific calibration tests were conducted in order to obtain the volumetric water content from the FTDR probes' data. FTDR output signals were measured at various moisture contents at few different soil types and were compared to water content values achieved by the gravimetric method. The calibration curve showed a linear correlation between the FTDR signals and the water content (appendix 1.1):

$$\theta = 0.2432\left({}^{L_a}\!/_{L}\right) - 0.3981 \qquad (2.1)$$

Where θ is the water content, *La* is the apparent probe's length and *L* is the real probe's length. An additional calibration test was performed in order to evaluate the potential influence of cable length on the measured apparent length. This experiment was conducted with FTDR probes of various cable lengths (3 - 75 m) immersed in few different liquid solutions of known permittivity (water, ethanol and acetic acid of several dilution levels). The calibration curve achieved from this test expresses the relationship between cable length and the FTDR output (*La/L*) (appendix 1.2). The calibration equation for the cable length effect was:

$$\left({L_a}/{L} \right)_c = \left({L_a}/{L} \right)_m - \{0.016 \cdot [(0.67 \cdot L_a) - 3]\} \qquad (2.2)$$

where *'c'* is the corrected value after cable length correction and *m* is the measured value. Procedures and full results of the calibration experiment can be found in Shani (2006) and Rimon et al. (2007).

2.4 Groundwater monitoring

Groundwater monitoring was done by a vertical observation well drilled at the monitoring station (fig. 2.1). The piezometer consists of a 3" PVC access pipe with perforated section in the groundwater and at least 1m above the water table. The piezometer is protected by a thick 6" steel casing penetrating at least 1.5m into the alluvial bed and rising high (at least 2m) above the channel bed. Groundwater parameters are being monitored using exactly the same equipment used at the surface: M5 Levelogger and a CS547A Conductivity and Temperature Probe. Both instruments are located inside the piezometer submerged in the upper part of the aquifer (~1 m) taking readings once every 15 minutes. Data obtained include response time of the groundwater to the recharge event, groundwater level fluctuations and groundwater EC.

2.5 Data acquisition

All the electronic devices for operation of the monitoring system are placed on top of the piezometer tower inside a shelter box (fig. 2.4). This includes: (1) TDR100 (*CSI*) for measurement of the water content by the FTDR probes (operated using PCTDR software), (2) SDMX50 coaxial multiplexers (*CSI*) were used to connect multiple probes at a single site to the TDR100, (3) AM 16/32 Relay Multiplexer (*CSI*) was used for connecting all thermocouples to the datalogger, (4) programming, scheduling and logging were done using a CR10X Measurement and Control System datalogger (*CSI*) operated by a PC208W 3.3 software (5) a CR10XTCR Thermocouple Reference (*CSI*) was connected to the datalogger, (6) A547 Interface (*CSI*) was used for the measurements of EC. Power was supplied by a 12V, 7 Amps hour battery connected to a solar panel via a charging regulator.

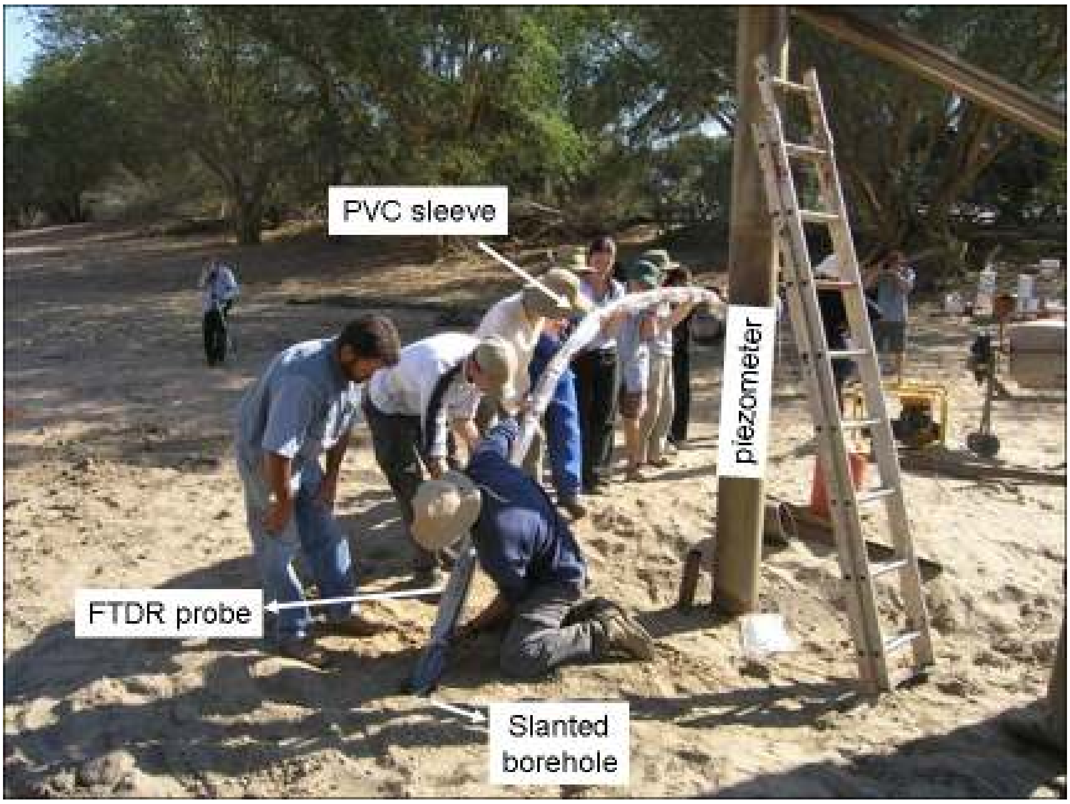

Figure 2.3 *The PVC sleeve with the FTDR probes facing upward is inserted into the slanted borehole, and later filled with high density resin.*

2.6 Sediment analysis

During the drilling of the piezometers at each site, sediment samples were collected approximately every 1 m and were analyzed for grain size distribution at the Department of Geology, University of Cape Town, RSA. Samples for bulk density and porosity were collected at few locations and depths around each site. **Bulk density** was calculated by dividing the dry net weight of a soil sample by the known volume of the sampling cup it was extracted with. Particles density was retrieved by dividing the dry net weight of the sample by the volume of water displaced when the sample was inserted into a water column. **Porosity** was then calculated according to:

$$n = 1 - \left({}^{b_d}\!/_{p_d} \right) \tag{2.3}$$

Where n is the porosity, b_d is the bulk density and P_d is the particles density.

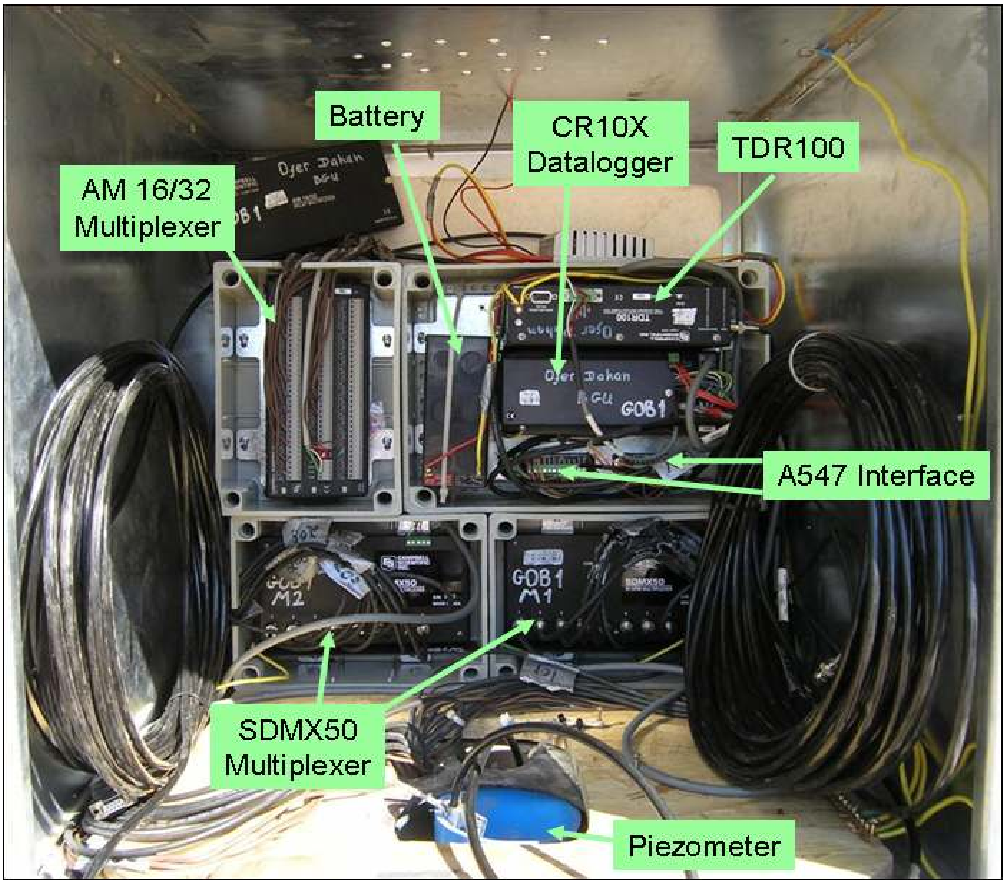

***Figure 2.4** The data control system and the access to the piezometer in the shelter box.*

3. Study sites

3.1 Kuiseb River, Namibia

3.1.1 Geography

The Kuiseb River is one of the largest ephemeral rivers of western Namibia, flowing from the high plateau east of the Great Escarpment westward into the Atlantic Ocean near Walvis Bay. Headwaters of the basin lie within the Khomas Hochland, west of Windhoek at ~2000 m above mean sea level (AMSL) (Scholz, 1972). The middle and lower reaches of the river cut their way through the central Namib Desert, forming the boundary between the vast sand dune sea to the south and the gravel peneplains to the north (fig. 3.1). The catchment area of the Kuiseb is ~15,500 km² and the total length of the river is approximately 500 km (Jacobson et al., 1995).

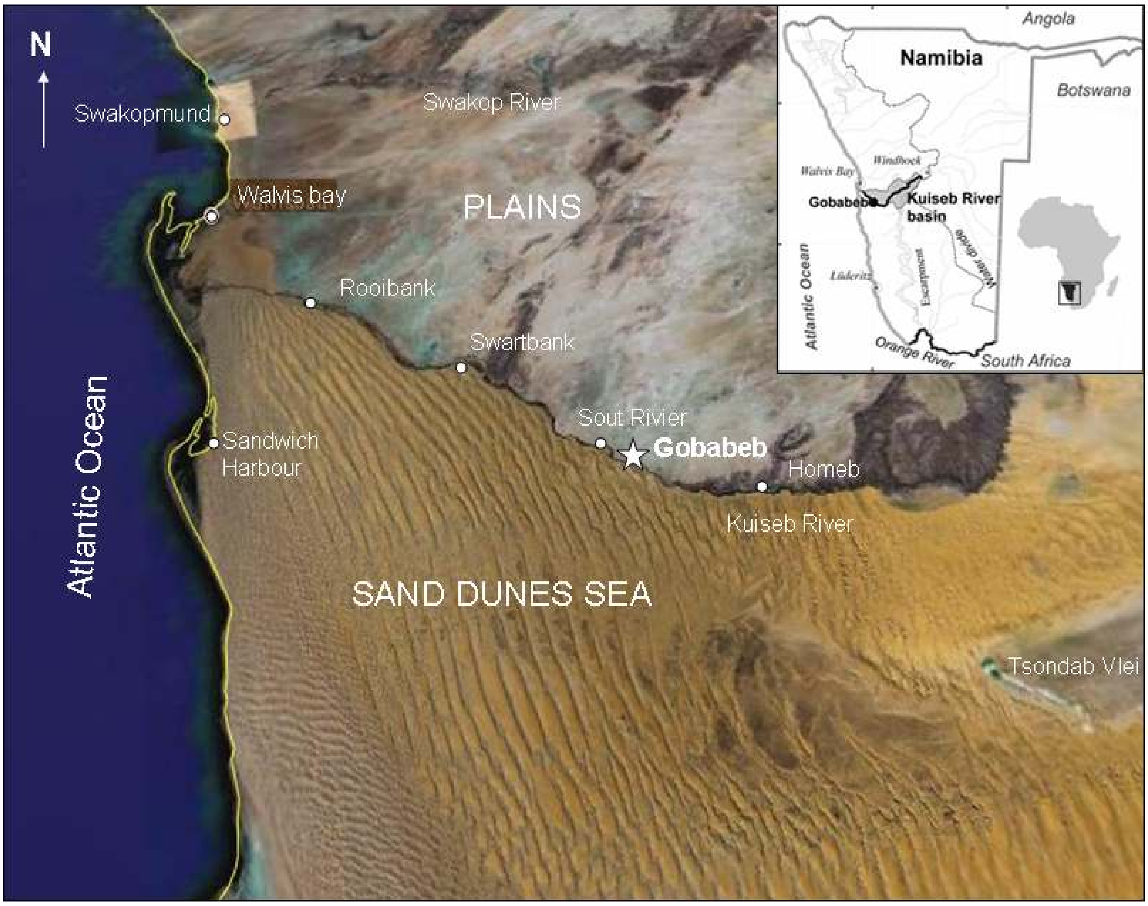

Figure 3.1 *Satellite image of the middle and lower Kuiseb River with the location of the Gobabeb study site.*

3.1.2 Climate

The aridity of the Namib Desert is caused by the cold Bengula Current, which reduces temperatures of the westerly winds limiting to minimum their ability to absorb moisture. Mean annual precipitation in the catchment varies between >300 mm/y in the highlands (5% of catchment area) to less than 20 mm/y in the lower reaches (~40% of the catchment area) with most of the basin receiving average rainfall of 100 mm/y (Botes et al., 2003). Mean March temperature is 24.2°C at Gobabeb compared with 17.7°C in July. Potential evaporation at Gobabeb is 3560 mm/y (Schmidt, 1998).

3.1.3 Geology

The Namib platform in the area of Gobabeb is underlain by late Proteorzoic rocks (1000 – 450 Ma) of the Damara System. These are metamorphic rocks of a wide variety including: mica schists, marble, granitic gneiss and quartzite. The Salem Granites of later Precambrian periods are intruded into the Damaran group, and in some places outcrop at the surface around Gobabeb (Goudie, 1972; Ward, 1987). The alluvial material of the riverbed varies in depth and composition along the flow path and its thickness is constrained by the depth of the crystalline bedrock. The Kuiseb River seems to play a dominant role in forming the northern boundary of the sand dunes sea and preventing the propagation of dunes northward (Ollier, 1977).

3.1.4 Hydrology

Runoff in the basin is primarily produced in the upper catchment, upstream of the flow gauging weirs of Schlesien on the main channel and Greylingshof on the Gaub River. In the middle and lower reaches, as the river flows through the Namib Desert, no south bank tributaries are found. On the northern bank, few small wadis exist like Soutrivier (downstream of Gobabeb), though these have very small and rare contributions of surface flow (Hattle, 1985). In the last 20 years, the Kuiseb flowed every year for an average of 12 days/year. The Kuiseb valley is underlain by a shallow alluvial aquifer which is being recharged during flood events. Subsurface inflows from the south are presumably nil, whereas some subsurface feeding from the northern bank is possible but considered to be insignificant in quantities. Contributions from the north however, present extremely high TDS values of ~5000 ppm comparable to only ~200 ppm in floodwater generated in the upper catchment. This is attributed to dissolution of sodium chloride and gypsum-rich tertiary sediments (Slabbert, 1991). Between 1975 and 1992 significant depletion of groundwater levels were recorded due to overexploitation. Water table drop of 2 - 6 m and 10 m were recorded in the Gobabeb and Swartbank areas, respectively (Lenz et al., 1995).

3.1.5 Vegetation

The shallow alluvial aquifer underlying the Kuiseb River supports a large, developed and dense vegetation community situated along the Kuiseb Valley (fig. 3.2). Approximately 80% of the vegetation is comprised of four woody tree species: (1) *Acacia erioloba,* found both on the river banks and on the edge of the dunes and plains (2) *Faidherbia albida*, found in proximity to the active channel. In the vicinity of Homeb these trees often reach 21 m in height (Theron et al., 1985).

Figure 3.2 *Dense woody vegetation along the Kuiseb Valley.*

(3) *Euclea pseudebenus* and *(4) Tamarix usneoides,* found on the riverbanks, floodplains and at the foot of the sand dunes (Bate and Walker, 1993). The active channel is usually bare of vegetation.

3.1.6 Population and water supply

The Kuiseb aquifer is a vital linear oasis in an otherwise inhospitable desert environment. It supports a large population of Namibians living along the course of the Kuiseb River. These include numerous private farms, few Topnaar villages, the Gobabeb Training and Research Center and the city of Walvis Bay, a total of >65,000 people. In addition, water from the Kuiseb aquifer are supplied to Swakopmund, Arandis, Rössing Mine and to the local fishing industry (Heyns et al., 2001).

3.1.7 Previous studies

The study by Stengel (1968) is probably one of the first studies carried around Gobabeb and addresses issues regarding water supply to Gobabeb. Findings from the Kuiseb Environmental Project are summarized in Huntley (1985). Slabbert (1991) aims to assess the impacts of proposed water resources development in the lower Kuiseb. According to Konig (1992), significant deterioration of water qualities associated with groundwater levels depletion was noticed at boreholes near Gobabeb between 1988 and 1992, which in some cases exceeded acceptable values for human consumption. Two phases of the German- Namibian Groundwater Exploration Project are summarized in Lenz et al. (1995) and Schmidt (1998). The reports present a thorough review of the physiography, geology and geohydrology of the region. Groundwater recharge during the floods of 1997 was estimated between 1 and 5 Mm^3. Lange (2005) applied a mathematical flow routing approach to evaluate temporal dynamics of transmission losses within a 150 km reach of the Kuiseb channel. He claims that high magnitude floods are the main source of groundwater recharge due to enhanced water losses in the over bank floodplains. Botes et al. (2002) present the conceptual approach of the Environmental Learning and Action in the Kuiseb (ELAK) project for development of sustainable basin management strategies.

3.1.8 Gobabeb monitoring station

The Gobabeb Training and Research Center is located in the lower Kuiseb approximately 85 km upstream of the river mouth with average annual rainfall of 20 mm. The GOB 1 monitoring station was constructed in the middle of the channel near Gobabeb (23°33'28.77" S 1°51'56.12" E) at an elevation of 387 m AMSL (fig. 3.3). The GOB 2 station was constructed ~300 m upstream of GOB 1 on the southern bank of the channel next to a ~15 m high acacia tree, known by the residents as "Marry's Caravan". Each station includes one observation piezometer and two slanted boreholes with attached FTDR probes. In the GOB 1 station two slanted boreholes (100, 200) were installed in the riverbed. However, borehole 100 was found to be malfunctioning and thus disregarded. In GOB 2, borehole 300 was drilled towards the middle of the channel whereas, borehole 400 heads southwards under the river bank and into the root system of the tree. Depth to the water table at the time of installation (July 2005) was ~5 m below surface. The GOB 1 station was protected with a robust metal structure to insure its durability during flash floods. Boreholes orientation and schematic cross sections of both stations can be found in appendix 2. The active channel presents a relatively flat uniform bed with an average width of 33 m. Average slope of the channel is 0.0026 (appendix 3). The sediments comprising the river bed in the vicinity of the stations are well sorted medium to coarse sands (tables 2, 3). Locations of probes in relation to the soil texture profile are presented in figure 3.4. Bulk density and porosity at two cross sections, in the middle of the channel and in the floodplains are presented in appendix 4.

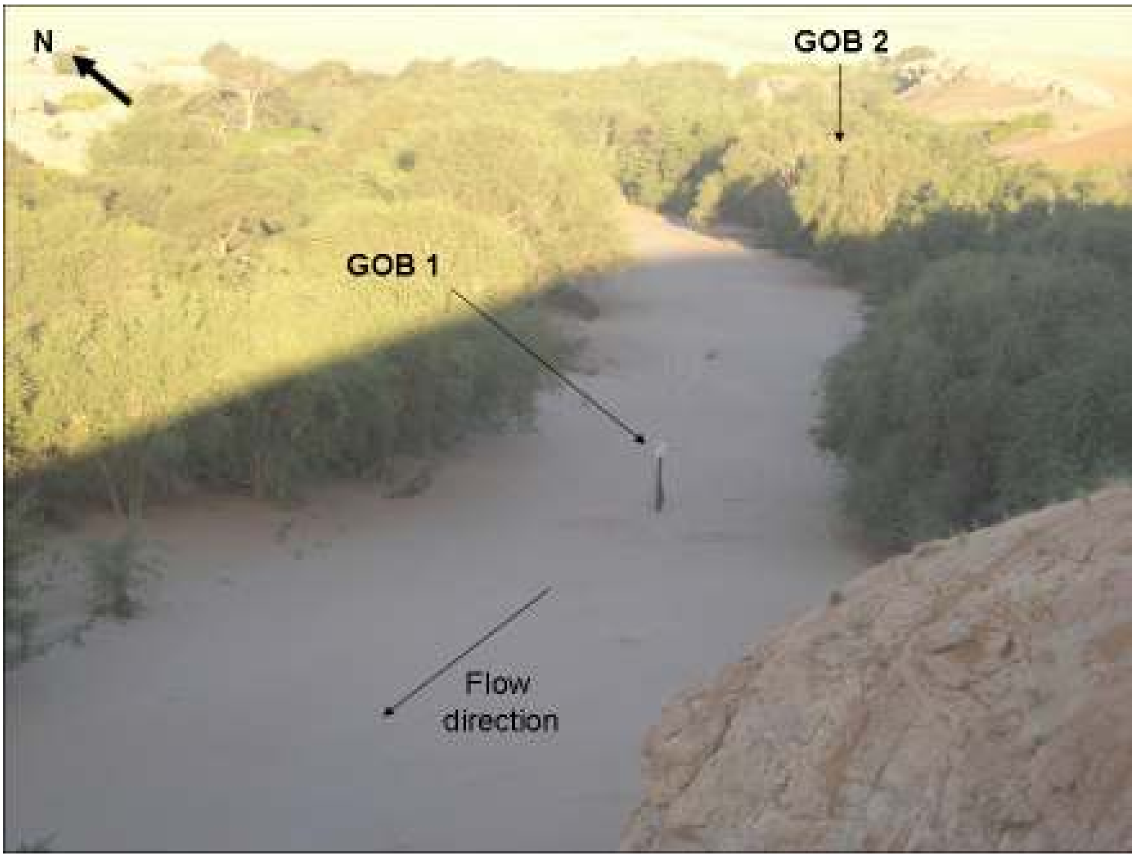

Figure 3.3 The active channel of the Kuiseb River with the monitoring stations

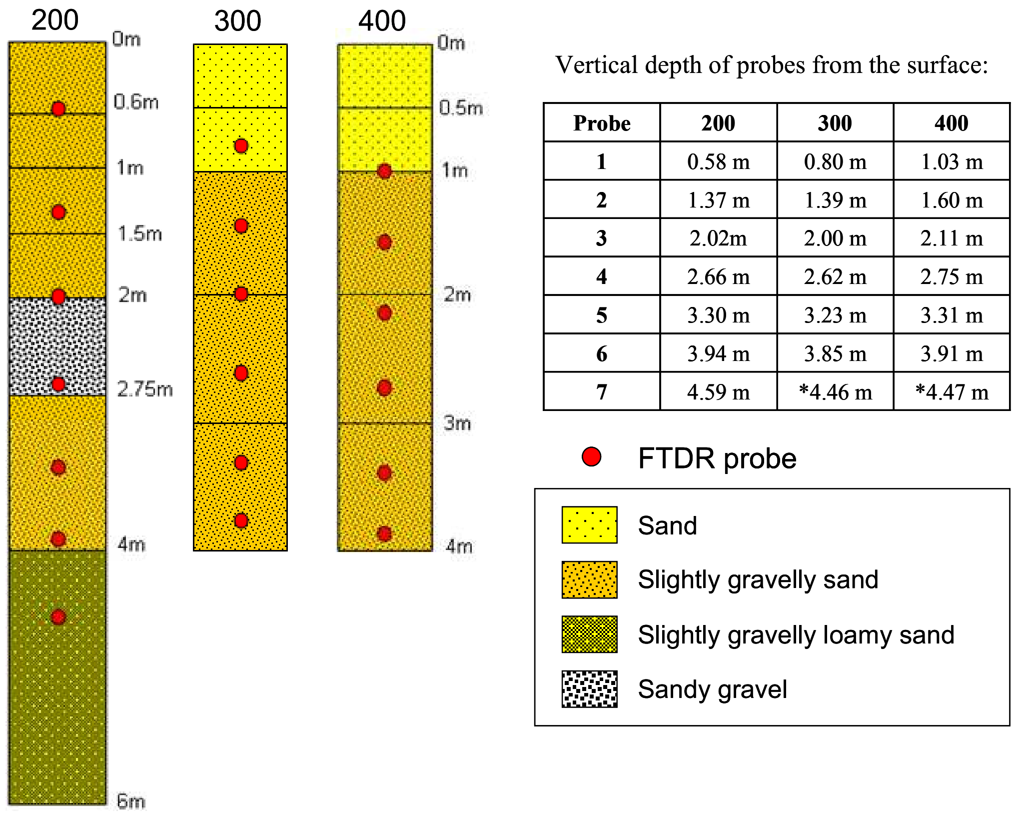

Vertical depth of probes from the surface:

Probe	200	300	400
1	0.58 m	0.80 m	1.03 m
2	1.37 m	1.39 m	1.60 m
3	2.02m	2.00 m	2.11 m
4	2.66 m	2.62 m	2.75 m
5	3.30 m	3.23 m	3.31 m
6	3.94 m	3.85 m	3.91 m
7	4.59 m	*4.46 m	*4.47 m

Figure 3.4 Location of FTDR probes at the Gobabeb stations (boreholes 200, 300, 400) in relation to the sedimentary sequence. *No texture data. Comment: estimated accuracy of probes' location is ±20 cm.*

Table 2. *Grain size distribution at GOB 1*

Depth (m)	**Gravel (%)**	**Sand (%)**	**Silt & Clay (%)**	**Texture (Folk, 1954)**
0 – 0.6	0.008	99.428	0.564	Slightly gravelly sand
0.6 – 1.0	0.001	99.347	0.652	Slightly gravelly sand
1.0 – 1.5	0.124	99.176	0.700	Slightly gravelly sand
1.5 – 2.0	8.818	90.759	0.423	Slightly gravelly sand
2.0 – 2.75	51.800	47.059	1.142	Sandy gravel
2.75 – 3.0	4.870	93.296	1.834	Slightly gravelly sand
3.0 – 4.0	0.671	97.137	2.192	Slightly gravelly sand
4.0 – 6.0	0.463	92.094	7.443	Slightly gravelly loamy sand

Table 3. *Grain size distribution at GOB 2*

Depth (m)	**Gravel (%)**	**Sand (%)**	**Silt & Clay (%)**	**Texture (Folk, 1954)**
0 – 0.5	0.000	98.602	1.398	Sand
0.5 – 1.0	0.000	98.292	1.708	Sand
1.0 – 2.0	0.061	98.995	0.944	Slightly gravelly sand
2.0 – 3.0	0.322	97.110	2.568	Slightly gravelly sand
3.0 – 4.0	0.268	97.534	2.198	Slightly gravelly sand

3.2 Buffels River, South Africa

3.2.1 Geography

The Buffels River is one of the largest ephemeral catchments along the western coast of South Africa located within the region of Namaqualand in the north-west (fig. 3.5). Namaqualand is situated between latitudes 17°00' – 18°30' and longitudes 29°00' - 30°00' and can be classified into three main physiographic regions. These regions include the higher lying Bushmanland Plateau to the east, the Namaqualand highlands (which includes the escarpment zone) and the lower lying coastal area to the west (visser, 1989). The Buffels River emerges in the Kamiesberge Mountains peaking ~1400 m AMSL, and flows westward along a 210 km channel into the Atlantic Ocean near Kleinsee, draining an area of approximately 9500 km^2 (Titus et al., 2002).

3.2.2 Climate

Three main factors affect the climate in the region: altitude, distance from the sea and topography. The mean annual precipitation increases from west to east due to the orographic affect, with values of ~45 mm at the coastal zone area and up to 480 mm in the Kamiesberge Mountains. Large variations between maximum and minimum temperatures (daily and seasonal) exist in the area, with an average maximum of 30°C in the summer and average minimum of 10°C in the winter. Mean annual evapotranspiration is 2200 mm (Titus et al., 2002).

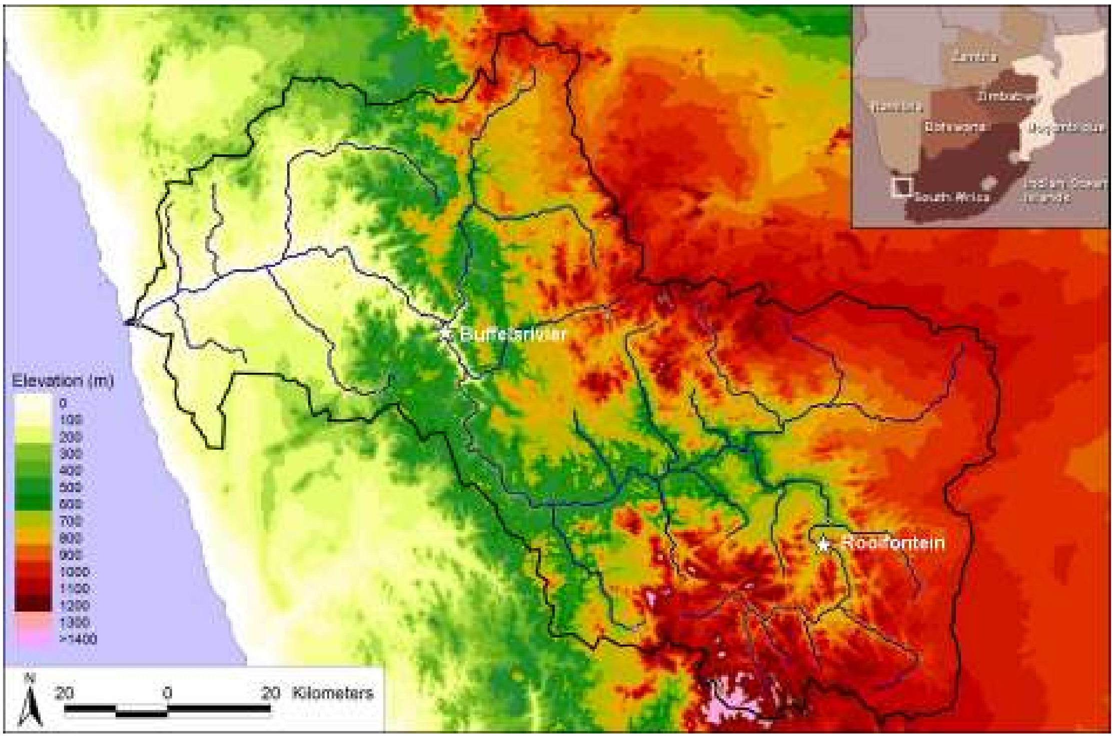

Figure 3.5 *A topographic presentation of the Buffels River catchment area with the location of the two study sites at Buffelsrivier and Rooifontein.*

3.2.3 Geology

The Buffels River catchment is predominantly underlain by Proterozoic crystalline basement rocks of the Namaqua Metamorphic Province which were intruded on a large scale by syntectonic granitic and gneissose rocks (Tankard et al., 1982). The upper Phanerozoic cover sediments of the Nama and Karoo groups are comprised mainly of Sand, Calcrete and alluvium in which the shallow aquifer of the Buffels River is located. The most prominent geomorphologic feature in the area is the bornhardts. These are inselbergs or "Island Mountains" with rounded dome-shape forms, comprised of granitic and gneissic rocks (Titus et al., 2002).

3.2.4 Hydrology

The drainage patterns in the catchment are well developed and are strongly interlinked with the geologic and structural features (Titus et al., 2002). Groundwater flow in the region is closely linked to the complex geomorphologic and hydrogeologic environments which create a dynamic system with more then one flow pattern. Three main aquifer systems are distinguished in the Namaqualand area: (1) in the fractured bedrock, (2) in the weathered zone (regolith) and (3) the alluvial aquifer associated with the river system which is usually of shallow depth of 1 – 15 m. These aquifers are closely interlinked though present different hydrologic features (Adams et al., 2004). Parameters such as hydraulic gradient, permeability and water table location will determine interflow directions and fluxes between the water bodies. Cornelissen (unknown year) concluded that subsurface lateral recharge of the alluvial aquifer does take place based on the existence of surface springs downstream of Buffelsrivier where the bedrock is exposed. Titus et al. (2000) characterized the different water bodies according to their chemical composition. Average measured EC of the groundwater of the fractured and weathered units is ~30,000 mS/cm whereas chloride concentration can reach >1000 mg/l. These high values are explained by (a) dissolution and leaching of highly soluble evaporitic salts (such as NaCl) (b) dissolution of hydrous minerals (such as biotite) in the host rock during water-rock interaction. Accordingly, the salinity is probably related to the residence time of the water in the hosting rock and hence to the length of flow path in the subsurface.

3.2.5 Vegetation

The vegetation in the catchment is dominated by a mixture of grasses, short leaf succulent shrubs and low woody shrubs of the Nama karoo biome (Low and Rebelo, 1996). Most of the shrubs are drought deciduous and tend to develop deep root systems. Out of the numerous plant species (over 200) found in the study reaches four main species comprise 70% of the perennial riparian vegetation: the *Acacia karoo* and *Tamarix useneoides* trees and the *Salsola aphylla* and *Suaeda fruticosa* shrubs. The active channel is usually bare of vegetation.

3.2.6 Population and water supply

The alluvial aquifers are the main source of water supply to most of the villages in the catchment, including Buffelsrivier and Rooifontein. At Rooifontein and the adjacent Kamassies village, 145 household are located (Lebert, 2005). Population at Buffelsrivier was estimated to be 1023 residents at 2005. Water is currently abstracted from the alluvial aquifer by the Nama Khoi Municipality for water supply for Buffelsrivier and for irrigation of a ~15ha private farm. The estimated total abstractions by these users are 0.157 Mm^3/y (Visser, 2006). According to Adams et al. (2004) 55% of the boreholes drilled in central Namaqualand are dry, 33% gave a yield of less than 1 l/s and only ~10% yield >1 l/s. Based on EC measurements most communities in the region use groundwater that do not comply with local and international water quality standards and guidelines (Adams et al., 2004).

3.2.7 Previous studies

Historic records of surface-water flows and groundwater in the basin are very scarce. One of the first detailed reports on the hydrogeology of the Buffels River and groundwater potential was written by Cornelissen (unknown year) for the O'okiep

Copper Company. Most of the few studies published since, focused on the lower catchment mainly in the vicinity of the Spektakel aquifer (next to the Buffelsrivier village, appendix 5). Historic hydrological information around the Rooifontein area is practically absent. The most thoroughly characterization of the region is probably the work published by Titus et al. (2002). Groundwater recharge assessment in the region is summarized by Adams et al. (2004). Recharge rates were estimated between 0.1 to 10 mm/y, with the higher values associated mainly with the alluvial aquifers and highlands and the lower values predominated the fractured rock. Historical water schemes from the Spektakel Aquifer are described by Marais (1981). In his report, Marais states the average width of the floodplain between the Eselsfontein and Schaap tributaries (equivalent to the average width of aquifer) is approximately 700 m. In 1973 abstractions had to be significantly reduced from approximately 2 to ~0.5 Mm^3/y due to over exploitation and nearly depletion of the aquifer. Between 1992 and 2006 groundwater levels in production boreholes along the Spektakel Aquifer declined by 30 to 40 m. Esterhuyse (2006) noticed a significant increase of several orders of magnitude in EC of the stream flow of the Buffels river during a prolong flow event on September 2006. This increase was attributed either to recharge from the underlying fractured rock which is "known to be of poor quality" or to contamination from the Buffelsrivier settlement.

3.2.8 Monitoring stations description

3.2.8.1 Rooifontein station

The Rooifontein Station was constructed in the upper catchment of the Buffels River near the village of Rooifontein (N 3321683 E -69945.5) at an elevation of 688 m AMSL (fig. 3.6). At the time of installation (July 2005) water table was located 2.8 m below surface. The sediments comprising the riverbed in the site are well sorted and relatively coarse, most of the profile is classified as sandy gravel (table 4). The monitoring station is located in the middle of the active channel which is about 30 m wide at this section, with an average longitude slope of 0.004 (appendix 6.1, 6.2). The station is located downstream from the confluence with a major tributary. Two slanted boreholes with FTDR probes were installed at this site. Boreholes orientation and a schematic cross section of the monitoring set-up are presented in appendix 7. Location of the probes in the soil profile is illustrated in figure 3.7.

Table 4. *Grain size distribution at Rooifontein station*

Depth (m)	Gravel (%)	Sand (%)	Silt & Clay (%)	Texture (Folk, 1954)
0 - 0.3	9.69	89.98	0.33	Gravelly sand
0.3 - 0.65	22.70	76.23	1.06	Gravelly sand
0.65 - 1.05	44.24	54.56	1.20	Sandy gravel
1.05 - 1.3	34.33	64.02	1.65	Sandy gravel
1.3 - 1.4	45.71	52.66	1.63	Slightly loamy sandy gravel
1.4 - 1.6	44.40	54.09	1.50	Sandy gravel

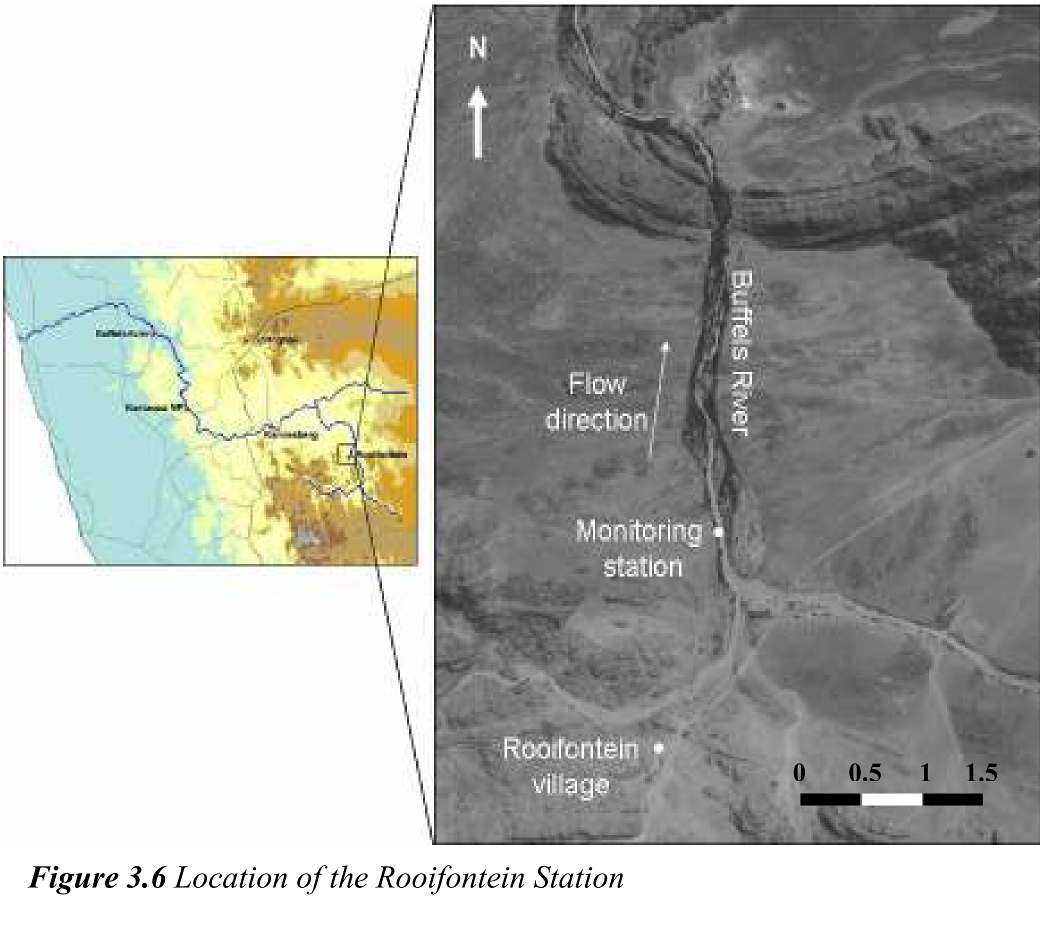

Figure 3.6 *Location of the Rooifontein Station*

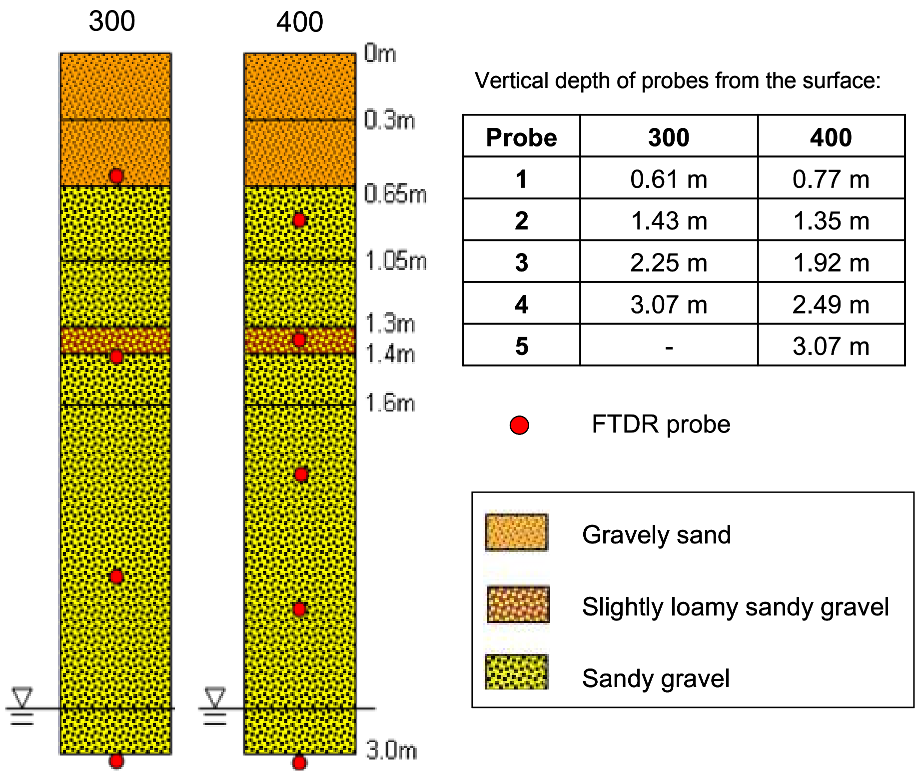

Vertical depth of probes from the surface:

Probe	300	400
1	0.61 m	0.77 m
2	1.43 m	1.35 m
3	2.25 m	1.92 m
4	3.07 m	2.49 m
5	-	3.07 m

Figure 3.7 *Location of FTDR probes at the Rooifontein station (boreholes 300, 400) in relation to the sedimentary sequence. Estimated accuracy of probes' location is ±20 cm.*

3.2.8.2 Buffelsrivier station

The Buffelsrivier station is located in the lower catchment of the Buffels River approximately 6.5 km upstream of the village of Buffelsrivier (N 3292620 E 62169) at an elevation of 208 m AMSL (fig. 3.8). Depth to the water table at the time of installation (July 2005) was 5 m below surface. The station is located in the middle of the active channel which is relatively flat and uniformly leveled with a width of approximately 40 m at this site (appendix 6.3). The alluvial profile at the vicinity of the station is comprised of well sorted mainly gravely sand (table 5). Two slanted boreholes 100 and 200, with attached FTDR probes were installed in the site, containing 7 and 6 probes respectively. Vertical depth of each probe in relation to the soil texture is presented in figure 3.9. Boreholes orientation and a schematic cross section of the monitoring set-up are presented in appendix 8.

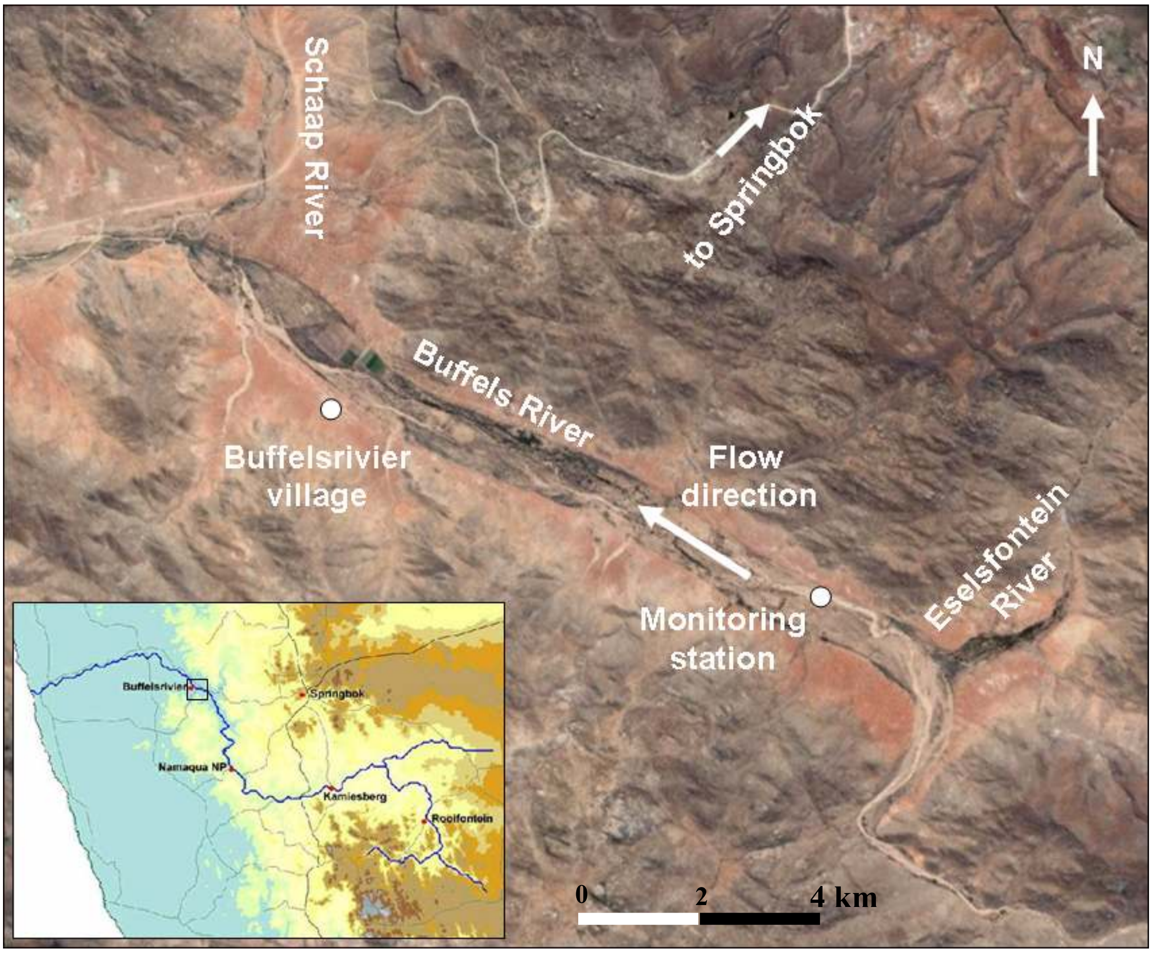

Figure 3.8 *Location of the Buffelsrivier station.*

Table 5. *Grain size distribution at Buffelsrivier station*

Depth (m)	Gravel (%)	Sand (%)	Silt & Clay (%)	Texture (Folk, 1954)
0 - 0.3	13.23	82.76	4.01	Gravelly slightly loamy sand
0.3 - 0.6	22.04	60.60	17.36	Gravelly loamy sand
0.6 - 0.85	16.98	82.02	1.01	Gravelly sand
0.85 - 1.05	31.21	66.33	2.46	Slightly loamy sandy gravel
1.05 - 1.45	16.98	80.76	2.26	Gravelly sand
1.45 - 2.05	34.26	64.71	1.03	Sandy gravel
2.05 - 2.95	26.29	70.97	2.74	Gravelly slightly loamy sand
2.95 - 3.95	21.26	76.11	2.63	Gravelly slightly loamy sand

Vertical depth of probes from the surface:

Probe	100	200
1	1.10 m	0.69 m
2	1.67 m	1.51 m
3	2.25 m	2.33 m
4	2.82 m	3.15 m
5	3.39 m	3.97 m
6	3.97 m	4.78 m
7	4.54 m	-

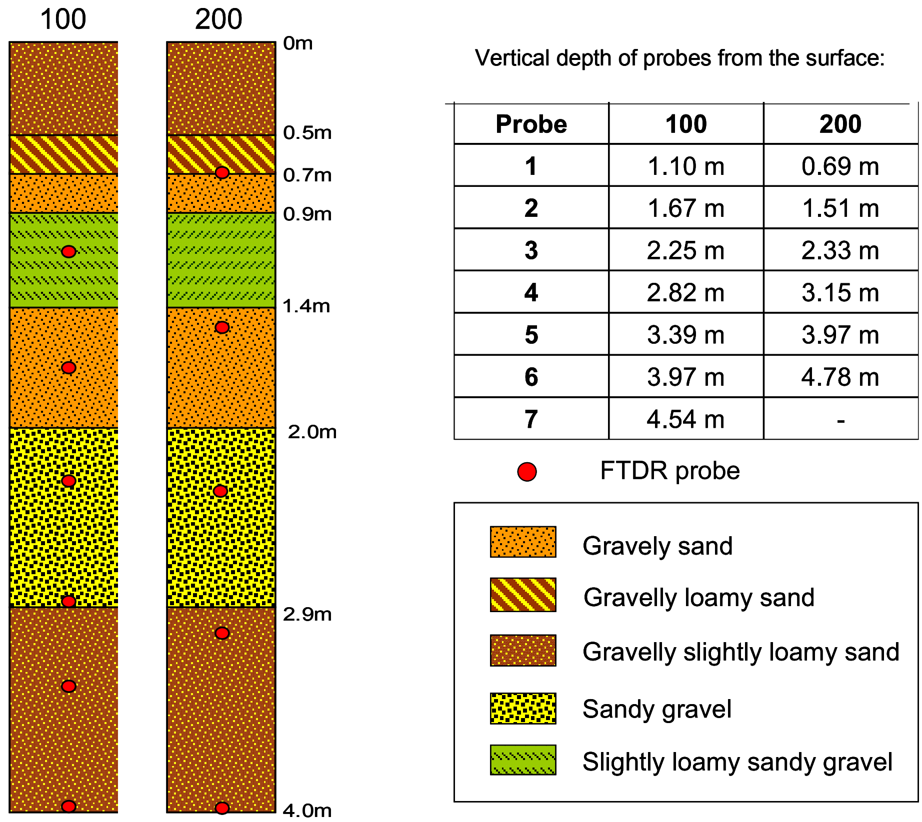

Figure 3.9 *Location of FTDR probes at the Buffelsrivier station (in boreholes 100, 200) in relation to the sedimentary sequence. Comment: estimated accuracy of probes' location is ±20 cm.*

4. Results

The infiltration dynamics and groundwater recharge were investigated during two years between July 2005 and July 2007 at the three monitoring stations. This chapter presents an overview of the data collected from each station throughout the study period. Only few representative events from each site will be presented in details, through which the natural processes taking place can be understood. The results are presented according to the monitoring setup, divided into the three hydrological domains participating in the percolation process: (a) the flood hydrograph – the source of the percolating and recharging water, (b) the spatial and temporal variations in water content along the unsaturated alluvium as recorded by the FTDR probes and (c) the water table fluctuations as a result of the recharge and dissipation processes. The results demonstrate well the strong interrelations between the three domains and reveal the main characteristics of the local hydrological systems.

FTDR data analysis

The percolation process was recorded by the FTDR probes located in the unsaturated profile as shown in figure 4.2b. For a better understanding of the results that follow, it is important to mention a few of the analytical guidelines that were followed during data analysis and interpretation: **(a)** Every line in the graph presents the water content measured by an FTDR probe at a certain depth in time **(b)** A rise in the line indicates an increase in water content (i.e. wetting) and thus the arrival of a wetting front to the depth at which the probe is located at. Accordingly, a drop in the line represents decrease in water content (i.e. drainage) **(c)** The middle of the probes (30 cm long) was regarded as the reference point for the distance calculations. The response time of the probes was taken as the point at which the probe reached the value of half the total increase in water content **(d)** Although the boreholes are slanted, all lengths and distances are already corrected to vertical distances from the surface unless mentioned else.

4.1 Gobabeb station, Kuiseb River, Namibia

4.1.1 Floods summary

During the study period five flood events of different magnitudes and durations flashed down the Kuiseb River at Gobabeb (Fig. 4.1). The fourth flood was the smallest of the season, flowing for 36 hours with a maximum water stage of 0.3 m. Flood number 5 was the last and largest of the season, lasting for approximately 13 days, reaching a maximum height of 3.2 m above the channel's surface. Appendix 9.1 summarizes all floods' characteristics.

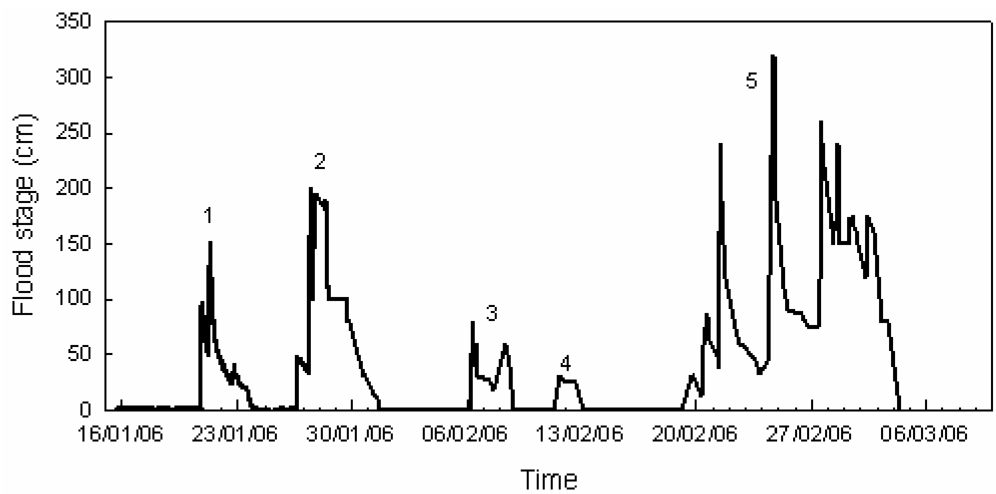

Figure 4.1 *The Kuiseb hydrograph at the Gobabeb station (numbers mark flood events)*

It is important to emphasize that the wet season of 2006 was not a "normal" year but rather displayed an extreme scenario of an exceptionally wet season with a number of floods much above the annual average. The data collected during this year gave the opportunity to investigate the infiltration-recharge processes related to an average season, as reflected from the two first floods, and the cumulative effect of a series of floods during an extreme year.

4.1.2 1st flood event

The first flood lasted for 76 hours and reached a maximum peak of 1.5 m above the channel bed. Figure 4.2 summarizes the patterns of the first event as recorded in the three hydrological domains: the stream flow (4.2a), the infiltration through the subsurface (4.2b) and the groundwater response to the recharge process (4.2c).

4.1.2.1 Infiltration dynamics

Figure 4.2b presents the response of the FTDR probes to the first flood. The upper probe (located at 0.58 m below surface) recorded an increase of 7.5% in water content 1h 45m after the arrival of the flood at the surface. Following the upper probe, the rest of the probes below it exhibit a similar response which takes place by the order of their depth, starting with the 2^{nd} probe (1.37 m) and ending with the response of the deepest probe (4.59 m). This observation suggests a uniform propagation of the wetting front downward through the porous media. The initial water content (θi) distribution along the entire soil column was quite uniform with an average of ~5%, representing the residual soil moisture at the end of the dry season. The average increase in water content along the entire cross section in response to the first percolation event was 6.9%. All probes recorded very similar changes in the water content except for probe 4 (2.66 m) which presents a rise of only 4%. This corresponds well with the significantly higher fraction of gravel present at this depth as appears in the sedimentary sequence (fig. 3.4). However, although the river was flowing bank to bank continuously for approximately 3 days, the water content surprisingly, did not exceed 15% (at none of the probes) and remained unsaturated during the whole time.

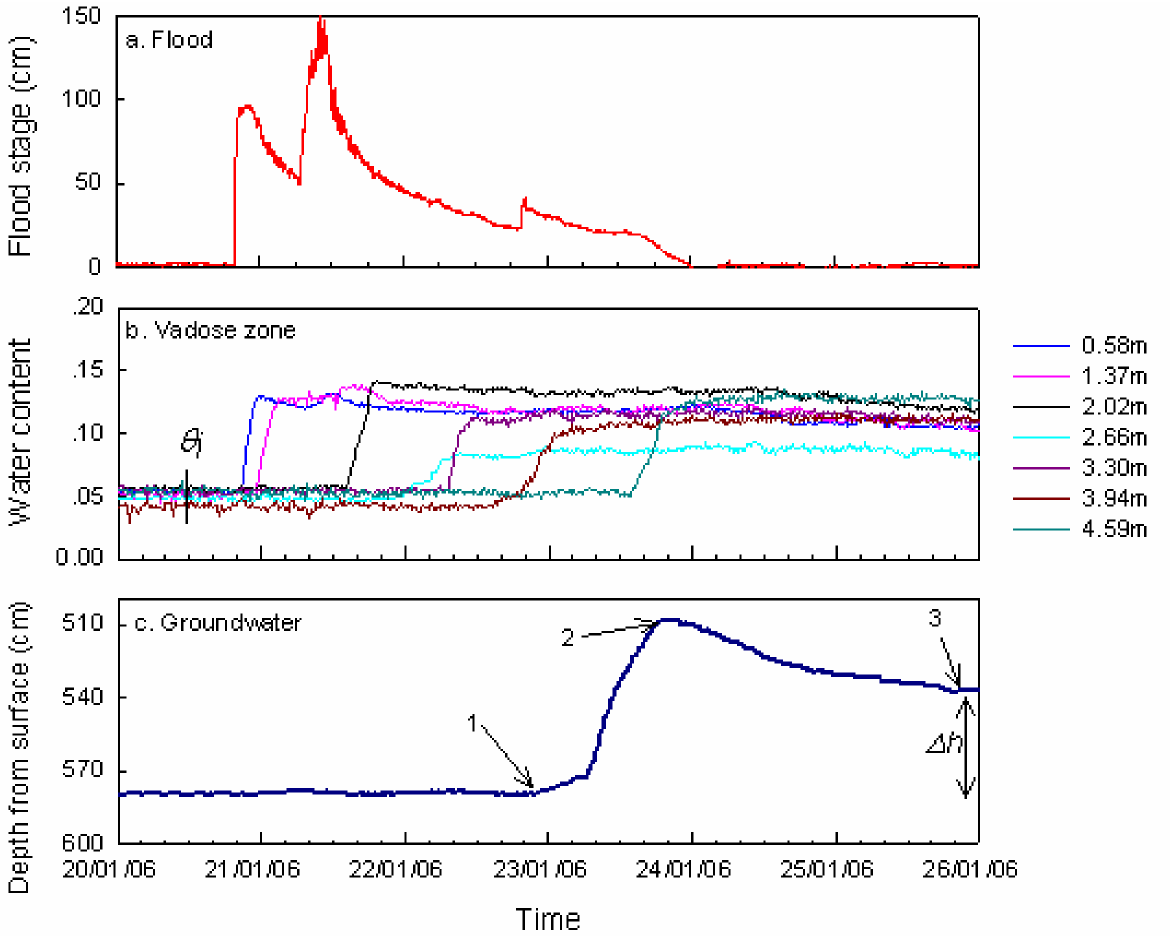

Figure 4.2 *The 1st flood event as recorded at: (a) the stream (b) the vadose zone and (c) the groundwater at Gobabeb (borehole 200).*

4.1.2.2 Groundwater level fluctuations

Groundwater starts to rise during the 23rd of January close to the wetting of probe 7 (1 in fig. 4.2c). Following the recharge event, water table rises from a depth of 5.80 m below surface to 5.08 m below surface, a rise of 72 cm. Since the effective zone through which recharge occurs is the active channel cross section, a mound of groundwater is formed underneath the river (2 in fig. 4.2c). At the second stage, water levels drop gradually down to 5.40 m below surface as a result of groundwater relaxation and a new water level (higher then the initial) is formed (3 in fig. 4.2c). The final increase in groundwater storage at the 1st flood was 40 cm (*Δh* in fig. 4.2c).

4.1.3 Second flood event

The second flood arrived at the monitoring station on the 26/01/2006 at 16:45, 2.5 days after the river ceased flowing from the first flood. During this event the river flowed for 5 days, reaching a maximum peak of 2 m above the stream bed.

4.1.3.1 Infiltration dynamics

The infiltration dynamics of the second flood as revealed from the FTDR probes (fig. 4.3) present more then a single response for every probe, each one with different characteristics, suggesting few wetting phases of different mechanisms. The first phase (2.1 in fig. 4.3) is similar to the response of the first flood showing a sequential wetting of all probes by the order of depth from the surface downwards. The average change in water content along the entire profile was 3.1%. The 2nd phase of the flood (2.2 in fig. 4.3) starts with a small response of the upper probe which is then followed by probe 2 (1.37 m) and probe 3 (2.02 m).

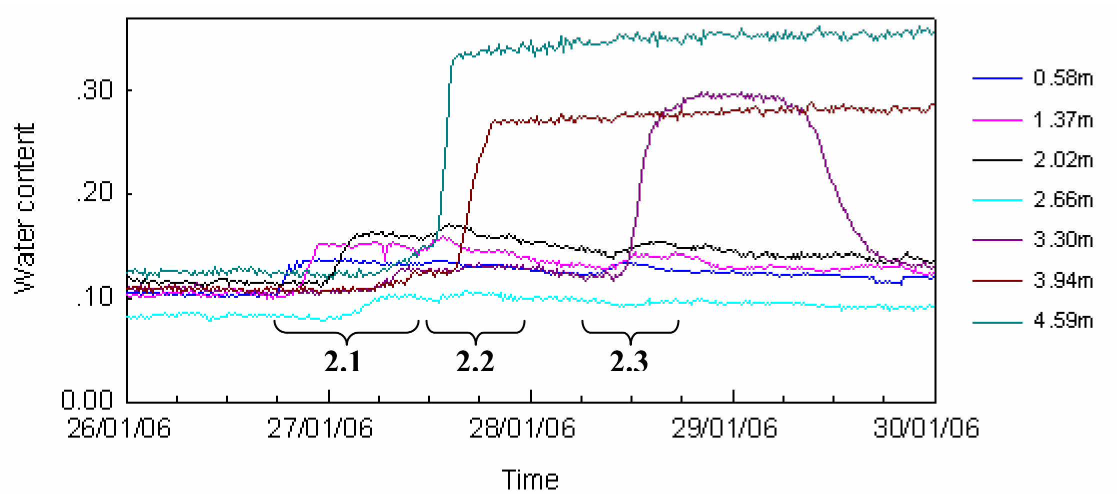

Figure 4.3 *Water content variation in the vadose zone during the second flood show three wetting phases (2.1, 2.2 and 2.3).*

The next probe that shows a wetting is probe 7 (4.59m), which rises sharply to a constant maximum value of 33.5%. Soon after, little wetting is recorded by probes 4 and 5 which are followed by a pronounced response of probe 6, rising to a constant value of 27% (similarly to probe 7). What seems to be a random irregular wetting of the profile can be divided into two wetting mechanisms taking place simultaneously. **The first mechanism** is initiated by the percolating floodwater (like the one already observed in the previous response), producing the propagation of a wetting front from surface downwards. This phase is responsible for the wetting of probes 1 to 5 showing an average increase of ~1% in soil moisture. **The second mechanism** is governed by the rising water table initiating the propagation of a wetting front from the saturated zone upwards into the unsaturated zone. This mechanism is responsible for the wetting of probes 7 and then 6 which reach considerably high values. The high and constant values (no drainage) represent saturation i.e. the probes are below the water table. The data obtained from the FTDR corresponds well to the groundwater levels as measured independently by the levelogger inside the piezometer.

In the 3rd phase of the second flood (2.3 in fig. 4.3), another small wetting is recorded in probes 1 to 4 with an average increase in water content of ~1.0%. During this stage probe 5 (3.30 m) records a prominent increase in water content from 12% to 30%, marking the arrival of the upward wetting front driven by the rising groundwater to its depth. Few hours later probe 5 shows a drainage phase bringing water content values back down to ~13%. The pattern of wetting and drainage as recorded by probe 5 correlates well to the pattern of groundwater fluctuations as recorded by the levelogger, reinforcing the model of an upward wetting mechanism controlled by the groundwater. Similar to the first flood, the significantly lower water content values of probe 4 can be observed. Also, during the whole time that the river flowed and recharge occurred, water content of probes 1 to 4 did not exceed 17% and remained unsaturated. Similar patterns of wetting and drying such as the ones mentioned for the 1st and 2nd floods were observed during the 3rd and 4th flood events.

4.1.4 Fifth flood event

Unfortunately, there is no data from the vadose zone during the first 6 days of the flood. However, when data collection resumed on the 25/02/2006, all probes measured saturation, indicating that the water table was located above probe 1 i.e., above 0.58m below surface. The high location of the water table is also revealed from a photograph that was taken at Gobabeb on the 04/03/2006 (fig. 4.4), showing a truck that was bogged in the loose sand of the riverbed and reached the shallow groundwater, causing local flooding at the surface. During this flood the uppermost probe was damaged and stopped functioning.

Figure 4.4 *A safari truck that got bogged in the riverbed hits the shallow water table, causing a local flooding at the surface (photograph taken by Hartmut Kolb).*

After all probes displayed saturation, the river kept flowing with over 2 m peaks, for almost a week. At this time the storage potential of the local aquifer reached its maximum capacity as the water table rose towards the surface and the entire vadose zone became saturated. As a result, the subsurface could no longer absorb any more water (end of recharge), and the termination point of the flood would be expected to shift downstream. Accordingly, during the fifth flood on the 25/02/2006, the water of the Kuiseb reached all the way to the Atlantic Ocean, a rare event that occurs only once in a few decades.

4.1.5 Vadose zone summary

Figure 4.5 presents water content variations along the vadose zone between December 2005 and May 2007. The initial water content (θi) in the beginning of January 2006 is ~5%, distributed uniformly along the unsaturated profile. The percolation events initiated by the floods at the surface are well reflected. All probes recorded saturation on the 25/02/2006. The saturation degrees shown by the various probes are different and vary between ~23% to ~43%. This can be attributed to variations in grain size distribution and porosity along the alluvium cross section. Most of the subsurface (at least up to 1.37 m below surface) is saturated for a long period of approximately 3 months. Only towards the end of May 2006 probe 2 starts to show a drainage phase, dropping down to field capacity, of less then 10% water content.

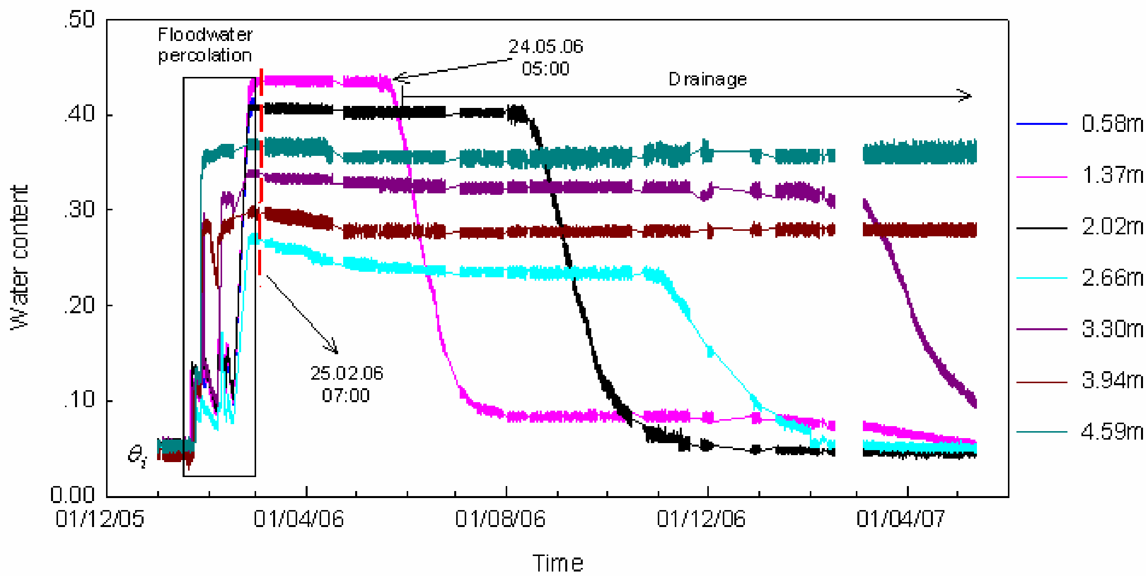

Figure 4.5 *Water content variations at various depths during Dec' 2005 – May 2007.*

4.1.6 Groundwater levels summary

Figure 4.6 presents the groundwater levels from July 2005 to June 2007 as recorded in GOB1 station in the middle of the channel. The floods period can be clearly recognized by the exceptional rise of the water table, between the two dry seasons during which levels drop gradually. The maximum stage of the groundwater was not recorded; however, the total increase in groundwater storage was >5m (!).

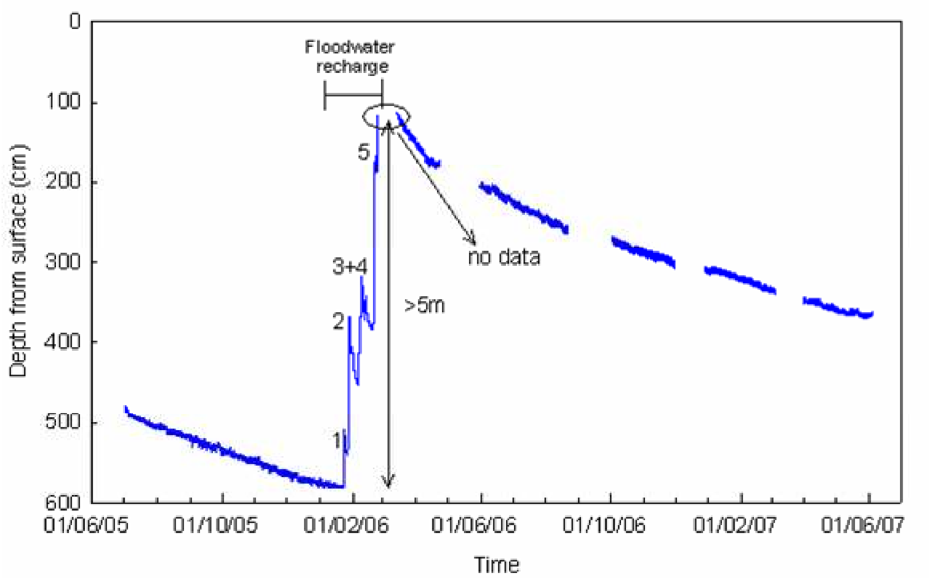

Figure 4.6 *Groundwater levels at Gobabeb between July 2005 and June 2007.*

4.1.7 Groundwater salinity summary

The different salinity properties of the groundwater and the floodwater may be used to differentiate between the two water bodies in the subsurface. Continuous EC measurements of the flood and groundwater give indication to the recharge events. Figure 4.7 presents EC values of the groundwater and floodwater with the water table fluctuations as recorded for the first four floods events. The most prominent feature from these results is the strong inverse relationship between groundwater levels and groundwater EC values. Each rise in the water table resulted in almost an instantaneous decrease in the groundwater EC which later gradually rose with water table relaxation, producing a mirror image of each other. The initial EC value of the groundwater was 0.8 mS/cm. The floods arrived with an average EC value of approximately 0.1 - 0.2 mS/cm (the third and forth floods were not recorded by the EC at the surface probably because it was buried under sand). The groundwater EC after four floods was almost half (0.475 mS/cm) the initial value. Straight after the first flood at the surface, a sharp rise is recorded in the EC values of the groundwater (almost to 1.2 mS/cm). This rise is recorded before any increase in the water table level is noted and therefore, probably does not represent a natural process and thus should be disregarded.

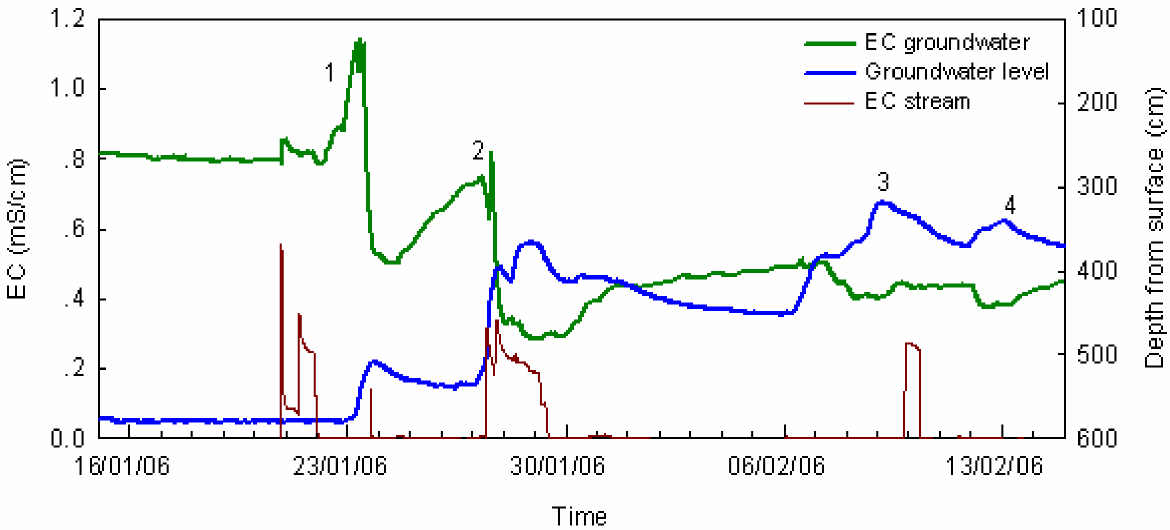

Figure 4.7 *EC values at the stream and groundwater (left y axis) and groundwater levels (right y axis) during the first four floods.*

The changes in groundwater EC during the beginning of the 5th flood were not recorded, however an interesting pattern was observed in the months that followed. After the 5th flood, around mid March 2006, EC of the upper groundwater stabilized on a relatively low constant value (0.3 mS/cm) with no change for a long period, till the end of May. During this time, no flooding occurred and thus groundwater levels drop steadily. Then without any notable reason, EC of the groundwater begin to increase around June 1st, reaching a maximum value of almost 0.8 mS/cm around mid August (fig. 4.8). During the following months EC drops gradually and eventually settles at a constant value of approximately 0.6 mS/cm.

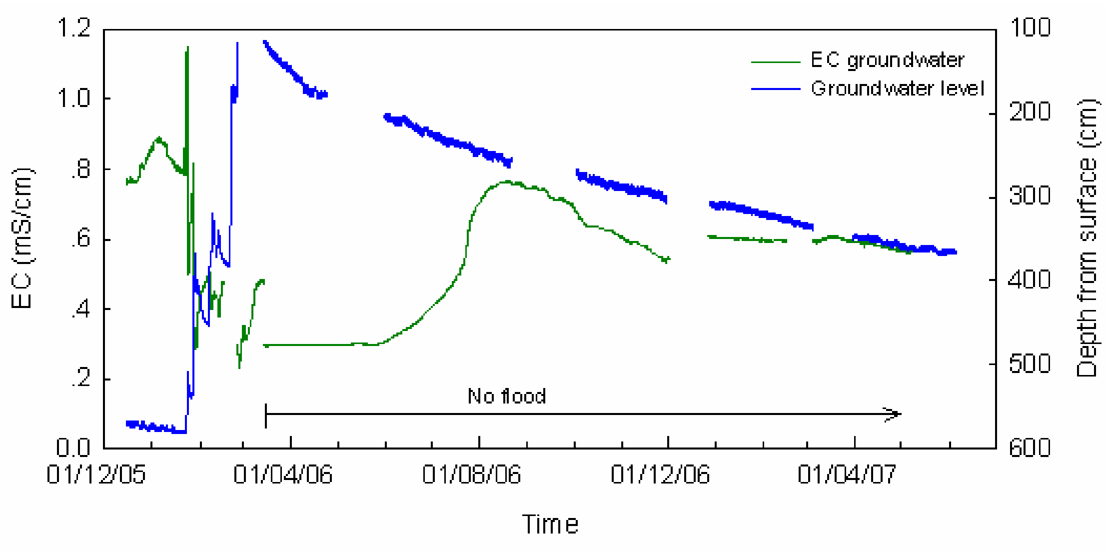

Figure 4.8 *Groundwater EC and levels at the Gobabeb monitoring station between December 2005 and June 2007.*

The rise in EC values can be the result of one or combination of the following: (a) evapotranspiration might be significant because the water table is relatively close to the surface (b) diffuse mixing process of the fresh recharged water at the upper layer of the groundwater with the entire aquifer body (c) salts contribution from subsurface brackish springs located at the northern boundary of the Kuiseb aquifer. A representative of those springs can be found at the surface few kilometers downstream of Gobabeb by Soutrivier where chloride concentrations reach up to ~5000 mg/l and sulfate concentrations reach ~4400 mg/l (Heidbüchel, 2007). Although the discharge rate of the springs is negligible in means of water quantities, theses springs might have a major effect on the salinity of the aquifer. The timing of the recorded rise in EC values might be related to: (a) rise in the discharge rate of the springs following the drop in the pressure induced on their outlets due to decrease in groundwater levels (b) arrival of a subsurface plume of high salinity propagating downstream at the saturated zone. This plume might be related to discharge of brackish springs upstream of the station. The pattern of EC rise followed by a drop in values supports the concept of a plume.

4.2 Buffelsrivier station, Lower Buffels River, South Africa

4.2.1 Floods number 1, 2 and 3

Figure 4.9 summarizes all flood events in the station during the 2 years of monitoring as recorded at the surface (4.9a), the vadose zone (4.9b) and the groundwater (4.9c). Seven flood events passed through the monitoring station at the lower Buffels River during the research period (appendix 9.2). At the first three events (17/10/05, 29/10/05, and 22/04/06) the river flowed for very short durations (10 to 30 hours) with relatively low water peak stages (14 – 45 cm). These flood events had a very limited signature in time and in space in the subsurface, causing some increase in vadose zone moisture content which soon after dropped down close to initial values (1-3 in fig. 4.9b). During all floods most of the vadose zone never exceeded ~15% water content and remained unsaturated.

The response of the upper probe in all 3 events was almost instantaneous (within 15-25 minutes) relative to the arrival of the first flood wave at the surface. Soon after, a sequential response by the order of depth of the FTDR probes was observed, suggesting a generally uniform propagation of a wetting front downwards into the subsurface. However, it was also observed that water table started to rise before the wetting front reached the lower probes, in all three events. This could be attributed to preferential flow pathways that bypass the slower propagation of the diffused wetting front. Groundwater in all events responded with sharp rises (between 30 and 130 cm) which immediately dropped back down to about initial levels. Final increase in groundwater storage in these events was negligible (1-3 in fig. 4.9c).

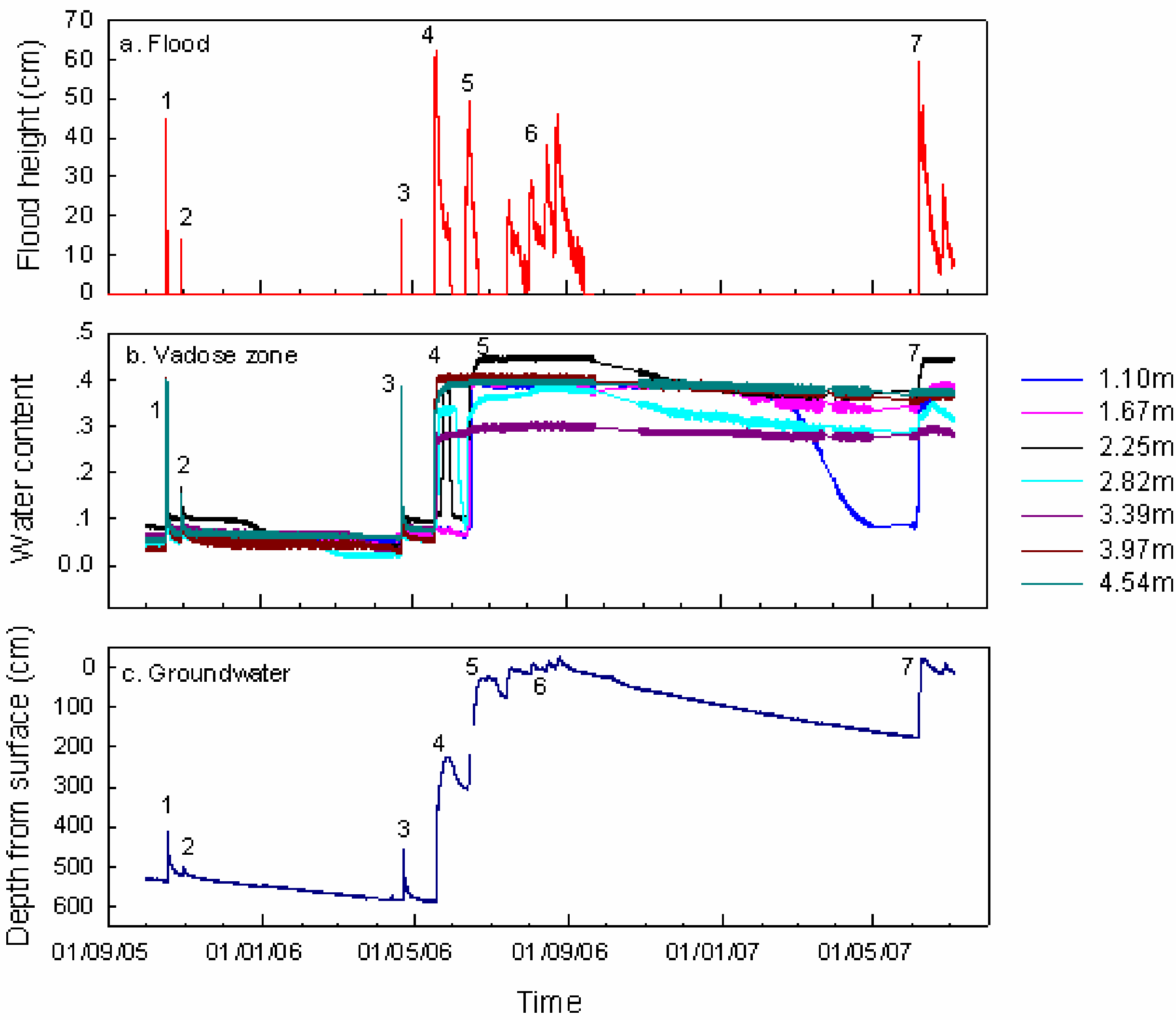

Figure 4.9 *(a) flood stage (b) vadose zone water content (c) groundwater level fluctuations as measured between September 2005 and August 2007 at the Buffelsrivier station.*

4.2.2 Groundwater EC response to the 1st and 2nd floods

In the first flood (1 in fig. 4.10), approximately 3 hours after the arrival of the flood at the surface with an average EC of ~0.2 mS/cm, water table rises abruptly followed by a dramatic drop in EC values of the groundwater (from ~1.2 to ~0.2 mS/cm). Soon after groundwater levels start to drop and return almost to initial levels. As a result of the water table relaxation and salts diffusion, EC values of the groundwater gradually increase, reaching 0.4 mS/cm just before the arrival of the second flood. The floodwater EC of the second event (2 in fig. 4.10) is slightly higher then that of the groundwater and reach a peak value of 0.6 mS/cm. Thus, in this case when recharge begins groundwater respond with a small increase in EC from ~0.4 mS/cm to ~ 0.6 mS/cm.

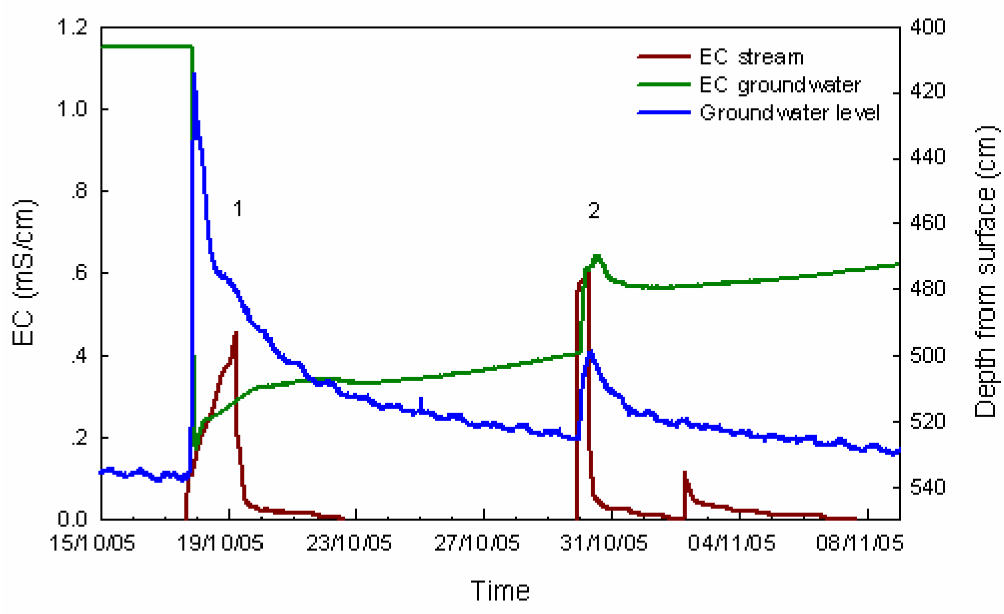

Figure 4.10 *EC measurements of the floodwater and the groundwater (left y axis) with groundwater levels (right y axis).*

Few hours later, water table drops sharply to approximately initial levels and groundwater EC continues to rise gradually at a similar rate to the one before the second flood. Eventually groundwater EC stabilizes at a value of almost 1.2 mS/cm (the initial value) at the beginning of January 2007.

4.2.3 The forth flood event

The infiltration dynamics recorded in this flood event are complex and can be divided into a few stages. At the first stage, a sequential response of all FTDR probes was recorded reflecting the downward propagation of a wetting front from the surface down to the water table (1 in fig. 4.11B). The beginning of water table rise before the wetting front reached its depth indicates that preferential flow takes places as well (a in fig. 4.11B). Once the wetting front reached the water table, the rising rate of the groundwater increases significantly (b in fig. 4.11B). At the second stage, probes 7, 6 and later 5 are wetted from below by the rising groundwater and record saturation values (2 in fig. 4.11B). Approximately 24 hours after the first infiltration event started, another flood wave initiates a second wetting front which advances from the surface downward, wetting probes 1 to 4 again one after the other (3 in fig. 4.11B). On the morning of May 20th, water table drop from 3.32 to 3.54 m below surface is also reflected by probe 5 (3.39m) which shows a sharp decrease in water content (4 in fig. 4.11B). This short drainage phase is soon interrupted by an increase in groundwater levels rising from 3.54 m to 2.24 m below surface. Accordingly, probes 5 (3.39 m), 4 (2.82 m) and 3 (2.25 m) record abrupt wetting and reach saturation (5 in fig. 4.11A). In the last stage, with the termination of flow at the surface, probes 3 and 4 follow the dropping water table and exhibit steep drainage phases almost back to initial water content values (6 in fig. 4.11A).

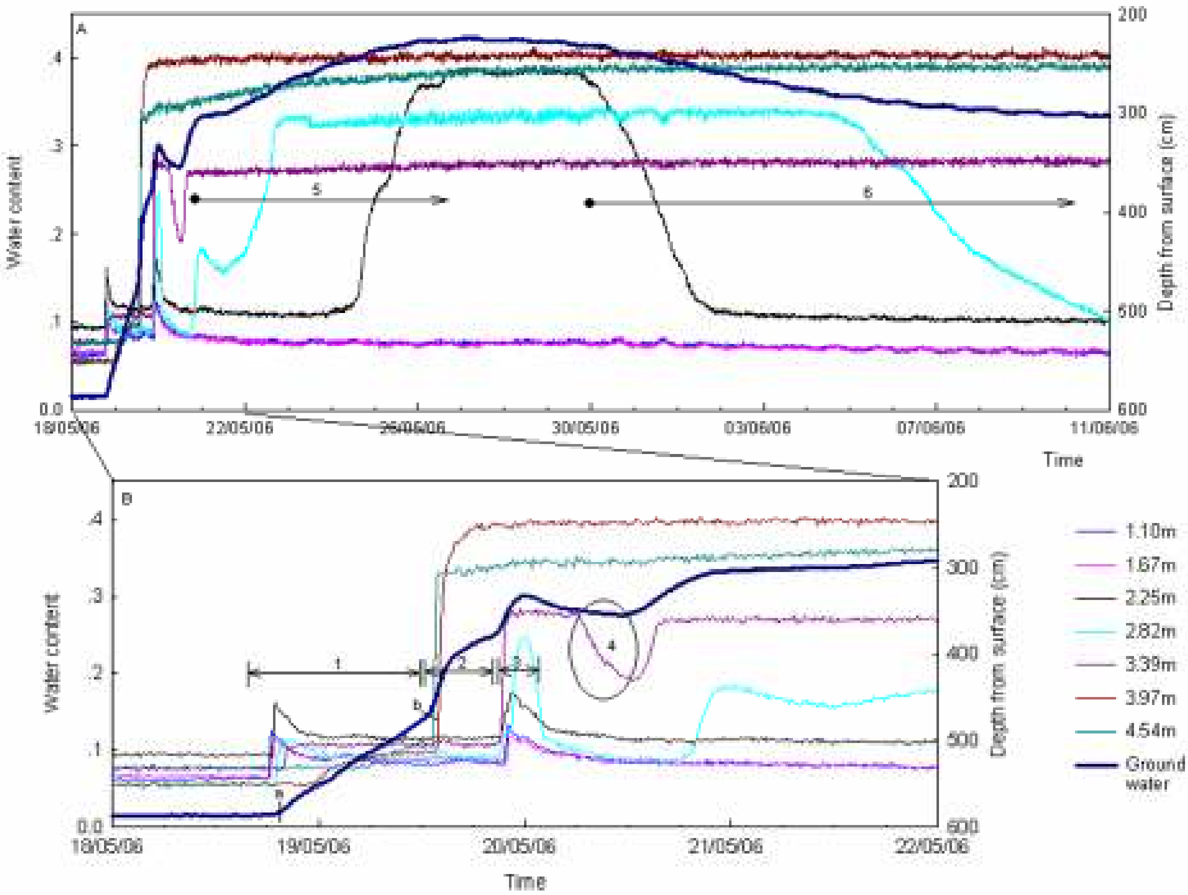

Figure 4.11 *(A) Water content variations in the unsaturated zone and groundwater levels during and after the 4th flood event (B) enlargement of the first 4 days.*

4.2.4 The 5th flood event

The prominent process that took place at the 5th flood is the saturation of the vadose profile from below by the rising groundwater. Figure 4.12 presents the almost instantaneous increase in water content from about field capacity to saturation, taking place in probe 4 at first and then in probes 3, 2 and 1. Water table location as recorded by the levelogger in the piezometer during this event corresponded exactly to the time of saturation of the different probes as recorded independently by the FDTR probes. During the whole time probes 5, 6, and 7 measured constant saturation values.

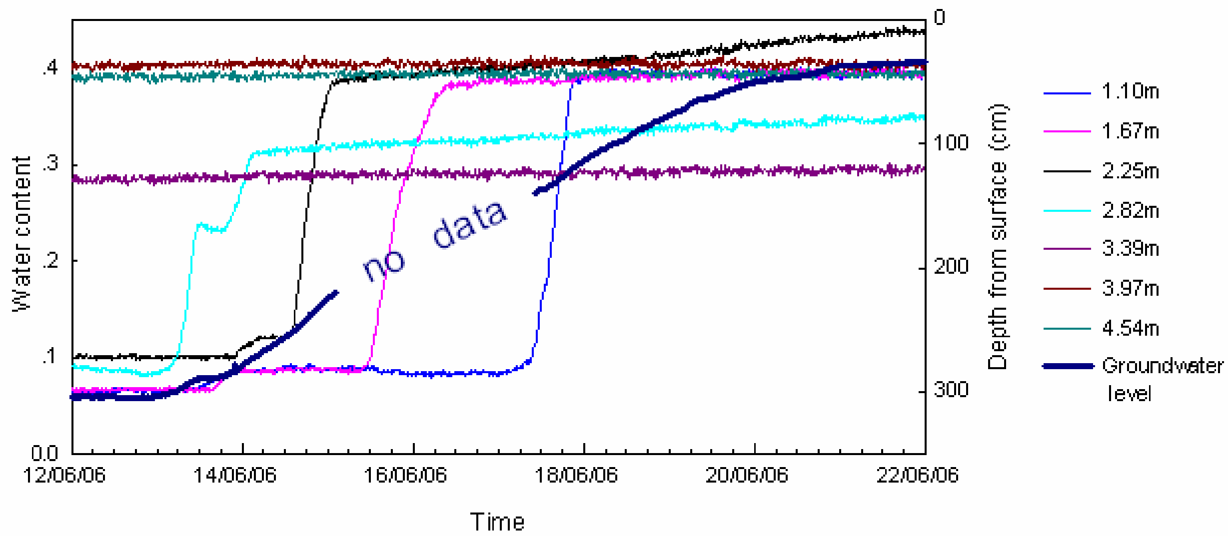

Figure 4.12 *Water content variations at various depths and groundwater levels as recorded during the 5th flood event.*

4.2.5 The 6th flood event

The 6th flood arrived at the monitoring station on the 14th of July and lasted for approximately 2 months with a maximum water stage of 0.45 m above surface. At the onset of the flood all probes measured saturation values while the water table was only 0.75 m below surface. Within three days of the flood on the 17th of July, groundwater rose and reached ground surface (1 in fig. 4.13). At this stage, the storage capacity of the aquifer reached its maximum limit and no more infiltration could take place. This might explain the extremely long duration of flow at the surface.

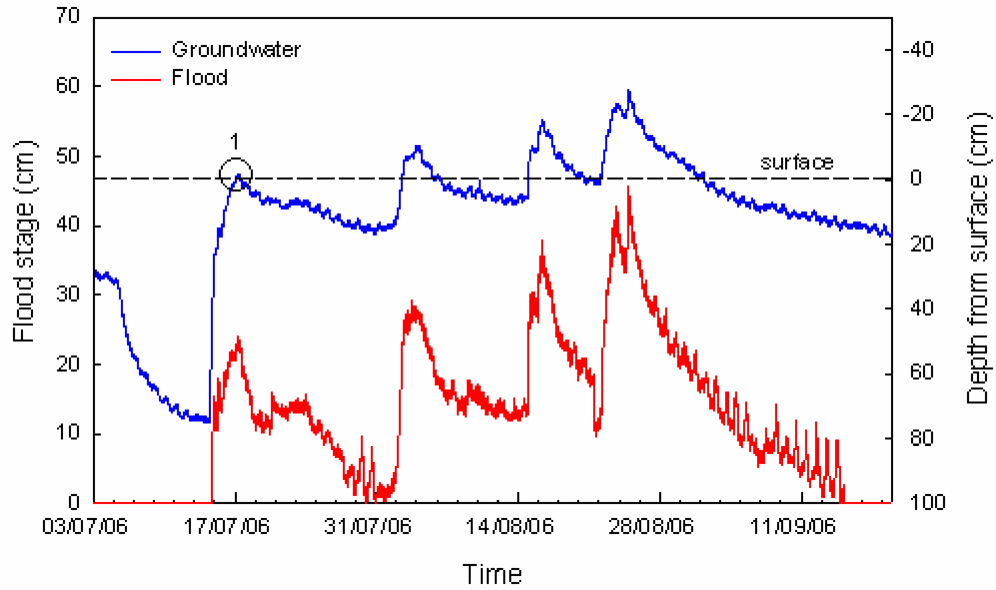

Figure 4.13 *Flood stage and groundwater levels during the 6th flood event.*

4.2.6 Groundwater levels summary

Every flood event that passed at the Buffelsrivier station was followed immediately by a rise in groundwater levels (fig. 4.14). The total increase in groundwater storage for the entire season at the site was ~5.5 m. In times of no flow in the river, water table dropped gradually at a constant rate.

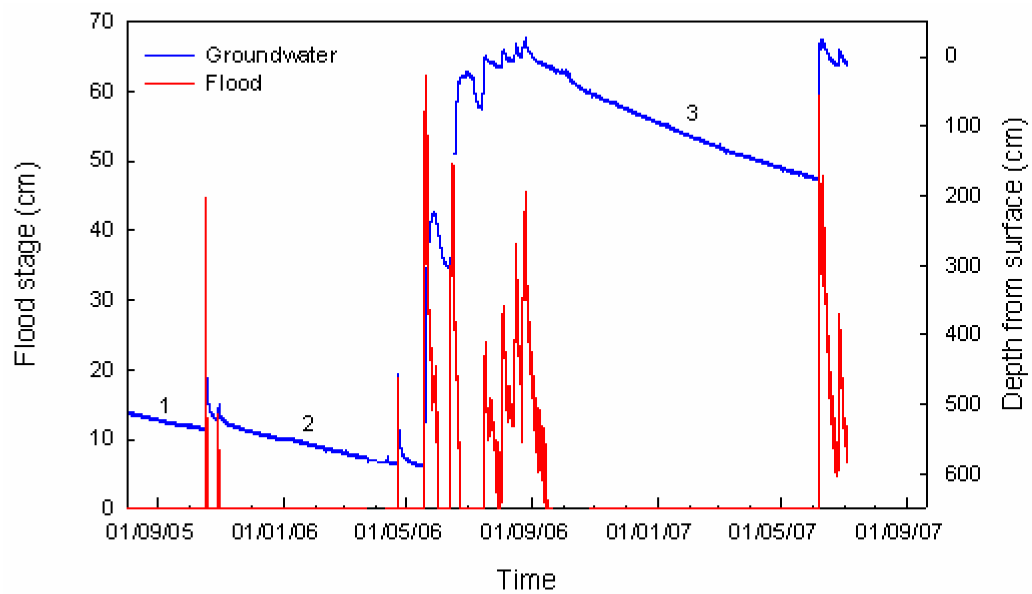

Figure 4.14 *Groundwater levels fluctuations in response to the flood events.*

The rate of level drop during deep water table (stages 1 and 2) is ~0.35 cm/d while during shallow water table (stage 3) the decline rate is 0.64 cm/h. This can be attributed to the shallow depth of the groundwater, being more available for evapotranspiration.

4.2.7 Groundwater salinity summary

Groundwater EC drops dramatically in response to the recharge events of floods 1-4 and 7 (1-4, 7 in fig. 4.15). However, within few hours to few days after each event, groundwater EC starts to increase gradually towards the initial value. Although the average EC value of flood no. 5 is less than 0.6 mS/cm, this event does not decrease groundwater EC significantly (as the first 4 floods). This might be related to the fact that the water table in this flood rises from 3 m below surface to ~0.3 m below surface. This zone is affected by evapotranspiration and might contain residual salt deposits. The dissolution of these salts in the rising groundwater might buffer the recharge effect of the fresh floodwater. The EC value of the 6th flood is much higher between 0.6 – 2 mS/cm and results in an increase in the groundwater EC. An unusual rise of groundwater EC was recorded during March-April 2007 to extremely high values of ~6 mS/cm.

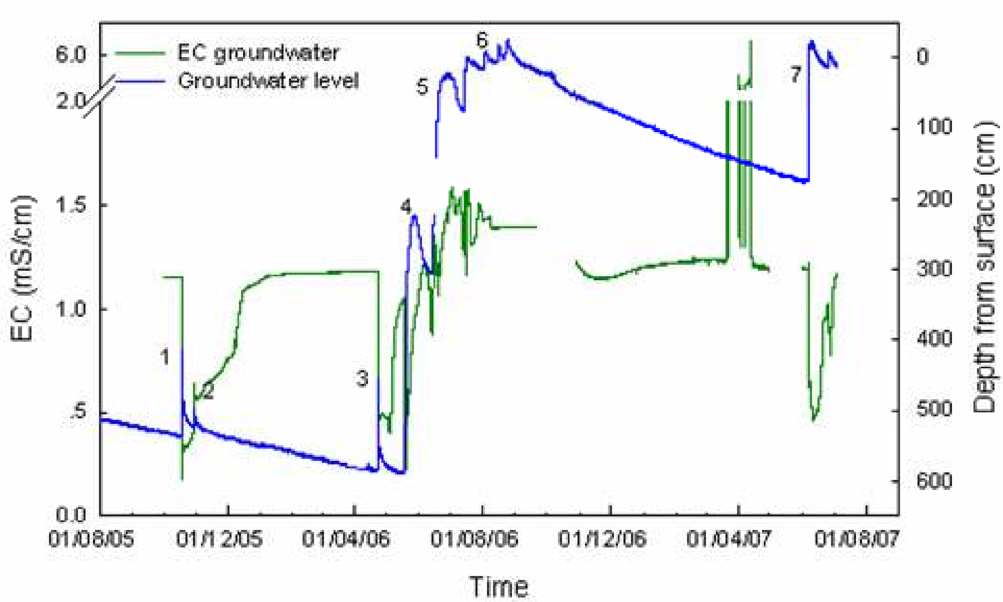

Figure 4.15 *Groundwater EC and groundwater levels (numbers indicate flood events).*

During this time no surface flow was recorded and groundwater exhibit gradual constant levels drop. A possible interpretation to this event is discussed in section 5.5.

4.3 Rooifontein station, Upper Buffels River, South Africa

4.3.1 Floods summary

Seven flood events passed through the Rooifontein station between July 2005 and July 2007 (fig. 4.16a). The floods varied in duration but were all similar in their maximum stage ranging from 20 to 50 cm above the river bed. The duration of the floods varied from ~40 to ~120 hours except for the 5th flood in which the river flowed continuously for approximately 2 months. The stage of the 2nd flood was not recorded probably because the flow did not take place across the entire width of the channel. However, the arrival time and salinity of the flood were recorded by the EC probe and the infiltration event that followed was recorded by the FTDR probes at the vadose zone. Appendix 9.3 summarizes the characteristics of all floods.

4.3.2 Infiltration dynamics

The Rooifontein site exhibits two prominent features: (a) very thin unsaturated thickness of ~3 m and (b) well sorted gravel deposits forming the alluvial bed at the subsurface. These features result in very fast processes of percolation and water table rise. Figure 4.16b shows the response of the FTDR probes to the percolation events. In all events a downward propagation of a wetting front from the surface was recorded by the upper probes while at the same time the lower probes were wetted from below by the rising water table. The response of the groundwater, before the arrival of the wetting front to the water table indicates clearly a recharge mechanism which is not related to the diffused infiltration observed by the FTDR probes. This mechanism is attributed to preferential flow pathways. The local features mentioned above together with the dominance of preferential flows, make the infiltration process almost entirely obscure at this site.

The 1st flood arrived at the station on the 18/10/2005 at 02:00. 1.5 hours later probes 1 and 2 respond with a small wetting from ~6% to ~9%. Soon after, probe 4 rises abruptly to saturation values (~40%). This is followed by a sequential response of probes 3, 2 and 1 (all rise to saturation values) as the groundwater rise up almost to the surface. Most of the vadose profile stays saturated for the next 5 days before probe 1 starts to drain.

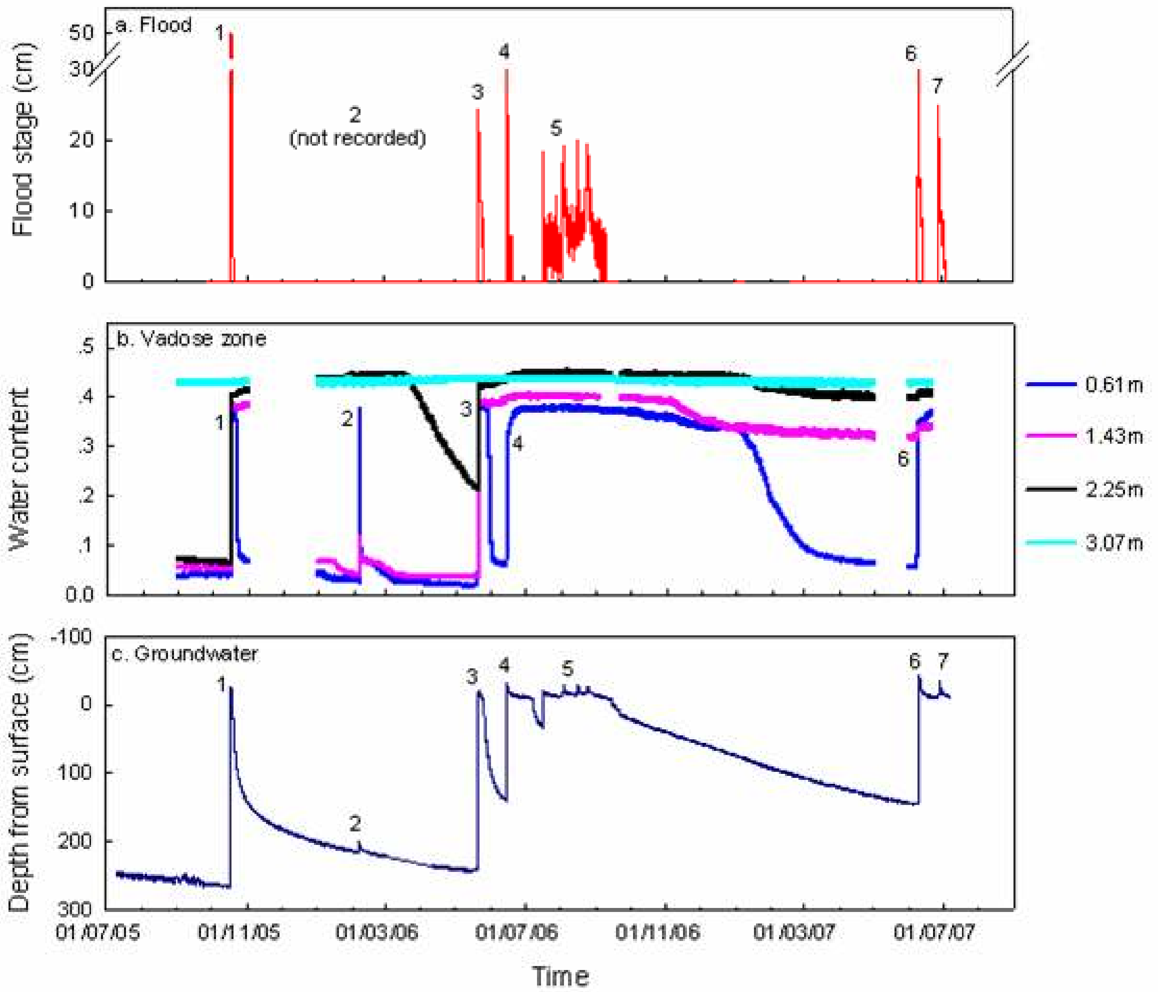

Figure 4.16 *(a) flood hydrograph, (b) water content variations in the vadose zone and (c) groundwater levels at the Rooifontein station, September 2005 to July 2007.*

The 5th flood event arrived at the station on the 16/07/2006 (fig. 4.17). At this time the water table was only 25 cm below surface and accordingly, all probes still measured saturation values. Within 1 hour from the beginning of the flood, groundwater rose to the surface and the storage capacity of the Rooifontein aquifer reached its maximum limit. This is directly related to the long duration of this flood (~2 months) although it was of relatively low magnitude.

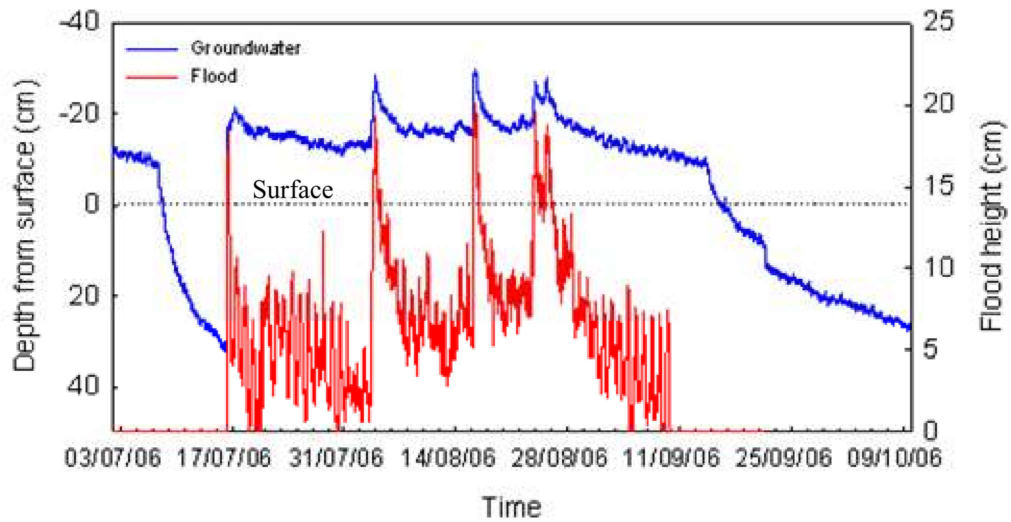

Figure 4.17 *Groundwater and flood levels during the 5th flood, Rooifontein station*

4.3.3 Groundwater levels summary

Figure 4.18 presents groundwater levels at the Rooifontein site between July 2005 and July 2007. Increase in groundwater levels (recharge) highly correlates to the times of flood events at the surface. In times of no flows in the river no notable recharge takes place. The total increase in groundwater storage was approximately 2.5 m over the entire season. The rate of water table drop after the fifth flood is considerably higher than the rate of drop at the beginning of the season, before the first flood. This is probably due to the shallow location of the groundwater (<1m below surface), making it more available for evapotranspiration. In every flood (except no. 2) the water table rises quickly to the surface during the first few hours. This has important consequences in terms of storage potential of the local aquifer as no recharge can take place from the point the water table reaches the surface.

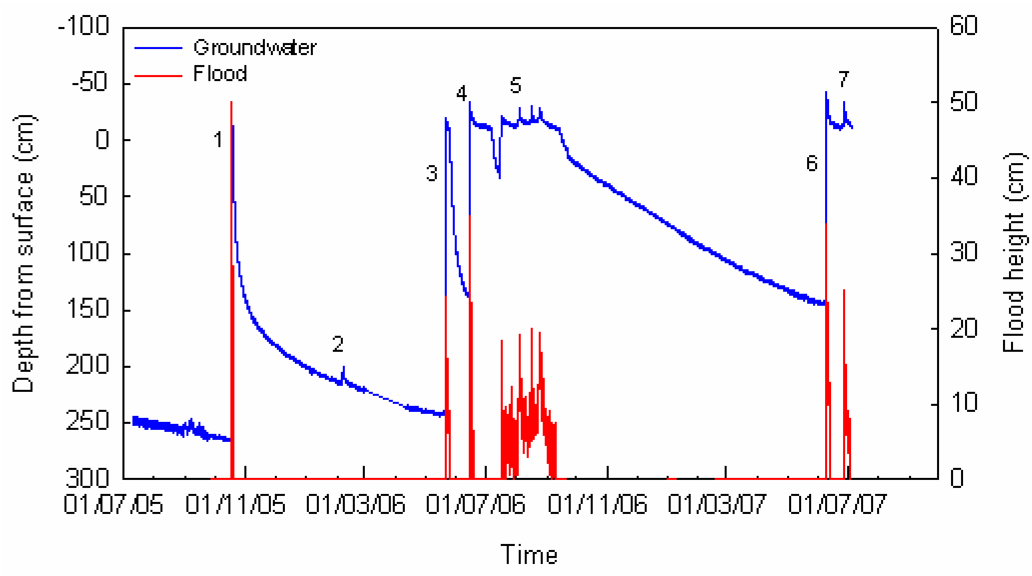

Figure 4.18 *Groundwater levels and flood height during July 2005 – July 2007*

4.3.4 Groundwater salinity summary

Groundwater EC variations at the Rooifontein site (fig. 4.19) in relation to the flood events are complex and present few unusual patterns which are discussed more throughly in section 5.5. The first two flood events had very small to no immediate impact on groundwater EC. EC values of the groundwater rise after these floods, reaching a maximum value of over 2 mS/cm at the end of April 2006. This stage is probably not related directly to floodwater percolation as it occurs many days after the floods ended. The 3rd and 4th floods are followed by a dramatic increase in groundwater storage, which results a sharp decrease in EC values of the groundwater. At the 5th flood event a delayed small rise of 0.1 mS/cm in groundwater EC was recorded, which soon after dropped back to initial values. This might be due to the high stage of the groundwater which are located very close to the surface. The recharge potential of the aquifer reached its maximum capacity, thus, very limited amount of water could be recharged into the aquifer. In addition, the loaction of the EC probe deep in the piezometer might cause the delayed response of small magnitude. At the 7th event, groundwater EC starts rising approximately a week before the arrival of the flood. This is a gradual rise from ~0.8 to ~0.9 mS/cm. With the flood arrival and rise of the water table, EC values rise abruptly to ~1.09 mS/cm.

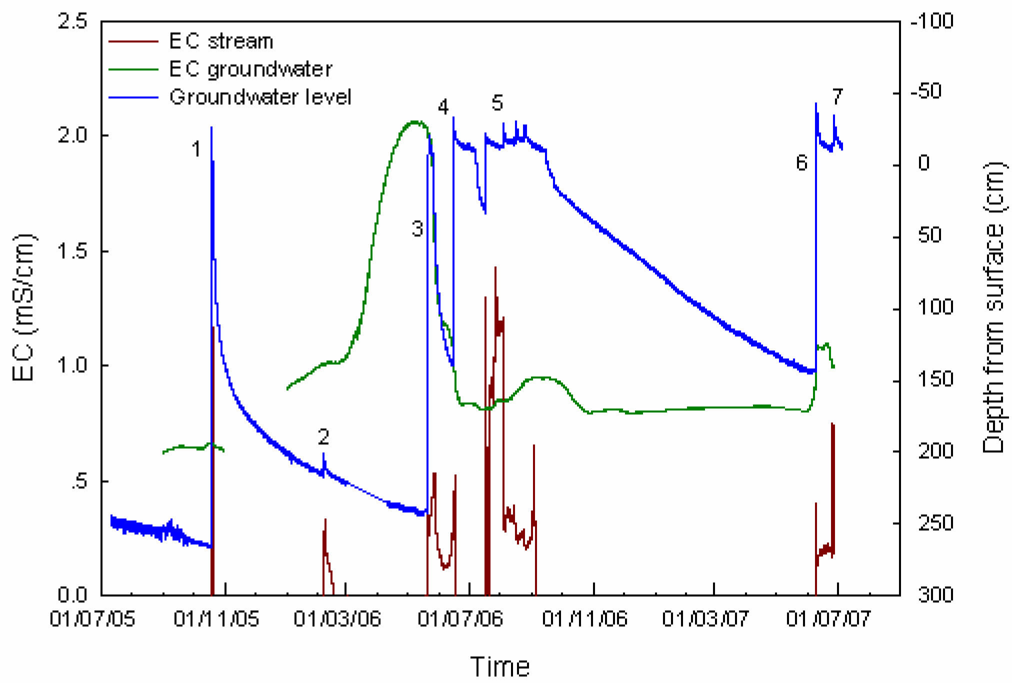

Figure 4.19 *Groundwater EC, groundwater levels and floodwater EC between July 2005 and July 2007 at the Rooifontein station.*

4.4 The conceptual model of the infiltration-recharge process

The recharge process (with no preferential flow) can be divided into three main stages: (a) Following the arrival of a flood at the surface, a wetting front propagates from the surface downwards through the vadose zone. The propagation of the wetting front is recorded by the FTDR probes in the vadose profile. Increase in the water content measured by a probe (fig. 4.20b) indicates the arrival time of the front to the depth at which the probe is located at. The change in water content ($\Delta\theta$) reflects the difference between the water content ahead of the wetting front (θi) and the water content behind the wetting front (θf) (fig. 4.20a). (b) As the wetting front reaches the water table recharge starts to take place (fig. 4.21a). This stage is reflected by the beginning of groundwater level rise as recorded by the levelogger inside the piezometer (1 in fig. 4.21d). The arrival of the rising water table to the depths of the FTDR probes is indicated by a pronounced rise in water content to saturation values (fig. 4.12). As a groundwater mound evolves underneath the active channel, a gradient is formed sideways of the mound producing lateral transverse fluxes in the saturated zone (fig. 4.21b). (c) The lateral fluxes increase with the building up of the mound. When these fluxes exceed the recharge fluxes, groundwater levels will start to drop (2 in fig. 4.21d). Later, as the flood at the surface ceases, drainage of the vadose zone takes place from the surface downwards and recharge fluxes decrease. Eventually recharge ends and the groundwater mound dissipates in a rate controlled by the groundwater hydraulic gradients, aquifer's hydraulic conductivity and aquifer's dimensions. Finally, the lateral fluxes cease and the water table settles at a final position across the entire aquifer width (h_f) (3 in fig. 4.21d). The height difference between the initial and final groundwater levels is the final increase in groundwater storage (Δh_f in fig. 4.21c and 4.21d).

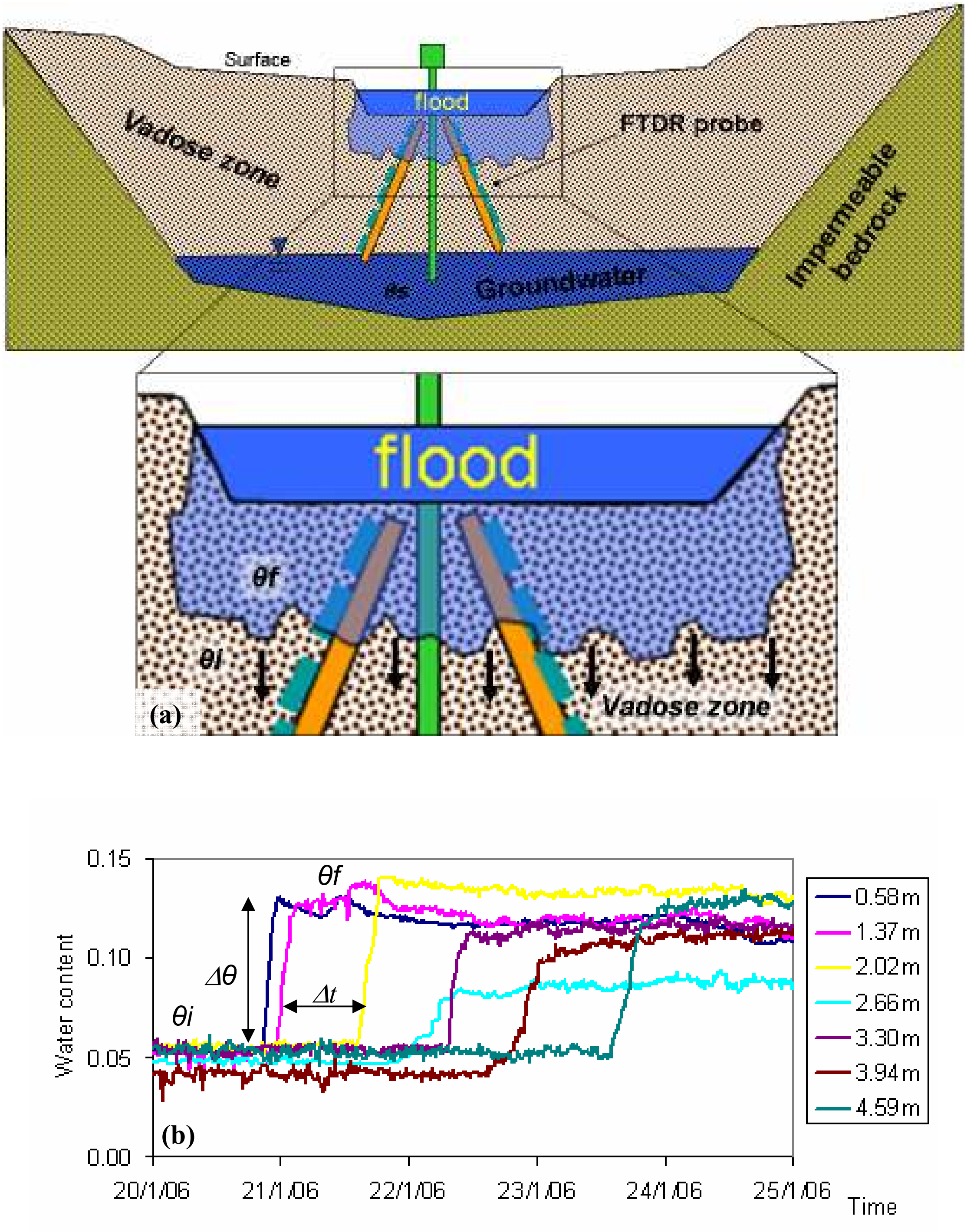

Figure 4.20 *The downward propagation of a wetting front is recorded by the FTDR probes in the vadose zone. (a) The water content in different areas is indicated by θi, θf, and θs (b) Sequential wetting of the FTDR probes during the 1st flood in Gobabeb.*

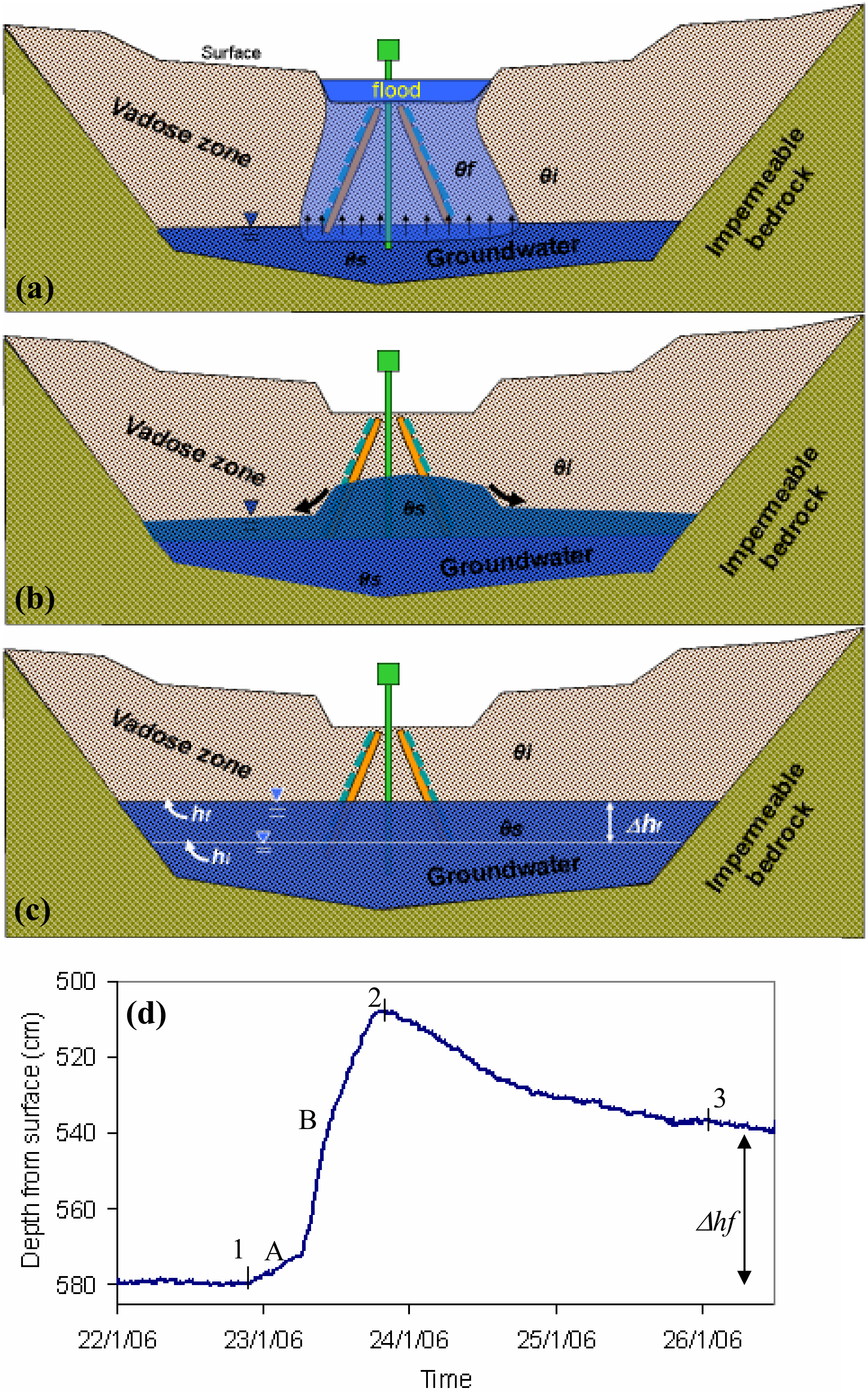

Figure 4.21 *Groundwater response to the recharge event (a) groundwater level starts rising as the wetting front reaches the water table (b) following the recharge event a mound evolves beneath the channel. As a result a gradient is formed sideways, resulting in lateral fluxes in a transverse direction to the channel flow direction (c) Eventually the water table is leveled uniformly across the entire aquifer (h_f). Final increase in groundwater levels is denoted by Δh_f (d) groundwater response (a to c) as recorded by the levelogger during the first flood at the Gobabeb station.*

4.5 Flow velocities and fluxes

Flow velocities and fluxes in the unsaturated zone are key factors for understanding infiltration dynamics and estimation of groundwater recharge. Section 4.5.1 presents the analytical procedure that was developed in this study for calculating these values. Every calculation method is followed by an example based on the 1st flood at the Gobabeb station. Section 4.5.2 presents the final results from the Gobabeb station for all floods. Sections 4.5.3 and 4.5.4 present the results from the Buffelsrivier and Rooifontein stations, respectively.

4.5.1 Analytical method

4.5.1.1 Wetting front propagation velocity (WFPV)

The propagation velocity of the wetting front can be calculated directly from the wetting sequence of the FTDR probs. The velocity is retrieved by dividing the vertical distance between two adjacent probes by the time gap between their wettings. The calculation was made for all sections between every two adjacent probes, from the surface down to the deepest probe, for all infiltration events. Table 6 presents the WFPV as calculated for each section for the 1st event at Gobabeb.

Example: in the first flood at Gobabeb, probe 3 (2.02 m) responded 16.25 hours after probe 2 (1.37 m) (fig. 4.20b). The vertical distance between these probes is 65 cm. The WFPV for this section is: $V = \Delta X/\Delta t = 65cm/16.25h = 4$ cm/h.

4.5.1.2 Percolation fluxes

Flux calculations were made using three independent methods based on (a) wetting front propagation rate (b) water table rising rate and (c) increase in aquifer storage. These methods are described below in details including calculation examples from the 1st flood event in the Kuiseb River.

(a) Wetting front propagation rate (WFPR)

This method applies to the downward propagation of a wetting front, resulting in a sequential wetting of the probes by their order of depth. Water flux calculations for the sections between every two adjacent probes were done based on the following equation:

(Fetter, 1988)
$$q = n \cdot v \tag{4.1}$$

where q is the flux (cm/h), n is the porosity (unit less) and v is the wetting front propagation velocity (cm/h). In our case since the flow of water takes place only in part of the pores volume the modified equation for unsaturated conditions will be:

$$q = \Delta\theta \cdot v \tag{4.2}$$

where $\Delta\theta$ is the change in water content (unit less) (fig. 4.20b).

Example: in the 1st flood at Gobabeb, the change in water content of the 3rd probe was 8% (fig. 4.20b). The downward flux therefore would be: q = 0.08 x 4 cm/h = 0.32 cm/h. Table 6 presents the flux values for each depth along the entire cross section for the 1st flood event at Gobabeb.

***Table 6**. WFPV and fluxes for each section as calculated for the 1st flood at Gobabeb*

Depth (m)	$\Delta\theta$ (%)	WVPV (cm/h)	q (cm/h)
0.58	7.5	33.1	2.5
1.37	8	28.7	2.3
2.02	8	4.0	0.3
2.66	4	5.4	0.2
3.30	6	16.0	1.0
3.94	7	4.7	0.3
4.59	7.5	3.3	0.3
Average	**6.9**	**13.6**	**1.0**

(b) Water table rising rate (WTRR)

The rise of water table that followed each flood event is a direct indication to active recharge. Accordingly, the local downward recharge flux can be calculated from the water table rising rate when the following conditions may be assumed: (1) the active stream channel is relatively flat and much wider comparable to the alluvial cross section of the unsaturated profile (2) the flood infiltrates across the entire width of the channel (3) the measuring point of groundwater levels (piezometer) is located in the middle of the channel away from the boundaries of the groundwater mound. These features allow assuming that during the first stages of the recharge process the water table rising rate is a direct consequence of the percolation flux. This is because in this stage and location the rising rate is not significantly affected by the lateral flows.

Groundwater response to the recharge event usually includes several stages represented by the magnitude (recharge rate) and direction (water table rise/drop) of the slope of the graph presenting groundwater levels in time (fig. 4.21d). Each stage (slope) is a result of the ratio between the downward recharge flux and the lateral flux produced by the developing groundwater mound. The steepest slope section in the graph (B in fig. 4.21d) will represent the highest recharge flux, while the average of all positive slope sections (rising water table) will represent the average flux for the entire event (A+B in fig. 4.21d). These values however, include within them the lateral flow component and thus can be regarded as minimum estimations of the real maximum and average fluxes.
The percolation flux calculated from the upward rising rate of the water table is based on groundwater levels data (as measured by leveloggers installed in observation boreholes) and variation in vadose zone water content (as measured by the FTDR probes). When water table rise, the increase in groundwater storage is equal to the surplus column of water added multiplied by the change in water content. Dividing this

value by the time gap between initial and final water levels will produce the rate of storage increase, which can also be defined as the recharge flux (q):

$$q = \frac{\Delta\theta \cdot \Delta h}{\Delta t} \tag{4.3}$$

where *Δθ* is the change in water content (unit less) and equals the measured saturation value minus the water content just before saturation, *Δh* is the groundwater levels difference between two chosen points of time during water table rise and *Δt* is the time measured for the *Δh* interval.

Example: groundwater response to the 1st flood at Gobabeb is shown in fig. 4.21d. In sections A and B together, groundwater rose by 72 cm during a period 22 hours. The average change in water content (based on the response of the lower probes at the second flood event) was 19.5%. The calculated average flux is: q = (72 x 0.195)/ 22 = **0.64 cm/h**. At section B only, groundwater rose by 64 cm in 13.5 hours. The maximum flux therefore, would be: q = (64 x 0.195)/13.5 = **0.92 cm/h**. According to the graph, most of the water table rise took place under the maximum flux value.

(c) Increase in groundwater storage (IGWS)

The following method requires knowledge of the aquifer width and is based on the assumptions that infiltration occurs across the entire width of the channel. A geomagnetic survey that was conducted near Gobabeb during 2006 found the aquifer width to be approximately 200 m.

Stage 1: Calculating increase in aquifer storage

The total increase in volume of aquifer storage per unit length of the river can be calculated according to the following equation:

$$V_L = \Delta h \cdot \Delta\theta \cdot W_{aq} \tag{4.4}$$

Where V_L is the volume increase per unit length of the river (cm^3/cm), Δh is the final increase in groundwater levels after relaxation (cm), $\Delta\theta$ is the change in water content (unit less) and Waq is the aquifer's width (cm). The change in water content ($\Delta\theta$) equals the change in the sediments water content from initial values (θi) to saturated values (θs). However, the initial water content is not uniform across the whole aquifer's width. Below the active channel, as a result of the percolation event (prior to any water table rise), soil moisture would be considerably higher in comparison the moisture below the terraces and the floodplains outside the active channel where no infiltration occurred (fig. 4.22). The adjusted equation therefore, will be:

$$V_L = (\Delta h \cdot \Delta\theta_{ch} \cdot W_{ch}) + (\Delta h \cdot \Delta\theta_t \cdot (W_{aq} - W_{ch})) \tag{4.5}$$

Where $\Delta\theta ch$ is the water content change below the channel (unit less), $\Delta\theta t$ is the change in water content below the terraces (unit less) and Wch is the channel's width (cm).

Example: in the 1st flood at Gobabeb, final increase in groundwater levels was 40 cm (fig. 4.21d). Channel width is 33 m and aquifer width is ~200 m. Average water content of saturation in the lower probes is 30% (based on the second flood event). Therefore, $\Delta\theta ch$ = 30%-12%=18% and $\Delta\theta t$ = 30%-5%=25%. The total storage increase per unit length would be V_L = (0.4 x 0.18 x 33) + (0.4 x 0.25 x 167) = 19.01 m^3/m.

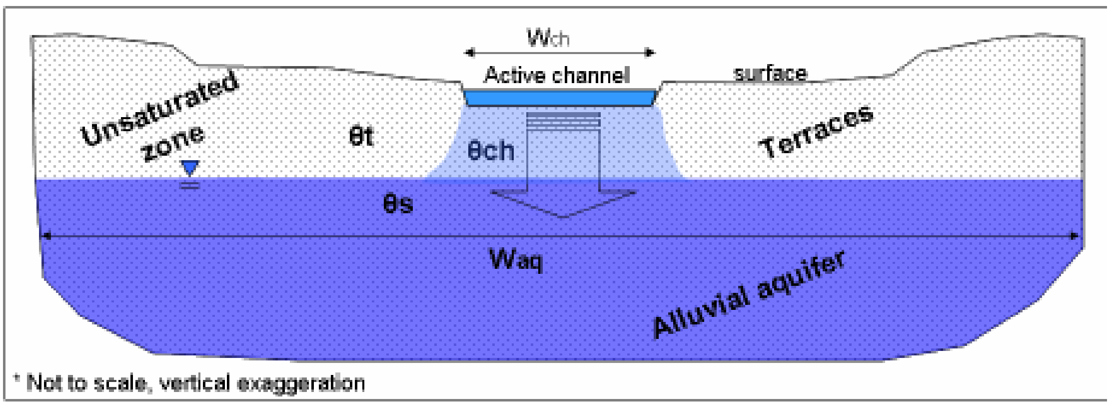

Figure 4.22 *Water content in different parts of the local hydrological system.*

Stage 2: Calculating the infiltration volume through the channel bed

As the effective cross section through which percolation takes place is bounded to the active stream channel, the percolating volume per river length may be calculated as:

$$V_L = q \cdot \Delta t \cdot W_{ch} \qquad (4.6)$$

Where q is the unknown infiltration flux that we want to find (cm/h), Δt is the duration of flood (hours) and Wch is the width of the active channel.

Stage 3: Retrieving the downward flux, q

The volume of water that percolated through the channel bed is practically equivalent to the increase in aquifer storage, thus, the values of V_L in stages 1 and 2 are the same (water losses at this stage are negligible, see section 5.2.1). The downward flux can be retrieved by using V_L from equation 4.6 in equation 4.5:

$$q = \frac{V_L}{\Delta t \cdot W_{ch}} \qquad (4.7)$$

Example: the 1st flood at Gobabeb lasted for 76 hours. The downward flux would be:

q = 19.01 m^3 / (76h x 33m) = 0.0076 m/h = **0.76 cm/h**.

As can be noted, all three methods described above, give very close fluxes between 0.64 cm/h to 1.0 cm/h, calculated independently for the first flood at the Gobabeb station.

4.5.2 Gobabeb station, Kuiseb River, Namibia

Table 7 summarizes the average WFPV and fluxes for the entire vadose profile during all flood events as calculated based on the FTDR probes' responses and groundwater rise. Some of the flood events included more than a single wetting phase as a response to multiple flood peaks. Each phase was regarded separately and the average value per flood is given here. The average WFPV for all the floods vary between 13.6 and 34.8 cm/h with an average velocity of ~22 cm/h for the whole season. No FTDR data is available for the early stages of the last flood. The significant increase in the average WFPV between the first and second floods which were similar in magnitude might be related to the differences in the initial water content values. The average initial water content along the entire profile at the onset of the second flood (arrived 2.5 days after the end of the first flood) was double (~10.5%) the value of the first flood (~5%). The influence of the initial water content on the WFPV is also well expressed from the comparison between the first and third floods. In both events the river flowed for approximately 70 hours (appendix 9.1).

Table 7. Average WFPV and fluxes at the Gobabeb station (borehole 200)

<table>
<tr><th rowspan="3">Flood no.</th><th colspan="2">Average for entire profile</th><th rowspan="3">WFPV (cm/h) FTDR</th><th colspan="4">Flux (cm/h)</th></tr>
<tr><th rowspan="2">θi</th><th rowspan="2">$\Delta\theta$</th><th rowspan="2">WFPR</th><th colspan="2">WTRR</th><th rowspan="2">IGWS</th></tr>
<tr><th>Ave.</th><th>Max.</th></tr>
<tr><td>1</td><td>5</td><td>6.9</td><td>13.6</td><td>1</td><td>0.64</td><td>0.92</td><td>0.94</td></tr>
<tr><td>2</td><td>10.5</td><td>3.1</td><td>34.8</td><td>1</td><td>0.80</td><td>1.40</td><td>0.50</td></tr>
<tr><td>3</td><td>9</td><td>5.7</td><td>16.4</td><td>1.3</td><td>0.27</td><td>0.38</td><td rowspan="2">0.38</td></tr>
<tr><td>4</td><td>10.5</td><td>3.2</td><td>23.0</td><td>0.7</td><td>0.06</td><td>0.10</td></tr>
<tr><td>5</td><td>9.5</td><td>-</td><td>-</td><td>-</td><td>1.35</td><td>2.84</td><td>0.85</td></tr>
<tr><td>Average:</td><td>-</td><td>-</td><td>21.94</td><td>1.00</td><td>0.62</td><td>1.13</td><td>0.67</td></tr>
</table>

The maximum stage of the first flood was 1.5 m compared to only 0.8 m of the third flood. Nevertheless, the average WFPV of the third flood was slightly higher then that of the first one (16.4 cm/h and 13.6 cm/h respectively). The reason for this seems to be the differences in initial water contents (9% and 5% at the 3rd and 1st floods respectively). These preliminary conclusions are strengthened by the results from the forth flood. Although it was the smallest of the season (0.3 m, 36 hours), the calculated WFPV was higher then that of the third flood, attributed again to the high initial water content values (10.5%). Similar patterns as described above are observed in all boreholes at the Gobabeb station (see appendix 10.1).

The fluxes of each flood were calculated separately, according to the three methods mentioned in section 4.5.1.2. All independent methods gave very similar values with an average between 0.62 – 1.13 cm/h for borehole 200 for the entire season. Although the average WFPV increased significantly between the first and second floods (table 7), the fluxes according to the WFPR of both events remained the same (1.0 cm/h). The higher velocity of the second event is balanced by a smaller change in water content compared to the first flood (3.1% in the 2^{nd} flood compared to 6.9% in the 1^{st} flood), resulting the similar fluxes (see equation 4.2). This pattern is noted in all the floods and boreholes. Flood number 4 which was the smallest and shortest, presents slightly lower fluxes comparable to the other floods. This corresponds to observations from other studies, that low water stages might reduce infiltration rates (section 1.2.3.2). At increased stages of the other floods, no correlation to infiltration rates was noted.

Appendix 10.1 summarizes the fluxes as calculated for each flood for boreholes 300 and 400. All boreholes present relatively similar values for all of the events ranging between 0.34 cm/h to 1.28 cm/h. However, the fluxes calculated by the WFPR for borehole 400 are consistently lower (0.47 cm/h) compared to boreholes 200 and 300 (1.0 cm/h and 1.28 cm/h respectively). This can be explained by the horizontal distance of the probes in borehole 400 from the active channel's boundary (evapotranspiration is negligible, see section 5.2.1). The fact that the borehole is drilled on the southern bank heading southward, away from the channel, and assuming the percolation process is primarily vertical, it might be that the probes are located on the boundaries of the downward flow cross section. For example, the horizontal distance of the 4^{th} probe (2.75 m below surface) from the channel's southern boundary is 2.3 m. The extension of the wetting front horizontally away from the channel is a function mainly of the grain size distribution and soil characteristic curve which determine the water retention. In this site the lateral propagation of the wetting is limited to the retention characteristics of well sorted medium sand and is reflected by the fluxes recorded in borehole 400.

4.5.3 Buffelsrivier station, Lower Buffels River, South Africa

Table 8 summarizes the average WFPV and fluxes as calculated for the entire vadose profile for all flood events at the Buffelsrivier site (borehole 100). Here, only two methods of calculation were applied. These are based on the wetting front propagation rate in the unsaturated zone and the rising rate of groundwater levels. The method based on storage increase could not be applied as it requires knowledge of the aquifer's width which is not known precisely for this site. From the fifth flood all FTDR probes in the unsaturated zone were submerged below the water table and showed saturated water content values (fig. 4.12). Accordingly, from this point onwards, no calculations based on water infiltration in the vadose zone were made. Nevertheless, during the first four floods WFPV ranged between 143 to 229.6 cm/h. Fluxes calculated by the WFPR method for the first four floods range from 6.2 to 20.5 cm/h with an average value of 11.74 cm/h. Fluxes for borehole 200 present similar values with an average of 7.11 cm/h (appendix 10.2). As can be seen from the table, fluxes calculated by the WTRR method varied by three orders of magnitudes between events and also differ from the fluxes calculated by the WFPR method. Nevertheless, the average fluxes calculated for the first four floods by the WFPR and by the max. WTRR are very similar (11.7 and 9.2 cm/h, respectively).

The hydrogeological conditions at the Buffels River site are significantly different from those observed at the Kuiseb River. As a result, some of the basic assumptions (mentioned in section 4.5.1.2b.) that were used for the calculations in the Kuiseb should be carefully examined when applied at the Buffels River. In comparison to the aquifer at the Kuiseb River the Buffelsrivier Aquifer is much wider (200 m compared to estimated measure of ~700 m, respectively). The alluvial deposits at the Buffels River are comprised of much coarser material with significantly higher gravel content (Tables 2-5). These two elements might enhance significant lateral fluxes that will develop immediately with groundwater mounding. Accordingly, these fluxes are expected to be more influential in reducing groundwater rising rate than at the Gobabeb site. In addition, the active channel bed at the Buffels River is wider with small scale variations in the surface level. Thus, channel "micro-topography" in the scale of 20 – 30 cm, might be significant in low magnitude floods <20 cm such as floods 2 and 3. In these cases, the assumption that the flow occurs across the entire width of the active channel will not be valid and thus groundwater mounding will be of limited extension and hence lateral fluxes are expected to be more significant (measuring point will not be in the middle of the mound). On the other hand, in floods exceeding ~50 cm, additional sections of the stream channel may be active which will result in a multi channel flow or a much wider stream flowing channel.

Table 8. *Average WFPV and fluxes at the Buffelsrivier station (borehole 100)*

Flood no.	**Average for entire profile**		**WFPV (cm/h) FTDR**	**Flux (cm/h)**		
				WFPR	**WTRR**	
	θi	**$\Delta\theta$**			**Ave.**	**Max.**
1	5	4.5	143	6.2	10.34	18.67
2	7	6.5	191	12	0.83	2.16
3	4.5	10	229.6	20.5	2.96	8.40
4	7	5	187.4	8.25	0.49	7.70
5	8	-	-	-	0.44	0.82
6	-	-	-	-	0.36	7.54
7	6	-	-	-	12.33	52.20
Average:	**-**	**-**	**187.75**	**11.74**	**3.96**	**13.93**

The beginning of groundwater rise before arrival of the wetting front to the water table indicates clearly preferential flow processes (fig. 4.11B). The existence of these patterns are revealed by the monitoring set up but can not be measured quantitatively. It might be expected that the preferential flow component will be expressed in higher values of fluxes calculated by the WTRR method compared to the WFPR method. However, this is not the case. This might be related to the fact that the location of such preferred pathways, in relation to the measuring point (piezometer) is unknown. The further away they will be from the piezometer, the smaller their affect will be.

4.5.4 Rooifontein station, Upper Buffels River, South Africa

Table 9 summarizes the average WFPV and fluxes as calculated for the entire vadose profile for all flood events at the Rooifontein site. Similar to the Buffelsrivier station, calculations were made based on the FTDR probes' response and the groundwater rising rate, but could not be done according to increase in storage due to lack of information regarding the aquifer's width. Infiltration and recharge processes in this site are very quick and together with the very small thickness of the unsaturated zone, the monitoring of these processes is difficult. In all events, the water table started rising before the wetting front reached it. In most cases, only the upper 1-2 probes were wetted from above before the water table rose to about their depth, making the infiltration process obscure. For this reason, calculating WFPV and fluxes based on FTDR data was impossible for most floods. However, a sequential response of the upper probes according to their depth could be identified in the first floods. Thus, the spatial and temporal resolution provided by the monitoring set-up was insufficient for adequate investigation of the infiltration processes in this site. In addition, similar hydrogeologic features to those mentioned for the Buffelsrivier site, question the validity of the groundwater rising rate method at this location. This might explain the wide range of fluxes obtained by the WTRR calculation method. WFPV calculated for the first three floods by the FTDR range from 61 to 190 cm/h with an average value of 138.6 cm/h. These values correspond well with velocities calculated according to the response of the FTDR probes to the rising groundwater (FTDR-GW). In this method, that was applied at this site only, the upward propagation velocity of the water table was retrieved by dividing the vertical distance between two adjacent probes by the time gap between their saturation time (marks the arrival of water table to the probe). During the 3rd flood, groundwater levels rose above the uppermost probe and thus from this point onwards no information regarding the infiltration process is available (all probes show constant saturation, fig. 4.16b). Average downward flux for the first three floods according to the WFPR method was 6.8 cm/h. Fluxes calculated by the WTRR method varied from 0.57 to 40.3 cm/h.

Table 9. *Average WFPV and fluxes at the Rooifontein station (borehole 300*)*

Flood No.	**Average for entire profile**		**WFPV (cm/h)**		**Flux (cm/h)**			
	θi	***Δθ***	**FTDR**	**FTDR-GW**	**WFPR**	**FTDR-GW**	**WTRR**	
							Ave.	**Max.**
1	7	3	190.7	131.3	4.8	37.1	21.70	40.3
2	4	11.5	164.0	-	12.3	-	1.80	2.48
3	4.5	5.5	61.0	32.1	3.4	8.41	4.61	6.23
4	6	32	-	-	-	-	4.70	9.74
5	6	34	-	-	-	-	0.57	18.6
6	6	34	-	-	-	-	2.25	17.73
7	6	34	-	-	-	-	-	-
Average:	-	-	**138.6**	**81.7**	**6.8**	**22.8**	**5.94**	**15.85**

** Results for borehole 400 at the Rooifontein station are presented in appendix 10.3*

Similarly to the Buffelsrivier site, preferred pathways and/or fingering probably play a major role in the infiltration dynamics and groundwater recharge. However, from the existing data it is difficult to access quantitatively the actual contribution of each process (diffuse wetting front vs. preferential flow). At the 7th flood event, the entire vadose profile was already saturated at the time of arrival of the flood and thus no actual recharge could take place.

4.6 Total recharge estimations

4.6.1 Calculation method

The volume of water recharged into the aquifer can be calculated based on three approaches that correspond to the three flux calculation methods. Extrapolation of the point measurements to larger sections is possible only where similar geomorphic characteristics and similar aquifer dimensions are found.

(1) Wetting front propagation rate (WFPR)

The total recharge per event can be calculated given the downward flux (as measured by the FTDR probes), the duration of flow at the surface and the width of the active channel (the effective cross section through which recharge takes place), based on the following equation:

$$V_L = q \cdot t \cdot w_{ch} \tag{4.8}$$

Where V_L is the recharge volume pet unit length of the river (m^2), q is the flux (m/h), t is the flood's duration (h) and W_{ch} is the active channel's width (m).

(2) Water table rising rate based on the levelogger (WTRR)

This approach is similar in concept to the first method only uses fluxes calculated based on the water table rising rate (see section 4.5.1.2b):

$$V_L = q \cdot t \cdot w_{ch} \tag{4.9}$$

Where this time q is the flux calculated according to the rising rate of the water table (m/h) and t is the duration from the beginning of groundwater rise to the peak level (h).

(3) Increase in groundwater storage (IGWS)

This approach calculates the added volume of water to the groundwater, across the entire aquifer. This is based on the final increase in groundwater levels, the change in water content and the width of the aquifer:

$$V_L = (\Delta h_f \cdot \Delta\theta_{ch} \cdot W_{ch}) + (\Delta h_f \cdot \Delta\theta_t \cdot (W_{aq} - W_{ch})) \tag{4.10}$$

Where Δh_f is the final increase in groundwater levels (m), $\Delta\theta_{ch}$ and $\Delta\theta t$ are the changes in water contents at the zone of water table rise below the channel and below the terraces outside the channel, respectively (unitless), W_{aq} is the width of the aquifer (m) and W_{ch} is the width of the active channel (m) (fig. 4.22).

4.6.2 Gobabeb station, Kuiseb River, Namibia

Table 10 presents the recharged volumes per each flood and the total recharge for the entire rainy season of 2006, as calculated by the three approaches described above. Because flood 3 was followed soon after by flood 4, final relaxation of the groundwater after the 3rd flood was not achieved and thus these two events were regarded as one for the calculation based on storage increase. An average flux value of 0.01 cm/h was taken for the recharge calculation of the 5th flood according to the WFPR method.

Table 10. *Groundwater recharge estimations for the Gobabeb station*

Flood no.	Flood duration (h)	Max. stage (m)	Recharged volume per unit length of the river (m^3/m)		
			WFPR	WTRR	IGWS
1	76	1.50	25.08	16.05	19.27
2	120	2.00	39.6	49.90	39.45
3	67	0.80	28.74	8.34	36.65
4	36	0.30	8.31	1.13	
5	324	3.20	106.92	122.96	127.48
Total:	**623**	**-**	**208.66**	**198.38**	**222.84**

For the calculations based on the WTRR, fluxes (either average or maximum) which represented best the pattern of groundwater rise were used. As can be noted from the table, all methods give very similar values. According to these results the Kuiseb aquifer was recharged during 2006 by approximately 210,430 m^3 per 1 km of stream reach (average of all methods).

4.6.3 Buffelsrivier station, Lower Buffels River, South Africa

Calculating total recharge at the Buffelsrivier site is more difficult due to the complex hydrogeological settings. Because the width of the aquifer is not known, the calculation based on increase in groundwater storage can not be applied. In addition, the large width of the aquifer results in longer time to relaxation and more difficulties to identify the final stage of the groundwater after relaxation. Table 11 presents the recharge estimations per event and for the entire study period by the WFPR and WTRR methods. The 6th and 7th flow events were extremely long during which groundwater reached the surface. The duration of actual recharge was taken up until water table reached the surface. No fluxes according to the WFPR method are available for floods 5-7 as all probes were submerged below the water table. For recharge calculations at these events, an average value (of floods 1-4) was used. The increase in groundwater storage was calculated independently of any flux value. The increase in storage per unit area equals the final increase in groundwater levels (after relaxation) as measured by the levelogger, multiplied by the change in water content. The significant differences in recharge estimations between the WFPR method (2364 m^3/m) and the WTRR method (213 - 517 m^3/m) arise probably from the problems and uncertainties associated with the flux calculations as mentioned in section 4.5.3. Two main reasons might account for some overestimation by the WFPR method: (a) the probes record the flux at a certain point of time which is on arrival of the wetting front. This method does not account for the fluxes at later stages which might be smaller (b) Clogging of the surface layer during the flood as observed in some of the cases (fig. 5.1) might reduce water supply rate from the surface to the vadose zone and thus significantly reduce recharge, although water still flows in the river. As a result the duration of the recharge event which was taken as the flood duration, might be much shorter in reality.

Table 11. *Groundwater recharge estimations for the Buffelsrivier station*

Flood no.	Flood duration (h)	Max. stage (m)	Storage increase per unit area (m)	Recharged volume per unit length of the river (m³/m)		
				WFPR	WTRR	
					Ave.	Max.
1	30	0.45	0.042	52.1	11.37	20.53
2	9.5	0.14	0.013	45.6	2.81	7.34
3	13	0.185	0.013	106.6	14.22	40.32
4	288	0.6	0.825	676.5	19.00	99.79
5	240	0.5	0.638	788.8	29.46	55.22
6	60*	0.45	0.174	281.7	10.15	211.12
7	336*	0.6	0.435	413.2	19.72	83.52
Total:	-	**-**	**2.1045**	**2364.40**	**213.056**	**517.84**

* Time until water table reached the surface

On the other hand, the WTRR method might be underestimating the total recharge due to: (a) fluxes calculated by this method include the lateral flow component which becomes more significant as the groundwater mound builds up. These fluxes might be very significant at this site due to the soil texture as discussed in section 4.5.3. Hence, the actual recharge fluxes might be much higher (b) The exact time of termination of the recharge event can not be identified in the groundwater hydrograph. Thus, duration of recharge was taken from the beginning of groundwater rise to the peak level. However, recharge continues to take place beyond this point also in the downward heading limb of the graph. The reason that groundwater levels at this stage drop is because the lateral fluxes exceed the recharge fluxes. As a result the actual duration of recharge is longer than the value taken for the calculations. Assuming an average width of the Buffelsrivier Aquifer of ~700 m (based on Marais, 1981), groundwater recharge could be approximated also by the IGWS method. According to this the total recharge would be 1498 m^3/m. This value corresponds better to the recharge estimation by the WFPR method, taking into account some overestimation.

4.6.4 Rooifontein station, Upper Buffels River, South Africa

The difficulties associated with calculating groundwater recharge at the Buffelsrivier site are relevant also regarding the Rooifontein site. Table 12 presents the total recharge estimations as calculated by the WFPR and WTRR methods. The height of the 2nd flood was not recorded but was probably of very low stage (<10 cm). Its contribution to groundwater storage was negligible.

Table 12. *Groundwater recharge estimations for the Rooifontein station*

Flood no.	Flood duration (h)	Max. stage (cm)	Storage increase (m)	Recharged volume per unit length of the river (m^3/m)		
				WFPR	WTRR	
					Ave.	Max.
1	41	50	0.25	4.32	13.02	24.18
2	7	?	0	25.83	3.79	5.21
3	116	25	0.32	13.77	16.58	22.41
4	118	35	0.45	11.28	6.35	13.15
5	1.5*	20	0.12	3.08	0.09	2.79
6	106	32	0.45	7.18	1.69	13.30
7	176	25	0	-	-	-
Total:	-	-	**1.59**	**65.45**	**41.51**	**81.04**

* Time until water table reached the surface. Duration of surface flow was ~ 2 month.

During most floods (except no. 2), groundwater levels rose to land surface very quickly during the first few hours of surface flow (1.5 – 12 h). Surface flow at some of the floods lasted for many days and got up to 2 months in the 5th event. This means that no significant recharge took place during most of this time as the storage capacity of the aquifer was totally full. When the 7th flood arrived at the station, water table was already above surface. Thus, all the water of this flood were actually "lost" to downstream sections and none of it infiltrated at the Rooifontein site. The long duration of flow is related directly to the fact that the vadose zone was fully saturated and no infiltration could take place. Total estimations for the entire period are relatively similar and are between 41 and 81 m^3/m. These relatively small recharge volumes are the result of the limited storage capacity of the aquifer at this site.

5. Discussion

5.1 Infiltration dynamics

5.1.1 Percolation mechanism

Some patterns associated with the wetting of the vadose zone and recharge of the aquifer following a flood, showed high similarities between all stations. Every flood initiated a wetting front that propagated from the surface downwards resulting in an increase in water content of the vadose zone from θi to θf. Interestingly, the vadose zone remained unsaturated ($\theta f < 20\%$) during all downward infiltration events in all stations. The sequential response of the FTDR probes according to their order of depth suggests a generally uniform/sharp front that reaches the water table within few hours from the flood arrival time at the surface. As the front reaches the water table, recharge starts to take place and is followed by water table rise. Saturation of the vadose zone took place from the bottom of the unsaturated profile upwards, and was governed by the rising water table. Once the vadose zone has been completely saturated and the aquifer reaches its full storage capacity, infiltration ceases and the flood will progress longer (time) and further downstream.

The downward propagation of a relatively fast moving wetting front was observed in all stations. However, while in the Kuiseb River this process is the primary wetting and recharge mechanism, **in the Buffels River preferential flow plays a major role** and takes place together with the uniform wetting. These preferred pathways initiate recharge before the arrival of the wetting front to the water table. In the Rooifontein site, because of the shallow groundwater and coarse soil texture, the downward infiltration process through the porous media is almost entirely obscured by the fast rising water table governed by preferential flows.

The results from borehole 400 at the Gobabeb station correspond well with the assumption that **water movement in the vadose zone during infiltration events is primarily vertical and takes place mainly beneath the active channel** (see section 4.5.2). Lateral flow outward of the stream boundaries is limited and thus the measured average fluxes below the bank are significantly lower than below the active channel.

One of the most interesting observations was that **the vadose zone remained unsaturated (<20%) during all infiltration events** in all sites although the rivers were flowing bank to bank for many hours. This observation contradicts the assumption that the water content above (behind) the wetting front is that of saturation. This assumption is often used in many conceptual models but was proven wrong in this study. Similar observations regarding the unsaturated nature of the wetting front during infiltration were reported by Sorman et al. (1997).

In several cases, decrease in water content of the upper probes was recorded before the end of the flow at the surface (fig. 5.1). Such decrease can be caused by reduction in the inflow flux of water from above. **This observation might be related to clogging of the surface layer towards the end of the floods**. Surface sealing can be caused by the physical and chemical breakdown of soil aggregates, the washing of fines into larger pores (filtration) and swelling of clay particles (Mualem et al., 1990; Romkens et al., 1990). Deposition of fine material due to decrease in water energy following a drop in flood stages might also lead to clogging. Such patterns were also reported by Maurer and Fischer (1988) and Dahan et al. (2007a).

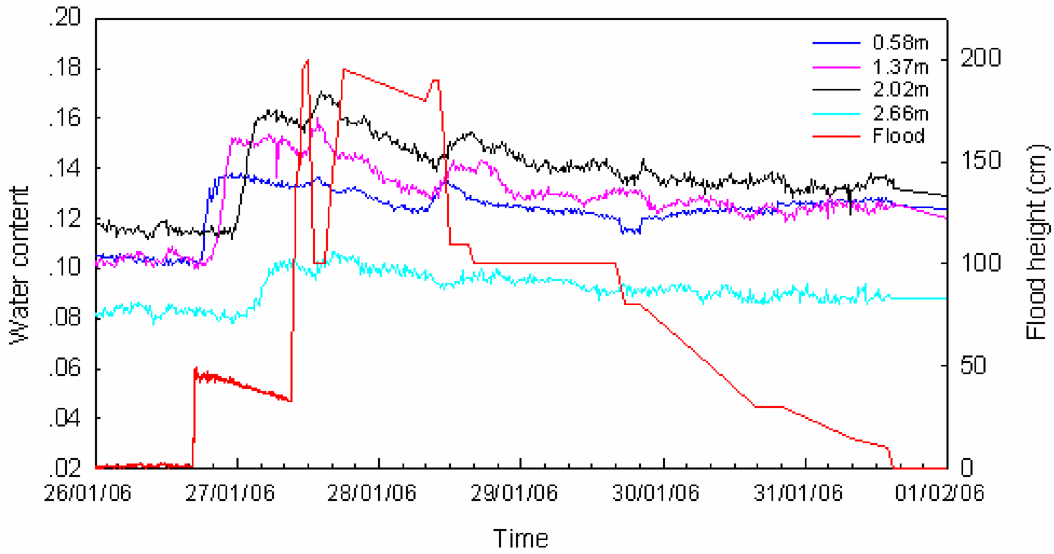

Figure 5.1 *Water content and flood stage during the 2nd flood event at Gobabeb.*

Results from all stations exhibit the **close relationship between the saturation of the vadose zone and surface flow**. Once the water table reaches the surface, the entire alluvial cross section is saturated and infiltration becomes negligible. As a result the termination point of the flood is expected to shift downstream. The arrival of the 5th flood in the Kuiseb River to the Atlantic Ocean (25/02/2006) and the long duration flows in the Buffels River (July 2006, June 2007) are directly related to the storage capacity of the alluvial aquifer and the rise of the water table to the surface.

5.1.2 Percolation rates

Wetting front propagation velocities differed between percolation events at the same site. Figure 5.2 presents the rate of propagation of the wetting fronts in floods 1 – 4 at Gobabeb. The slope of the lines (propagation rate) corresponds to the initial water content of each flood. Initial values were 5%, 10.4%, 9%, and 10.4% for floods 1, 2, 3 and 4, respectively. **This suggests that percolation rates increase with increase in the**

initial water content. Various studies and text books indicate that infiltration rates at the surface are expected to be highest when the initial water content is lowest (Warrick, 2002). This is also expressed by Horton's curve (1940) and is attributed to a higher matrix potential due to higher suction forces in a dry soil (section 1.2.1). However, this applies to the very early stages of infiltration (first few hours) and to the near-surface zone only. In the case of deep percolation, as the wetting front moves down away from the surface, the hydraulic potential approaches a unit gradient and the infiltration rate asymptotically approaches the saturated hydraulic conductivity (Marshall et al., 1996). In a pre-wetted soil, permeability increases because the hydraulic connectivity between the pores is already established. As the hydraulic conductivity is directly proportional to the water content in unsaturated conditions, a higher initial content along the profile will produce higher average percolation rates. Haimerl (2004) found similar dependency between the WFPV and the initial water content.

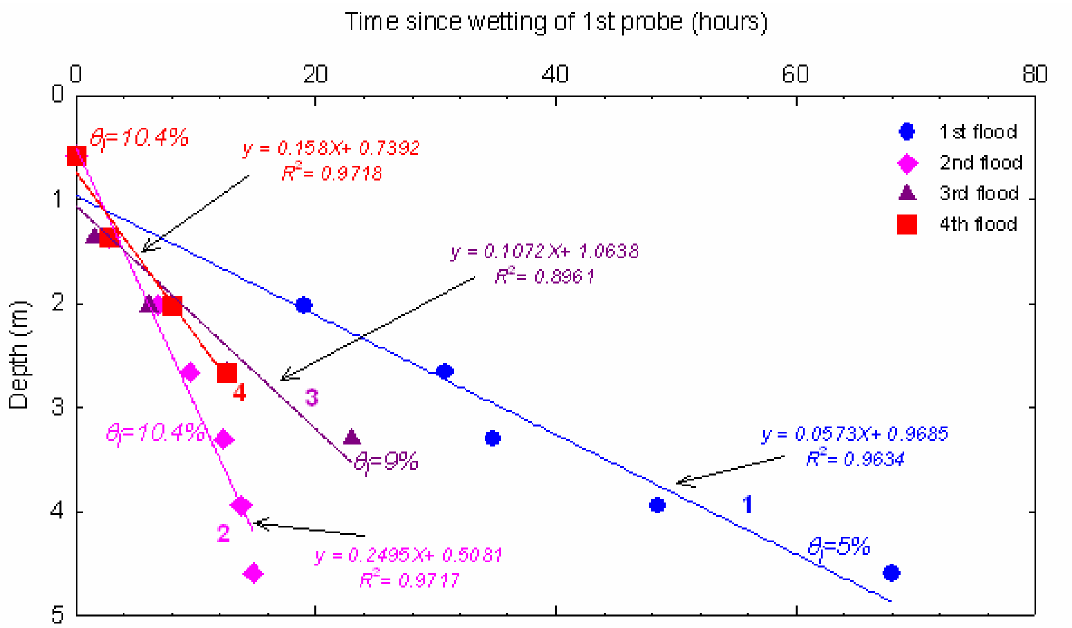

Figure 5.2 *Depth of the wetting front vs. time as measured for floods 1-4 at the Gobabeb station. Flood number and initial water content are marked next to each line (no FTDR data exists for the 5th flood).*

In the Buffels River, the correlation between initial water content and WFPV is not as distinct as in the Kuiseb site. It is suggested that the effect of antecedent water content will decrease with increase in average grain size.

The texture and structure of the sediments comprising the alluvial profile are expected to have major influence on the percolation characteristics. Percolation fluxes are strongly related to the porosity and grain size distribution (GSD). The second order relationship between pore size (d) and permeability (k) [$k=d^2$] means, that even a small change in 'd' might result a significant change in 'k' of one order of magnitude or more. The coarser and better sorted the material is, the faster the fluxes would be. Fluxes and WFPV measured at the Rooifontein and Buffelsrivier sites (dominated by relatively coarse sand to gravely sediments) were significantly higher (at least one order of magnitude) compared to those measured at the Kuiseb River near Gobabeb (more fine sand dominates).

Variations in the porosity and GSD along the profile are reflected from field capacity and saturation values of the probes at different depths (fig. 4.5). Such variations might potentially impede infiltration either by a low permeability layer or as a result of capillary barriers in the interface between a fine-grained layer and an underlying coarse-grained layer. This phenomenon might be reflected from the response of the FTDR probes in a few cases (fig. 5.3). In some of the probes an unusual rise in water content (>25%) during downward infiltration was observed, reaching a peak value followed by an immediate sharp drop down to 'regular' values (~10%-15%). **This might represent the accumulation of water above a thin impedance layer or capillary barrier.** Once the water potential at the wetting front reaches the air entry potential (pressure required to fill the large pores with water), then the accumulated water quickly percolates downwards, draining the upper layer. The observation that the flow is impeded only temporarily and the pattern of quick drainage after the peak values supports the explanation of a capillary barrier. As a result of this mechanism, a delayed response of the probe below the impedance layer is noticed, in comparison to the responses above that layer. Similar observations were reported by Talby (2006) and Shani (2006) who termed this pattern of the FTDR probes as "step increase".

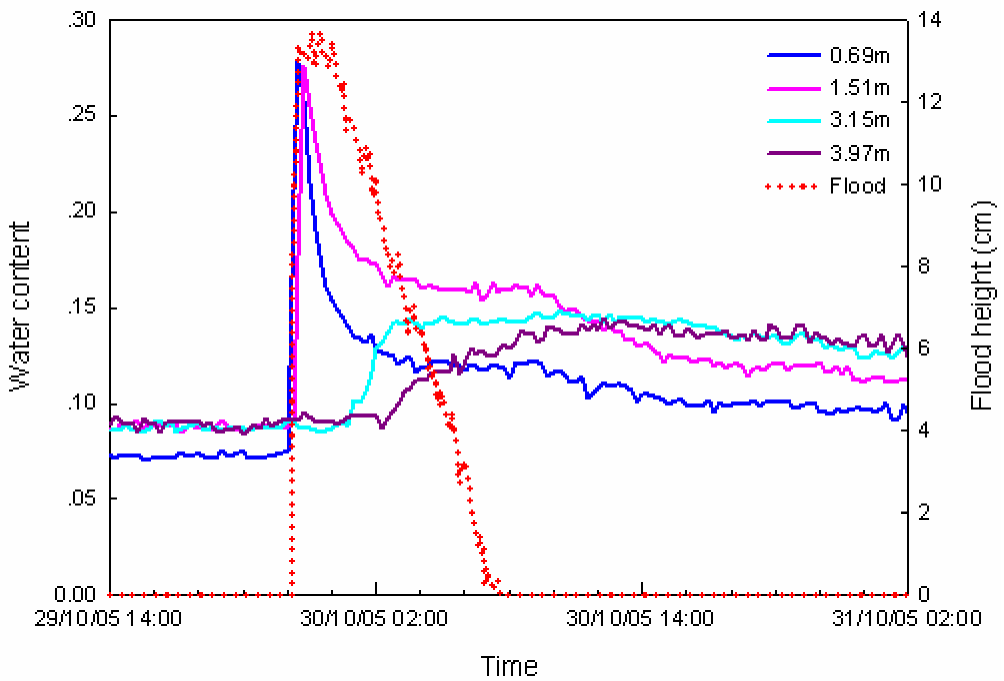

Figure 5.3 *Water content and flood height during the 2nd flood at Buffelsrivier.*

Comparison of all events at a given site shows that the flood stage had limited influence on the average percolation rate (fig. 5.4). The above observations propose that factors such as antecedent water content and sediments properties are more significant than the flood stage in controlling percolation rates. This observation was strongly demonstrated at the Gobabeb site. **Although floods varied widely in their maximum stage, the calculated average percolation fluxes for all events were surprisingly very similar** (table 7). It is suggested here that this unexpected feature might be the result of a natural regulating mechanism that controls maximum percolation fluxes at a certain channel. This mechanism can be related to the stratified structure of the vadose zone beneath ephemeral channels. Two main features can be responsible for the regulation of fluxes. First, the alternation between fine and coarse layers along the profile (fig. 5.5b) creates sharp differences in the hydraulic conductivity in the interfaces between those layers (as mentioned previously).

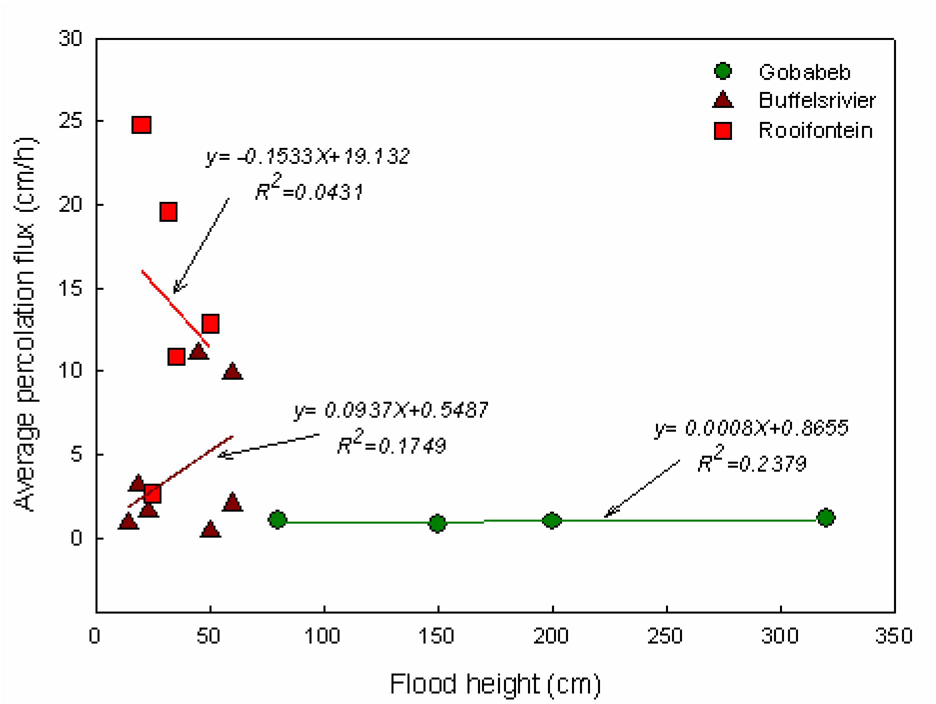

Figure 5.4 *Average percolation fluxes vs. flood height*

Capillary barriers might also be a result of the layered structure and can possibly account for a significant reduction in the average vertical fluxes. The second feature is in the form of very fine layers (fig. 5.5a) of very low hydraulic conductivity and of small thickness (few cm) that might have a disproportional effect on the propagation of a wetting front downwards. These fine layers might be deposited towards the end of flow in the channel following a decrease in the floodwater energy. If the next flood to run down the channel is of low magnitude and gradual level rise, there is a good possibility that the fine layer will be buried by new deposits and become part of the sedimentary sequence. Because of their small thickness, these layers can be easily overlooked by GSD and other soil analysis procedures. Shani (2006) observed the impact of such layers on the propagation of a wetting front in a field scale experiment in the Arava, Israel. Baver et al. (1972) referred to the potential impedance of a buried fine layer as a check valve.

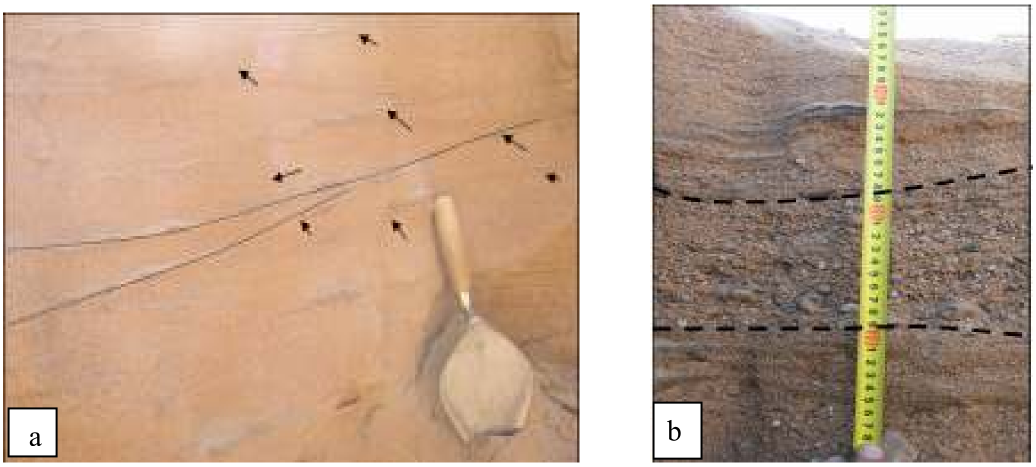

Figure 5.5 *(a) Fine grain layers in the Kuiseb alluvial cross section (b) alternating fine and coarse layers along the Rooifontein site alluvial cross section.*

At the Buffelsrivier and Rooifontein stations, although most of the flux values within the same calculation method do not differ much, this pattern is less distinct and larger variations are observed between events. However, the significantly coarser sediments at these sites might produce a wide range of hydraulic conductivities of several orders of magnitude higher than those at the Gobabeb station. Considering the potential wide distribution of fluxes at these sites, it is possible that some regulation is active at these channels as well. It is suggested that without the regulating mechanism described above, fluxes might have varied even more widely. In addition, technical limitations associated with the local conditions at the sites in the Buffels River might contribute to the observed variations in fluxes.

5.2 Recharge processes beneath ephemeral channels

Groundwater recharge during a flood event starts at the moment the wetting front arrives at the water table. At this stage, the groundwater are hydraulically connected to the floodwater and any water that will further infiltrate at the surface will contribute directly to the recharge of the aquifer. Once the flow in the channel ceases, no more water is added to the vadose profile, and redistribution starts to take place. This stage is dominated mainly by free drainage of the excess water in the sediment, governed by gravity. In the case of a shallow water table, as in all the study sites, most of the draining water will eventually reach the water table and recharge the aquifer. When the building tension forces within the soil matrix (resulting from the drying process) will equal gravity, redistribution will cease. At this stage the water content along the unsaturated profile represents the field capacity of the various layers.

5.2.1 The effect of evapotranspiration

Evapotranspiration is difficult to assess in the field due to the difficulties associated with actual measurements of these components. **In the case of flash floods and the associated percolation rates observed in this study, it is argued that evapotranspiration is insignificant for recharge estimations**. This is based on the following guidelines: (a) direct evaporation of surface-water during stream flow can be neglected due to the short duration of flow (few hours to a few days). Long flow durations (>2 weeks) occurred when the entire vadose profile was already saturated and thus these flow periods are irrelevant for recharge calculations (b) The subsurface water is available to evaporation only when stream flow ceases. This stage marks the beginning of the redistribution phase and takes place after most of the recharge already occurred (c) Due to the relatively fast percolation velocities and the short duration of this stage, evaporation from the subsurface during redistribution can be probably assumed as insignificant (d) The potential water losses to transpiration during a recharge event are practically insignificant due to the relatively higher recharge rate in comparison to the transpiration rate. **Evapotranspiration is however partially responsible for the gradual drop in groundwater levels, taking place all year round and especially after the floods season when the water table is close to the surface** (1, 2, and 3 in fig. 4.14). During high groundwater levels, some drop might be related to the longitude flow downstream but most of the decline is attributed to evapotranspiration (the monitoring stations are not affected by pumping).

The FTDR probes recorded the drainage process of the subsurface taking place from the surface downwards, following the descending water table (fig 4.5). The rate of drainage can be estimated according to: (a) FTDR probes - by dividing the time interval between the beginnings of drainage of two adjacent probes by the vertical distance between them (b) Levelogger – by calculating the slope of the graph presenting water levels in time. Figure 5.6 shows a decrease in the drainage rate as a function of depth at the Gobabeb station based on the FTDR data. This decrease is expected as the water table propagates further away from the surface and evapotranspiration becomes less effective. The average evapotranspiration rate from the subsurface to a depth of 3 m was 0.84 cm/d. This value corresponds with the depth of the water table at Gobabeb, as measured by the levelogger a year after the end of the last flood. At that time (March 2007) groundwater level was ~3 m below surface. These findings are very similar to the estimations made by Bate and Walker (1993) at Gobabeb. According to their study water table would fall just under 2.92 m below surface 51 weeks after a flood. Average falling rates of the water table calculated based on the levelogger measurements were very similar and were found to be ~0.57 cm/d at depths between 1 to 3.5 m below surface. Similar values were calculated for the Buffels River based on Levelogger data. Drainage rates at the Buffelsrivier site ranged from 0.73 cm/h in the upper ~1 m of the channel bed to 0.59 cm/h at 2 m below surface. At the Rooifontein site rates varied from 0.67 cm/h at the top soil to 0.51 cm/h at a depth of 1.5 m.

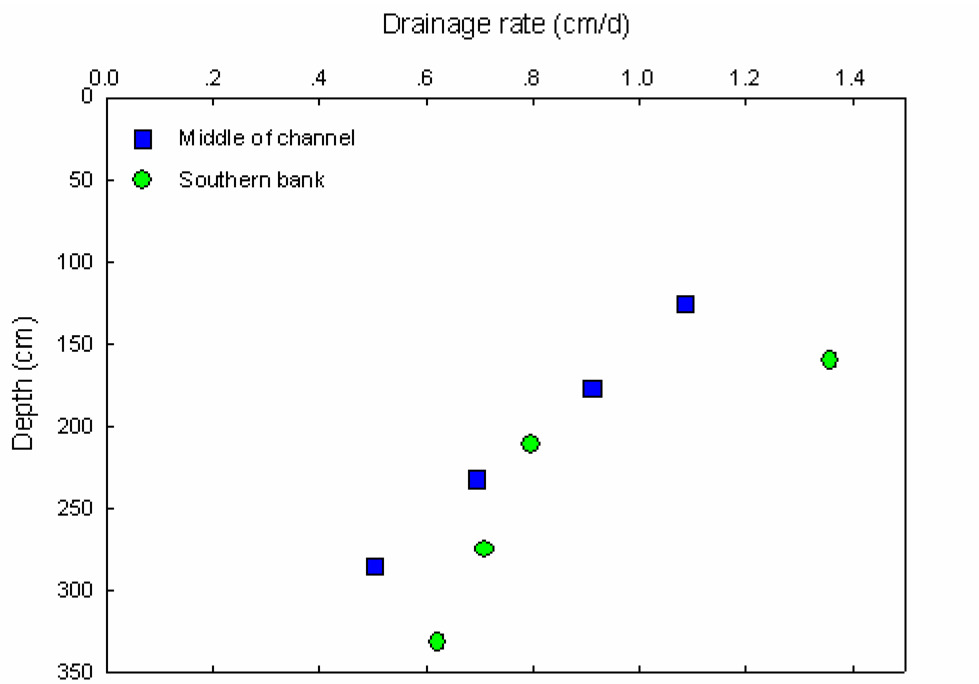

Figure 5.6 *Drainage rate vs. depth according to FTDR probes at Gobabeb.*

5.2.2 Total recharge quantities

The total amount of water recharged into the aquifer was found to be primarily related to the duration of flow in the active channel (fig. 5.7). In general, the longer the flow in the channel is, the larger the total recharge volume will be. However, the maximum volume of recharge is also a function of the storage potential and aquifer dimensions. The WFPV and unsaturated thickness will determine the beginning time of recharge. Thus, the faster the wetting front will reach the water table, the earlier recharge will begin and hence, the recharge duration will be longer. Lange (2005) attributes a significant amount of recharge in the Kuiseb River to high magnitude events that exceed the active channel and cover the floodplains. During high magnitude floods, water flows out of the active channel and floods the banks and floodplains. Although this might increase significantly transmission losses (which was the parameter studied by Lange, 2005) due to the major increase in wetted area, it will probably have insignificant affect on the total recharge.

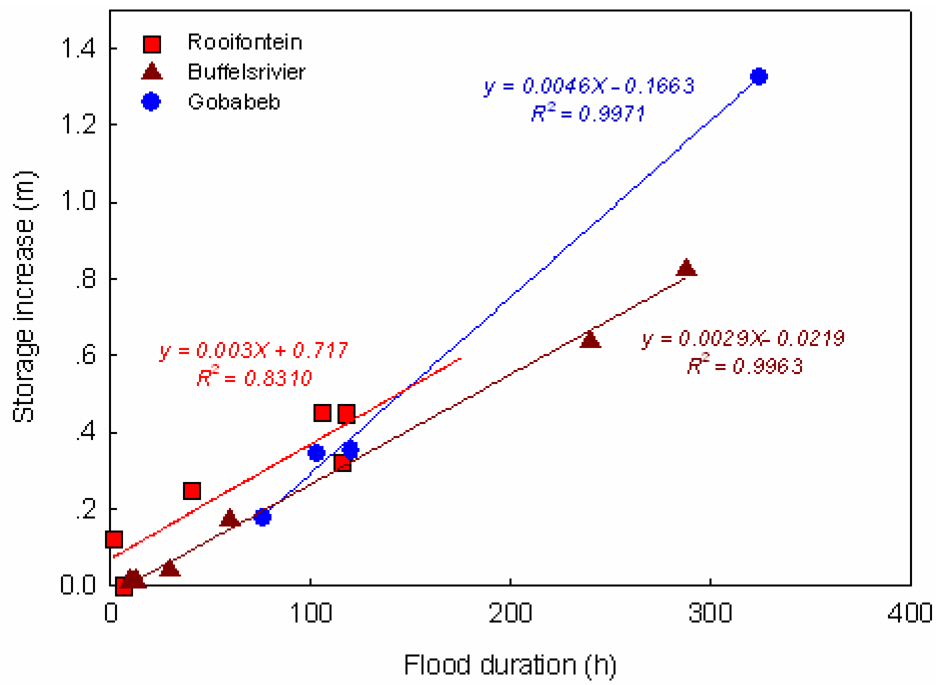

Figure 5.7 *Storage increase vs. flood duration in all study sites.*

Based on the rates and patterns observed in this study it is argued that very limited infiltration is possible outside the active channel: (1) the stratigraphy of the floodplains is characterized by layers with high fraction of fine-grained deposits of low hydraulic conductivity, resulting from the relatively low stream power that dominates these areas. Thus, percolation rates are expected to be several orders of magnitude lower than those in the active channel (2) the vadose zone thickness is much larger outside the active channel (includes the height of the banks). This means that more water will be held in the pore space as soil storage and the travel time of a wetting front from the surface to the water table will be longer (3) flooding of the floodplains will be very limited in time (several hours) due to the short duration of peak stages as revealed from the hydrographs. Considering the low percolation rates expected below the floodplains, the larger depth to the water table and the short flooding time, the possibility that floodwater infiltrating into the floodplains will reach the water table is assumed to be very low. Moreover, due to rare deep percolation in the floodplains, water that will eventually reach the aquifer will be considerably saltier as a result of flushing salts from the profile.

The cumulative effect of a series of floods in the same rainy season is very significant in terms of the total recharge. This is mainly due to two reasons: (a) assuming the time interval between two successive floods is not too long (few weeks), when the subsequent flood arrives, the sediment is already pre-wetted (around field capacity values) and not totally dry to residual values following the long dry season. According to the relationship between the initial water content and the WFPV observed earlier, the travel time of the wetting front to the water table will be shorter. Consequently, the amount of recharged water will be larger in comparison with initially dry conditions. Schwartz (2001) found out that transmission losses into the bed of a natural channel in southern Israel during flood events were significantly reduced if the time interval between the events was more then one week; (b) following the first recharge event, depth to groundwater will decrease hence travel time of the wetting front to the water table will be shorter. These features are mainly significant in the case of low magnitude short duration floods that arrive after the river had flowed earlier in the season. As a result, even in these floods significant recharge takes place (for example, the 3rd and 4th floods at Gobabeb).

5.3 Groundwater recharge mechanism

The results clearly indicate that the source of groundwater recharge in the Kuiseb aquifer is primarily floodwater infiltration. The local geology and geomorphology eliminate the possibility of substantial recharge from the north or south of the channel. The groundwater response (timing and quantities) corresponds directly to floods occurrences in the river and the infiltration processes that follow.

The results from the Buffelsrivier site also demonstrate a direct link between floodwater infiltration and recharge of the alluvial aquifer. Every flood resulted in increase in groundwater storage. No recharge was noted during no-flow periods in the river. Recharge at the first phase is initiated by flows through preferential pathways within the alluvial channel bed. Not long after, a second recharge phase can be noticed in most cases with the arrival of the wetting front to the water table (fig. 4.11B). As the water table gets closer to the surface and the unsaturated zone "shrinks", it becomes more difficult to differentiate between these phases.

The hydrological system at the Buffels River is dynamic and the channel seems to change from a loosing stream type to a gaining stream type (see section 1.1) during the 6th flood. The data suggests that the long duration flow during July-September 2006 did not originate from accumulation of runoff in the active channel but rather represents base-flow (drainage of groundwater at the surface). Three main observations support this conclusion: (1) groundwater levels reach the surface according to the levelogger measurements (2) comparison of floods occurrence in the channel and precipitation records suggests that rainfall alone could not account for the long duration (~2 month) flow (fig 5.8) (3) The floodwater carry the salinity signature of their source. High EC values (>1 mS/cm) associated with the long flows in the river present similar values to those of the groundwater for the same period (fig 5.10). These values are too high to be attributed to direct evaporation merely. The source of the high EC values at the groundwater might be one or a combination of the following: (a) some inflows into the alluvial aquifer from the surrounding granite bedrock might take place. The water within the bedrock was characterized in other studies as extremely saline. Hydraulic connectivity between the alluvial aquifer and the granite aquifer was reported in previous studies (section 3.2.7) (b) the upper part of the vadose zone, just below the surface is expected to contain large amounts of salt residuals due to evapotranspiration. As the water table rises to the surface, these residuals are dissolved into the aquifer (c) the concentration of these evaporitic residuals probably increases at the boundaries of the alluvial aquifer with increase in the distance from the active channel. As the water table rises above the surface and into the terraces at the floodplains, saline water from the margins of the aquifer might drain into the channel.

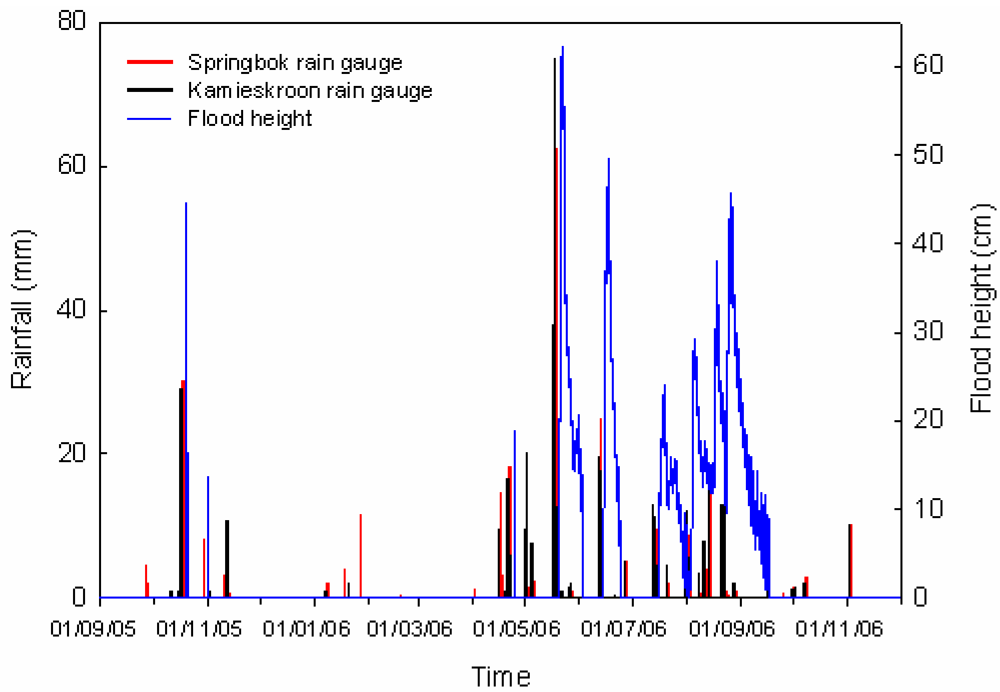

Figure 5.8 *Rainfall and flood height at the Buffelsrivier station.*

The Rooifontein site presents very similar characteristics to those in the Buffelsrivier site. **The main source of recharge of the alluvial aquifer at Rooifontein is infiltration of floodwater**. This seems to take place through two mechanisms: a more or less uniform wetting front propagating through the porous media and fast percolation through preferential pathways in the channel bed. The shallow depth of the groundwater and the fast rates of percolation result in almost instantaneous response of the groundwater to the floods, and abrupt water table rise up to the surface in most events. Similar to the Buffelsrivier station, the long flows at this site are thought to be associated with base-flow, as the stream changes into a gaining type. The evidence for this conclusion emerges from the same observations mentioned at the Buffelsrivier site. These are: the water table location, the rainfall pattern in relation to the extreme events of long flow duration (fig. 5.9) and the salinity of the floodwaters as a marker of their source (fig. 5.10).

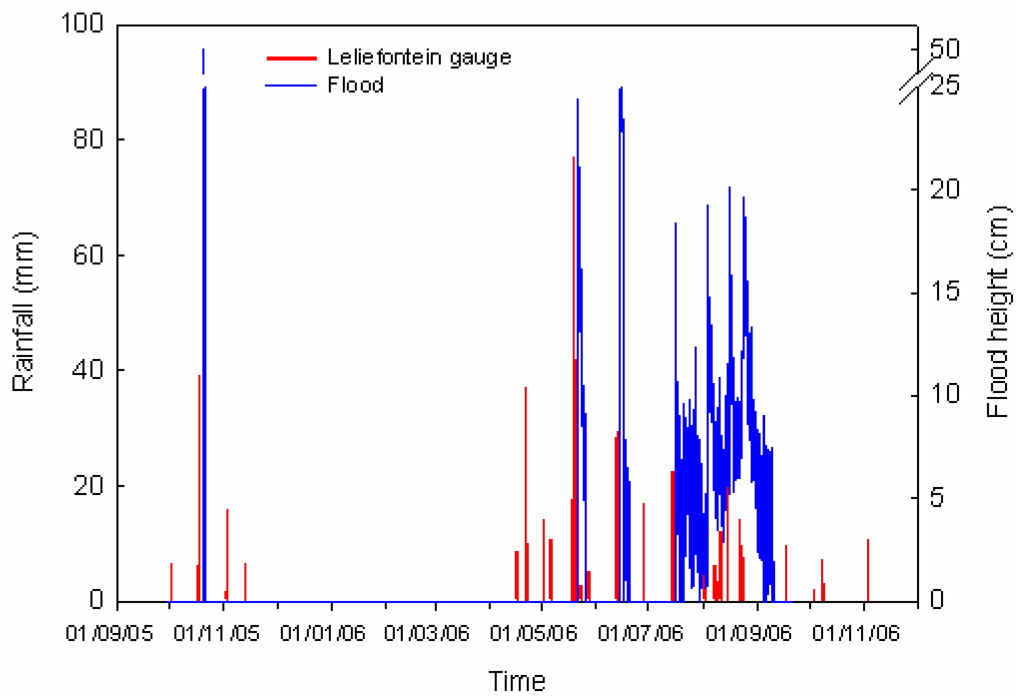

Figure 5.9 *Rainfall vs. flood height at the Rooifontein station.*

The hydrological systems at Rooifontein and Buffelsrivier are complex and dynamic. Data obtained in this study is insufficient to reveal all the local groundwater flow patterns and the interrelations between the alluvial and granite aquifers. However, the data suggests (similarly to previous studies) that the two reservoirs are hydraulically connected and affect each other. These conditions create a dynamic relationship between the river and aquifer where the channel can be of both gaining and loosing types (see section 1.1). For a better and through understanding of these systems, further work should be carried. Geochemical tools might reveal more of the recharge component from the granite bedrock and subsurface flow patterns.

5.4 Aquifer storage and recharge potential

The storage potential of an unconfined aquifer is a function of its porosity, width and thickness of the saturated plus unsaturated zones. Because the alluvial aquifers in all sites are of shallow depths and of limited extent, bounded by granite bedrock from three directions, their storage potential is relatively small. This is most evident in the Rooifontein aquifer where the entire vadose profile is saturated within few hours of flooding. When groundwater levels reach the surface, the storage capacity of the aquifer is full and no more water could infiltrate. As a result, the flood is expected to last longer and reach further downstream. At this stage water arriving from the upstream are "lost" to downstream reaches (and eventually to the ocean) instead of being recharged at site.

At Gobabeb and Buffelsrivier sites, because the alluvium is thicker, the storage potential is larger and a good rainy season with sufficient floods can compensate on a following drier season. For instance, during the rainy season of 2006 the aquifer at Gobabeb got full to its maximum storage. This enabled regular exploitation in the following year of 2007 even though the river did not experience even a single flood. Moreover, groundwater levels at the end of 2007 were still higher then the levels prior to the floods of 2006. This has great importance for water management especially in arid regions, were flood occurrence is of large variation in time. In the case of small storage potential, such as in Rooifontein, there is almost no "reserve" storage volume and there is a necessity for floods to recharge the aquifer every year, even after good rainy seasons to avoid water shortage. **Results from this study suggest that the main**

limiting factor for groundwater recharge at the Rooifontein site is the small storage potential of the aquifer.

5.5 Aspects of water quality and groundwater recharge

All sites exhibit the positive affect of fresh floodwater recharge on groundwater qualities by lowering the salinity of the aquifer. Following the floods in the Kuiseb at the beginning of 2006, a major improvement was felt in the quality of the drinking water at Gobabeb. This is directly related to the drop in groundwater EC from ~0.8 to ~0.3 mS/cm between January to mid March 2006. Similar patterns were observed in the Buffelsrivier site where groundwater EC dropped from ~1.15 to ~0.3 mS/cm following floods 1-4. At the Rooifontein site EC values of the groundwater decreased from ~2 to ~0.8 mS/cm following floods 3 and 4. The fresh recharged water is accumulated in the first stage at the top of the aquifer due to their lower specific density in relation to the more saline groundwater. **However, in all sites, following the recharge event, groundwater EC gradually rises back towards initial values**. This stage represents the mixing of the upper fresh groundwater layer with the underlying water body. The duration of this stage is mainly a function of the concentration gradient, the thickness of the fresh layer and the hydraulic conductivity within the saturated zone. Because the recharged volume will always be small relatively to the volume stored in the entire aquifer, the improvement in groundwater qualities following a flood would be limited in time and in space. Accordingly, in the case of relatively low quality aquifers such as in all sites in this study, shallow pumping near the active channel after floods can provide water of high quality before they are "lost" in the aquifer. These water can replace water that are stored in surface reservoirs/tanks for drinking purposes and special irrigation needs.

As mentioned in section 5.3, high EC values of the floodwater that are associated with long surface flows both in Buffelsrivier and Rooifontein stations, are most likely related to base-flow (fig. 5.10). However, some unusual patterns were observed in these stations. These patterns include gradual increase in EC values of the groundwater in Buffelsrivier during March and April 2007 (from ~1.2 to ~6.5 mS/cm, fig. 4.15) and in Rooifontein between February to May 2006 (from ~1 to ~2 mS/cm, fig. 4.19). During both cases, the channels were dry (no surface flow) and the water table was gradually dropping (no recharge recorded by groundwater levels). **An optional explanation for these phenomena is some inflows from the saline granite complex into the alluvial aquifer**. These fluxes might be insignificant in quantities but of very high salinity. Any discharge of saline groundwater (spring) upstream of the stations is expected eventually to reach the station probably in the form of a plume of high EC values. Similar patterns observed at the Gobabeb station might also be related to discharge of subsurface brackish springs (see section 4.1.7).

Nevertheless, in all stations, in large timescales of few months, the hydrological system tends to return back to initial, 'near steady state' conditions and presents the same or close EC values as in the pre-flood time. The range of measured EC values for all sites is summarized in table 13. Salt transport dynamics at the groundwater and into the alluvial aquifers are complex. Unusual patterns were observed at different times at all sites. A complete picture is impossible to gain based on a single measurement point within the alluvial aquifer. Further investigation of the subsurface lateral flows on a larger scale based on chemical approaches might give answers to some of these unsolved issues.

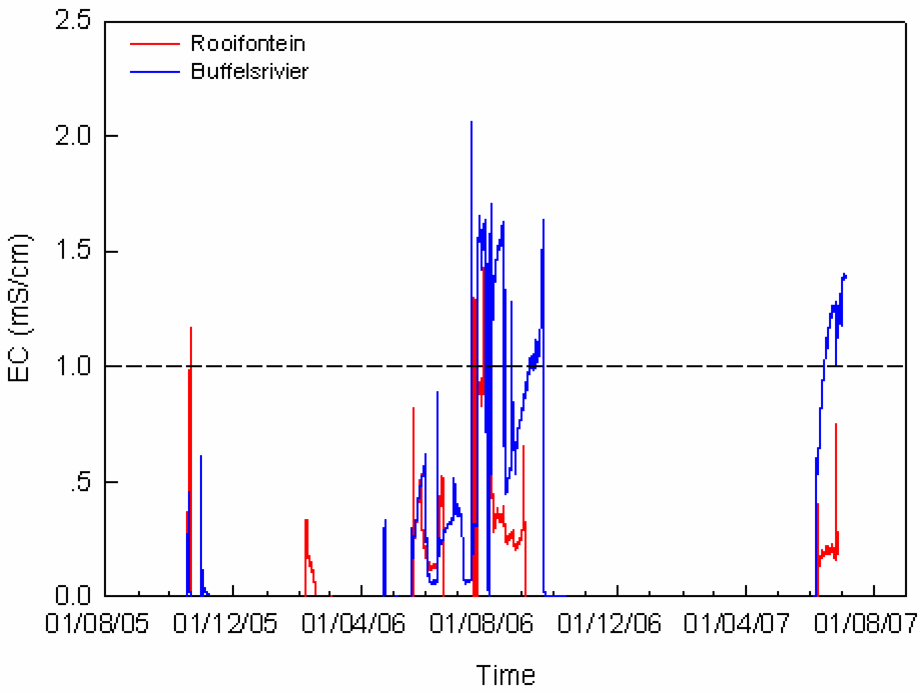

Figure 5.10 *EC values of the floods in the Buffelsrivier and Rooifontein stations. Long durations floods (> 1 month) are characterized by high EC values (>~1 mS/cm,). See July 2006 in both stations and June 2007 at Buffelsrivier.*

Table 13. *Groundwater EC values range for each site (mS/cm)*

	Buffelsrivier	Rooifontein	Gobabeb	
			GOB1	GOB2
Initial (pre-floods)	1.15	~0.7	0.87	1.34
Maximum	1.6	2.06	1.12	1.5
Minimum	0.2	0.7	0.28	0.34
Final (1 year after last flood)	1.2	0.82	0.6	1.12

5.6 Practical implications for wise groundwater management

The available amount of surface-water, which is mainly in the form of flash floods in arid regions, is a function of the natural climatic and physiographic factors at a given basin. This amount might be highly variable in space and in time, while one of the most problematic features of it is its unknown reoccurrence time. Nevertheless, some practices are available in order to enhance replenishment of alluvial aquifers, once stream flow does take place. Human interference in these processes that aim to maximize groundwater recharge is known as **artificial recharge**. These practices are based on the concept that the soil is the most available and suitable reservoir for storage of water and that by controlling the duration, location and surface area of the flow, recharge potential can be significantly enlarged. Commonly used artificial recharge methods include: percolation reservoirs, damming of natural streams (and controlled release of the water to recharge downstream of the dam), ditch and furrow and injection wells. The following is a proposed conceptual scheme designed specifically for the case studies presented in this work with special relevance to the Rooifontein site, where storage potential of the aquifer seems to be the main limiting factor for groundwater recharge.

The scheme is based on a controlled pumping wells system along a section of the river course. During large flood events groundwater can be pumped intensively and be transported in closed pipes to a distant downstream location, to be spread over different recharge areas. Pumping should be carried simultaneously in a series of wells along a stream reach (~1 km) to obtain a regional water table lowering in contrast to a localized depression cone around a single well. This will increase storage potential in the upstream area and will supply more water quantities to infiltrate in the downstream area. Moreover, in the case that the downstream recharge site is within the river course, the pre-wetting of the soil in the downstream section will result enhanced percolation rates once the flood arrives. Shentsis (2003) reported significant increase in transmission losses in Wadi Paran, Israel due to groundwater extraction. In the case of the Kuiseb River, the buried paleo-channels located under the sand dunes to the south of the Kuiseb River and west of Gobabeb, could provide excellent unlimited storage volume for such management approach. The well sorted quartz grains comprising the dunes are ideal for natural quick percolation and can also provide a protective buffer zone from possible contamination. Theses sites could act as emergency reservoirs for the city of Walvis Bay during drought years. In the case of Rooifontein and Buffelsrivier, an appropriate site for groundwater storage would be more difficult to locate due to the local settings. For this case, a method of **subsurface damming** of large tributaries is suggested in order to create suitable recharge sites without loosing the groundwater due to downstream flow. Water pumped from the main channel during large floods can be spread over near by tributaries which will be dammed before the confluence with the main channel. This method might produce medium size groundwater reservoirs in addition to the main alluvial aquifer.

Subsurface damming of the main alluvial aquifer across the flow direction might also be a useful tool during years of low precipitation. Such a construction can maximize recharge around the pumping wells and once the local aquifer reaches full capacity, water will over flow at the surface and percolate downstream of the dam. Planning and locating the recharge sites should consider the following criteria: high infiltration rates, sufficient mounding potential, available storage capacity, groundwater quality, proximity to residential communities and proximity to potential contamination sources (Bouwer, 2002). Any management plan or implementation of an artificial recharge scheme will also require addressing the following issues:

(1) Ability to recognize the high magnitude/long duration flood events as they evolve, in order to activate a suitable management scheme (such as intensive pumping). This can be achieved by basin scale monitoring of rainfall in real time combined with live updates supplied by the local communities.

(2) Constructing surface-water harvesting scheme and artificial recharge sites distribution plan along the main channel and large tributaries. This scheme should define the water quantities that are to be cultivated at each section of the basin in order

to ensure wise distribution of surface-water to all reaches without drying the downstream sections on one hand, but also avoiding the loss of water to non rechargeable areas, on the other hand. This requires a dynamic scheme that is being constantly updated by field data and water budgets at different locations in the basin in real time and should be adjusted accordingly.

(3) Community involvement and active participation of the residents is a key factor for the success of any water management program. This includes guidance and education at every village regarding efficient water use and reduction of water consumption and water waste. Emphasizing groundwater contamination hazard from domestic sources and waste sites and how it can be prevented. Part of the guiding should include professional qualification of some of the residents to carry regulated monitoring of the surface-water and groundwater as well as to be able to identify "red line" levels of water qualities and quantities that require immediate notification of the authorities. Other aspects of responsibility of the local hydrologists are to generate real time "live" reports to decision makers during flood events and to operate and maintain local artificial recharge sites.

6. Summary

The purpose of this work was to investigate the dynamics of floodwater percolation and recharge of alluvial aquifers below ephemeral channels in arid regions. Three monitoring stations were constructed in two large basins in southwestern Africa: (1) the Gobabeb station in the lower Kuiseb River, Namibia, (2) the Buffelsrivier station in the lower Buffels River, South Africa and (3) the Rooifontein station in the upper Buffels River, South Africa. At each station, simultaneous monitoring of the surface, vadose zone and groundwater was conducted for a period of 2 years. Data retrieved included continuous water content measurements along the unsaturated profile from the surface to the water table, before, during and after flood events. Groundwater and floodwater levels and electrical conductivity were recorded as well.

During the two wet seasons between July 2005 and July 2007, five flood events were monitored at the Gobabeb station and seven flood events were monitored at both the Rooifontein and Buffelsrivier stations. As a result of these exceptionally wet seasons, the water table at all three sites rose to the surface and the aquifers were fully replenished. The innovative apparatus implemented in this study enabled detailed monitoring of the complete infiltration-recharge processes. A few main stages were identified: (a) arrival of a flood at the surface, (b) propagation of a wetting front through the vadose zone down to the water table, (c) groundwater mounding and (d) groundwater relaxation at a higher level relative to its initial location. Some similar patterns were observed at all stations:

- Every flood at the surface initiated the propagation of a relatively fast moving wetting front that reached the water table within a few hours.
- Recharge of the alluvial aquifers was directly related to floodwater infiltration. No detectable recharge took place during times of no flow at the surface.

- During the downward percolation, the vadose zone remained unsaturated (<20% water content) even though the rivers were flowing bank to bank for many hours.
- Saturation of the sediments took place from the bottom of the unsaturated profile upward and was governed by the rising water table.
- As the aquifers reached their maximum storage capacity with the arrival of the water table to the surface, no more infiltration took place on site. As a result, surface flow lasted for long periods and the flood traveled further downstream.
- Recharge by floodwater significantly improved groundwater quality.
- The wetting front propagation velocity was found to be directly related to the initial water content along the unsaturated profile. Flood stage had only a limited influence on the infiltration rate.
- Total groundwater recharge was mainly a function of the flow duration in the active channel. No correlation was found between the total recharge and flood stage.
- The recharge potential of the aquifers was a function of the aquifer's dimensions and mainly the unsaturated thickness.

All sites presented relatively limited storage potential. At the Rooifontein site, this appeared to be the main limiting factor for the aquifer's replenishment. However, although all sites presented generally similar physiographic and hydrologic characteristics, some distinct differences were recognized:

- Both the Buffelsrivier and Rooifontein sites exhibited dominant preferential flow processes.

- Recharge fluxes at the Buffels River were one order of magnitude higher than those measured at the Kuiseb channel (0.36-52 cm/h and ~1.0 cm/h, respectively). This was attributed to the coarser sediments comprising the alluvium at the Buffels River compared to those found in the Kuiseb.

Fluxes at the Gobabeb site were calculated by three independent methods according to the vadose zone flow, the groundwater rising rate and the final increase in groundwater storage. All methods gave very similar values. Two of these methods were applied at the Buffels River sites where some variation in values was noticed. These variations were attributed to the different settings in the Buffels River and to limitations of the monitoring system. Although floods at the Kuiseb varied significantly in stage and duration, average fluxes were surprisingly similar in all events. This might be the result of a natural regulating mechanism related to the stratified structure of the channel alluvium and inter-bedding of very fine material along the vadose profile.

Total groundwater recharge for the entire study period was calculated at each site based on the measurements at the monitoring stations. Extrapolation of these point measurements to larger sections is applicable only where the geomorphic characteristics and aquifer dimensions are similar to those at the monitoring stations. Total recharge at the Gobabeb site was estimated to be ~210,000 m^3 per 1 km of stream reach. Recharge estimations for the Rooifontein site varied between 41,000 and 81,000 m^3/km. Minimum recharge estimation at the Buffelsrivier site was 200,000 m^3/km.

7. References

Abdulrazzak, M.J. and Morel-seytoux, H.J., 1983. Recharge from an ephemeral stream following wetting front arrival to water-table. Water Resources Research, 19(1): 194-200.

Abdulrazzak, M.J. and Sorman, A.U., 1994. Transmission losses from ephemeral stream in arid region. Journal of Irrigation and Drainage Engineering-Asce, 120(3): 669-675.

Abdulrazzak, M.J., Sorman, A.U. and Alhames, A.S., 1989. Water-Balance approach under extreme arid conditions - a case-study of Tabalah Basin, Saudi-Arabia. Hydrological Processes, 3(2): 107-122.

Adams, S., Titus, R. and Xu, Y., 2004. Groundwater recharge assessment of the basement aquifers of Central Namaqualand. 1093/1/04, Water Research Commission, Pretoria.

Adar, E. and Nativ, R., 2003. Isotopes as tracers in a contaminated fractured chalk aquitard. Journal of Contaminant Hydrology, 65(1-2): 19-39.

Allemmoz, M. and Olive, P., 1978. Recharge of groundwater in arid areas: case of the Djeffara plain in Tripolitania, Lybian Arab Jamahiriya, IAEA, Vienna.

Allison, G.B., Gee, G.W. and Tyler, S.W., 1994. Vadose-zone techniques for estimating groundwater recharge in arid and semiarid regions. Soil Science Society of America Journal, 58(1): 6-14.

Allison, G.B. and Hughes, M.W., 1983. The use of natural tracers as indicators of soil-water movement in a temperate semi-arid region. Journal of Hydrology, 60(1-4): 157-173.

Amin, M.H.G., Hall, L.D., Chorley, R.J. and Richards, K.S., 1998. Infiltration into soils, with particular reference to its visualization and measurement by Magnetic Resonance Imaging (MRI). Progress in Physical Geography, 22(2): 135-165.

Amin, M.H.G., Richards, K.S., Chorley, R.J., Gibbs, S.J., Carpenter, T.A. and Hall, L.D., 1996. Studies of soil-water transport by MRI. Magnetic Resonance Imaging, 14(7-8): 879-882.

Anderson, T.W., Freethey, G.W. and Tucci, P., 1992. Geohydrology and water resources of alluvial basins in south-central Arizona and parts of adjacent states. 1406-B, U.S. geological survey.

Bailey, M.A., 2002. Analysis of one-dimensional vertical infiltration using heat as a tracer in Rillito Creek University of Arizona, Tucson, 152 pp.

Bate, G.C. and Walker, B.H., 1993. Water relations of the vegetation along the Kuiseb River, Namibia. Madoqua 18: 85-91.

Baver, L.D., Gardner, W.H. and Gardner, W.R., 1972. Soil Physics. John Wiley and Sons, New York, NY.

Bear, J., 1972. Dynamics of fluids in porous media. Elsvier, New York.

Bell, J.P., Dean, T.J. and Baty, A.J.B., 1987. Soil moisture measurement by an improved capacitance technique, part 2, field techniques, evaluation and calibration. Journal of Hydrology, 93: 79.

Bellon-Maurel, W., Orliac, O. and Christen, P., 2003. Sensors and measurements in solid state fermentation: a review. Process Biochemistry, 38(6): 881-896.

Besbes, M., Delhomme, J.P. and De Marsily, G., 1978. Estimating recharge from ephemeral streams in arid regions, a case study at Kairouan, Tunisia. Water Resources Research, 14(2): 281-290.

Blasch, K., Ferre, T.P.A., Hoffmann, J., Pool, D., Bailey, M. and Cordova, J., 2004. Processes controlling recharge beneath ephemeral streams in Southern Arizona.

In: J.F. Hogan, F.M. Phillips and B.R. Scanlon (Editors), Groundwater recharge in a desert environment: The southwestern United States. Water Science and Application 9. AGU, Washington DC, pp. 69-76.

Botes, A., Henderson, J., Nakale, T., Nantanga, K., Schachtschneider, K. and Seely, M., 2002. Environmental learning and action in the Kuiseb, 3rd WaterNet/Warfsa Symposium: Water demand management for sustainable development, Dar Es Salaam, Tanzania, pp. 630-638.

Botes, A., Henderson, J., Nakale, T., Nantanga, K., Schachtschneider, K. and Seely, M., 2003. Ephemeral rivers and their development: testing an approach to basin management committees on the Kuiseb River, Namibia. Physics and Chemistry of the Earth, 28(20-27): 853-858.

Bouwer, H., 2002. Artificial recharge of groundwater: hydrogeology and engineering. Hydrogeology Journal, 10(1): 121-142.

Brooks, R.H. and Corey, A.T., 1966. Properties of porous media affecting fluid flow. Journal of Irrigation and Drainage Div., American Society of Civil Engineering, 92(IR2): 61-88.

Bruce, R.R., Quisenberry, V.L., Scott, H.D. and Snyder, W.M., 1985. Irrigation practice for crop culture in the southeastern United States. Advances in irrigation, 3: 51-106.

Buckingham, E., 1907. Studies on the movement of soil moisture. 38, U.S. Department of Agriculture Bureau Soils.

Bull, L.J. and Kirkby, M.j., 2002. Dryland rivers - hydrology and geomorphology of semi arid channels. John Wiley & Sons, England, 388 pp.

Cancela, J.J., Dafonte, J., Martinez, E.M., Cuesta, T.S. and Neira, X.X., 2006. Assessment of a water activity meter for rapid measurements of soil water potential. Biosystems Engineering, 94(2): 285-295.

Cary, J.W., Gee, G.W. and Simmons, C.S., 1991. Using an electro-optical switch to measure soil water suction. soil Science Society of America Journal, 55: 1798.

Cataldo, J., Behr, C., Montalto, F. and Pierce, R.J., 2004. A summary of published reports of transmission losses in ephemeral streams in the U.S., eDesign Dynamics, LLC, New York.

Chanzy, A., Chadoeuf, J., Gaudu, J.C., Mohrath, D., Richard, G. and Bruckler, L., 1998. Soil moisture monitoring at the field scale using automatic capacitance probes. European Journal of Soil Science, 49(4): 637-648.

Childs, E.C. and Bybordi, M., 1969. Vertical movement of water in stratified porous material .I. infiltration. Water Resources Research, 5(2): 446.

Chow, V.T., 1964. Handbook of applied hydrology. McGraw-Hill Book Company.

Constantz, J., Thomas, C.L. and Zellweger, G., 1994. Influence of diurnal-variations in stream temperature on streamflow loss and groundwater recharge. Water Resources Research, 30(12): 3253-3264.

Cook, P.G., Walker, G.R., Buselli, G., Potts, I. and Dodds, A.R., 1992. The application of electromagnetic techniques to groundwater recharge investigations. Journal of Hydrology, 130(1-4): 201-229.

Cornelissen, A.K., unknown year. Water from the Buffels River, Ookiep Copper Company.

Dahan, O., McDonald, E.V. and Young, M.H., 2003. Flexible time domain reflectometry probe for deep vadose zone monitoring. Vadose Zone Journal, 2(2): 270-275.

Dahan, O., Rimon, Y., Tatarsky, B. and Talby, R., 2006. Deep vadose zone monitoring system, TDR 2006: 3rd International Symposium on Time Domain Reflectometry for Innovative Soils Applications, Purdue University, USA.

Dahan, O., Shani, Y., Enzel, Y., Yechieli, Y. and Yakirevich, A., 2007a. Direct measurements of floodwater infiltration into shallow alluvial aquifers. Journal of Hydrology, doi:10.1016/j.jhydrol.2007.06.033.

Dahan, O., Tatarsky, B., Enzel, Y., Kulls, C., Seely, M. and Benito, G., 2007b. Flood-water infiltration and ground-water recharge in the hyperarid Kuiseb River, Namibia. Journal of Hydrology, in press.

Dalton, F.N. and Van Genuchten, M.T., 1986. The time domain reflectometry method for measuring soil water content and salinity. Geoderma, 38: 237-250.

de Vries, J. and Simmers, I., 2002. Groundwater recharge: an overview of processes and challenges. Hydrogeology Journal, 10(1): 5-17.

Dregne, H., 1991. Global status of desertification. Annals of Arid Zone(30): 179-185.

Duliu, O.G., 1999. Computer axial tomography in geosciences: an overview. Earth-Science Reviews, 48(4): 265-281.

Edmunds, W.M., 1998. Recharge to groundwater in arid and semi-arid regions from the Holocene to the present. In: A.S. Alsharhan, K.W. Glennie, G.L. Whittle and C.G.S.C. Kendall (Editors), Quaternary deserts and climate change. A.A Balkema, Rotterdam, pp. 419-431.

El-Hames, A.S. and Richards, K.S., 1998. An integrated, physically based model for arid region flash flood prediction capable of simulating dynamic transmission loss. Hydrological Processes, 12(8): 1219-1232.

Enzel, Y., 1990. Hydrology of a large, closed arid watershed as a basis for paleohydrological and paleoclimatological studies in the Mojave River drainage system, southern California. PhD Thesis, University of New Mexico, 315 pp.

Enzel, Y. and Wells, S.G., 1997. Extracting Holocene paleohydrology and paleoclimatology information from modern extreme flood events: An example from southern California. Geomorphology, 19(3-4): 203-226.

Esterhuyse, 2006. Report back on Buffelsrivier Hydrocensus conducted on 3 and 4 September 2006, SRK Consulting SA (Pty) Ltd, Rondebosch.

Faybishenko, B.A., 1995. Hydraulic behavior of quasi-saturated soils in the presence of entrapped air - laboratory experiments. Water Resources Research, 31(10): 2421-2435.

Ferre, T.P.A., Knight, J.H., Rudolph, D.L. and Hachanoski, R.G., 1998. The sample area of conventional and alternative time domain reflectometry probes. Water Resources Research, 34: 2971-2979.

Feth, J.H., 1964. Hidden recharge. Ground Water, 2((4)): 14-17.

Fetter, C.W., 1988. Applied hydrogeology. Macmillan Publishing Company, New York.

Flint, A.L., Campbell, G.S., Ellett, K.M. and Calissendorff, C., 2002a. Calibration and temperature correction of heat dissipation matric potential sensors. Soil Science Society of America Journal, 66(5): 1439-1445.

Flint, A.L., Flint, L.E., Kwicklis, E.M., Fabryka-Martin, J.T. and Bodvarsson, G.S., 2002b. Estimating recharge at Yucca Mountain, Nevada, USA: comparison of methods. Hydrogeology Journal, 10(1): 180-204.

Flischer, A., Flischer, L. and Frizlander, A., 1997. Hydrogeology of the Idan - Ein-Yahav region. 820/147/96, Israel geophysical Institute (in Hebrew).

Freyberg, D.L., Reeder, J.W., Franzini, J.B. and Remson, I., 1980. Application of the Green-Ampt model to infiltration under time-dependent surface-water depths. Water Resources Research, 16(3): 517-528.

Gardner, W.H., 1986. Water content. In: A. Klute (Editor), Methods of soil analysis. Agronomy, pp. 493-544.

Gardner, W.R., Hillel, D. and Benyamini, Y., 1970. Post-irrigation movement of soil water: 2. Simultaneous redistribution and evaporation. Water Resources Research, 6: 1148-1153.

Gat, J.R. and Issar, A., 1974. Desert isotope hydrology: water sources of the Sinai Desert. Geochimica et Cosmochimica Acta, 38(7): 1117-1131.

Gee, G.W., Campbell, M.D., Campbell, G.S. and Campbell, J.H., 1992a. Rapid measurement of low soil-water potentials using a water activity meter. Soil Science Society of America Journal, 56(4): 1068-1070.

Gee, G.W., Fayer, M.J., Rockhold, M.L. and Campbell, M.D., 1992b. Variations in recharge at the Hanford site. Northwest Science, 66(4): 237-250.

Gee, G.W. and Hillel, D., 1988. Groundwater recharge in arid regions - review and critique of estimation methods. Hydrological Processes, 2(3): 255-266.

Gelt, J., Henderson, J., Seasholes, K., Tellman, B. and Woodard, G., 1999. Water in the Tucson area: seeking sustainability, Water resources research center, Tucson AZ.

Goodrich, D.C., Williams, D.G., Unkrich, C.L., Hogan, J.F., Scott, R.L., Hultine, K.R., Pool, D., Alissa, L.C. and Miller, S., 2004. Comparison of methods to estimate ephemeral channel recharge, Walnut Gulch, San Pedro River Basin, Arizona. In: J.F. Hogan, F.M. Phillips and B.R. Scanlon (Editors), Groundwater recharge in a desert environment: The southwestern United States. AGU, Washington, DC, pp. 77-99.

Goudie, A., 1972. Climate, weathering, crust formation, dunes and fluvial features of the Central Namib Desert, near Gobabeb, South West Africa. Madoqua, 1: 15-31.

Green, W.H. and Ampt, G.A., 1911. Studies on soil physics:1. The flow of air and water through soils. Journal of Agriculture Science, 4: 1-24.

Gurr, C.G., 1962. Use of gamma rays in measuring water content and permeability in unsaturated columns of soil. Soil Science, 94: 224-229.

Guzman, A.G., Wilson, L.G., Neuman, S.P. and Osborn, M.D., 1989. Simulating effect of channel changes on stream infiltration. Journal of Hydraulic Engineering-Asce, 115(12): 1631-1645.

Haimerl, G., 2004. Groundwater recharge in wadi channels downstream of dams - efficiency and management strategies. PhD thesis., 167 pp.

Hattle, A., 1985. Surface water hydrology of the Kuiseb. In: B.J. Huntley (Editor), The Kuiseb environment: the development of a monitoring baseline. South African national scientific programmes, Pretoria, pp. 27-32.

Healy, R.W. and Cook, P.G., 2002. Using groundwater levels to estimate recharge. Hydrogeology Journal, 10(1): 91-109.

Heidbüchel, I., 2007. Recharge processes in ephemeral streams derived from a coupled stream flow routing / groundwater model -application to the Lower Kuiseb (Namibia). Thesis., University of Freiburg Freiburg, Germany.

Heimovaara, T.J., 1994. Frequency domain analysis of time domain reflectometry waveforms. 1. Measurement of the complex dielectric permittivity of soils. Water Resources Research, 30: 189-199.

Hendrickx, J.M.H. and Walker, G.R., 1997. Recharge from precipitation. In: I. Simmers (Editor), Recharge of phreatic aquifers in (semi-) arid areas. International association of hydrogeologists. A.A. Balkema, Rotterdam, pp. 19-111.

Heyns, P., Coetzee, M., Hoffmann, K.H., Mendelsohn, J., Schneider, G. and Seimons, W., 2001. Groundwater in Namibia - an explanation of the hydrogeological map, Depatment of Water Affairs, division Geohydrology, Windhoek.

Hillel, D., 1980. Fundamentals of soil physics. Academic Press, New York.

Hillel, D., 2004. Introduction to environmental soil physics. Elsevier Science, San Diego, California.

Hughes, D.A. and Sami, K., 1992. Transmission losses to alluvium and associated moisture dynamics in a semiarid ephemeral channel system in Southern Africa. Hydrological Processes, 6(1): 45-53.

Huisman, J.A., Hubbard, S.S., Redman, J.D. and Annan, A.P., 2003. Measuring soil water content with Ground Penetrating Radar: a review. Vadose Zone Journal, 2: 476-491.

Huntley, B.J., 1985. The Kuiseb environment: the development of a monitoring baseline, Report No. 106. South African national scientific programmes, Pretoria, 138 pp.

Issar, A. and Passchier, R., 1990. Regional hydrogeological concepts. In: D.E. Lerner, A.S. Issar and I. Simmers (Editors), Groundwater Recharge: A guide to understanding and estimating natural recharge. International Contributions to Hydrology. Verlag Hientz Hiese, pp. 21-37.

Jackson, T.J., 2002. Remote sensing of soil moisture: implications for groundwater recharge. Hydrogeology Journal, 10(1): 40-51.

Jacobson, P.J., Jacobson, K.M. and Seely, M., 1995. Ephemeral rivers and their catchments: sustaining people and development in Western Namibia. Desert Research Foundation of Namibia, Windhoek, 160 pp.

Jones, S.B., Wraith, J.M. and Or, D., 2002. Time domain reflectometry measurement principles and applications. Hydrological Processes, 16(1): 141-153.

Knighton, A.D. and Nanson, G.C., 1994. Flow Transmission Along an Arid Zone Anastomosing River, Cooper Creek, Australia. Hydrological Processes, 8(2): 137-154.

Konig, E.H., 1992. Investigation into poor drinking-water quality at Gobabeb research station. WQ/92/06, Ministry of Agriculture, Water and rural Development, Windhoek.

Kruseman, G.P., 1997. Recharge from intermittent flow. In: I. Simmers (Editor), Recharge of phreatic aquifers in (semi-) arid areas. International association of hydrogeologists. A.A. Balkema, Rotterdam, pp. 145-184.

Lange, J., 2005. Dynamics of transmission losses in a large arid stream channel. Journal of Hydrology, 306(1-4): 112-126.

Lebert, T.S., 2005. Land tenure reform in Namaqualand: elite capture and the new commons of Leliefontein, University of the Western Cape, South Africa.

Ledieu, J., de Ridder, P., De Clerck, P. and Dautrebande, S., 1986. A method of measuring soil moisture by time-domain reflectometry. Journal of Hydrology, 88: 319-328.

Lenz, R., Grobbelaar, H. and Djama, M., 1995. Groundwater exploration in the Kuiseb dune area, Reports of the German Namibian Groundwater exploration project (GNGEP), BGR, Hannover.

Lerner, D.E., Issar, A.S. and Simmers, I., 1990. Groundwater recharge: A guide to understanding and estimating natural recharge. International Contributions to Hydrology, 8. Verlag Hientz Hiese.

Logsdon, S.D., 2000. Effect of cable length on time domain reflectometry calibration for high surface area soils. Soil Science Society of America Journal, 64: 54-61.

Low, A.B. and Rebelo, A.G., 1996. Vegetation of South Africa, Lesotho and Swaziland, Department of Environmental Affairs and Tourism, Pretoria.

Marais, J.A.H., 1981. Update technical report on the Spektakel water scheme in the district of Springbok C.P., Nababeep.

Marshall, T.J., Holmes, J.W. and Rose, C.W., 1996. Soil physics. Cambridge University Press, New York, 453 pp.

Mattikalli, N.M., Engman, E.T., Jackson, T.J. and Ahuja, L.R., 1998. Microwave remote sensing of temporal variations of brightness temperature and near-surface soil water content during a watershed-scale field experiment, and its application to the estimation of soil physical properties. Water Resources Research, 34(9): 2289-2299.

Maurer, D.K. and Fischer, J.M., 1988. Recharge to the Eagle Valley groundwater basin by stream flow in Vicee Canyon, West-Central Nevada. 88-4158, USGS Water-resources investigation report.

Mualem, Y., Assouline, S. and Rohdenburg, H., 1990. Rainfall induced soil seal .a. A critical-review of observations and models. Catena, 17(2): 185-203.

Mudd, S.M., 2006. Investigation of the hydrodynamics of flash floods in ephemeral channels: Scaling analysis and simulation using a shock-capturing flow model incorporating the effects of transmission losses. Journal of Hydrology, 324(1-4): 65-79.

Ollier, C.D., 1977. Outline geological and geomorphic history of the Central Namib Desert. Madoqua, 10(3): 207-212.

Osterkamp, W.R., Lane, L.J. and Savard, C.S., 1994. Recharge estimates using a geomorphic distributed-parameter simulation approach, Amargosa River Basin. Water Resources Bulletin, 30(3): 493-507.

Owe, M., Vandegriend, A.A. and Chang, A.T.C., 1992. Surface moisture and satellite microwave observations in semiarid Southern Africa. Water Resources Research, 28(3): 829-839.

Parissopoulos, G.A. and Wheater, H.S., 1991. Effects of Wadi flood hydrograph characteristics on infiltration. Journal of Hydrology, 126(3-4): 247-263.

Philip, J.R., 1957. The theory of infiltration. 1. The infiltration equation and its solution. Soil Science, 83: 345-357.

Philip, J.R., 1971. General theorem on steady infiltration from surface sources, with application to point and line sources. Soil Science Society of America Proceedings, 35(6): 867-&.

Phillips, F.M., 1994. Environmental tracers for water-movement in desert soils of the American Southwest. Soil Science Society of America Journal, 58(1): 15-24.

Phillips, F.M., 1995. The use of isotopes and environmental tracers in subsurface hydrology. Reviews of Geophysics, 33: 1029-1033.

Phillips, F.M., Hogan, J.F. and Scanlon, B.R., 2004. Introduction and overview. In: J.F. Hogan, F.M. Phillips and B.R. Scanlon (Editors), Groundwater recharge in a desert environment: the Southwestern United States. Water Science and Application 9. AGU, Washington DC, pp. 1-14.

Raats, P.A.C., 2001. Developments in soil-water physics since the mid 1960s. Geoderma, 100(3-4): 355-387.

Reid, I. and Frostick, L.E., 1997. Channel form, flows and sediments in deserts. In: D.S.G. Thomas (Editor), Arid zone geomorphology: Process, form and change in drylands. John Willey & Sons Ltd., pp. 205-229.

Richards, L.A., 1931. Capillary conduction of liquids through porous mediums. physics, 1: 318-333.

Rimon, Y., Dahan, O., Nativ, R. and Geyer, S., 2007. Water percolation through the deep vadose zone and groundwater recharge: Preliminary results based on a new vadose zone monitoring system. Water Resources Research, 43(5).

Robinson, D.A., Jones, J.M., Wraith, J.M., Or, D. and Friedman, S.P., 2003. A review of advances in dielectric and electrical conductivity measurement in soils using Time Domain Reflectometry. Vadose Zone Journal, 2: 444-475.

Romkens, M.J.M., Prasad, S.N. and Whisler, F.D., 1990. Surface sealing and infiltration. In: M.G. Anderson and T.P. Burt (Editors), Process studies in hillslope hydrology. Wiley, Chichester.

Rushton, K.R., Eilers, V.H.M. and Carter, R.C., 2006. Improved soil moisture balance methodology for recharge estimation. Journal of Hydrology, 318(1-4): 379-399.

Sanford, W., 2002. Recharge and groundwater models: an overview. Hydrogeology Journal, 10(1): 110-120.

Scanlon, B. and Cook, P., 2002. Theme issue on groundwater recharge. Hydrogeology Journal, 10(1): 3-4.

Scanlon, B., Healy, R. and Cook, P., 2002. Choosing appropriate techniques for quantifying groundwater recharge. Hydrogeology Journal, 10(1): 18-39.

Scanlon, B.R., Keese, K.E., Flint, A.L., Flint, L.E., Gaye, C.B., Edmunds, W.M. and Simmers, I., 2006. Global synthesis of groundwater recharge in semiarid and arid regions. Hydrological Processes, 20(15): 3335-3370.

Scanlon, B.R., Langford, R.P. and Goldsmith, R.S., 1999. Relationship between geomorphic settings and unsaturated flow in an arid setting. Water Resources Research, 35(4): 983-999.

Scanlon, B.R., Tyler, S.W. and Wierenga, P.J., 1997. Hydrologic issues in arid, unsaturated systems and implications for contaminant transport. Reviews of Geophysics, 35(4): 461-490.

Schmidt, G., 1998. Kuiseb dune area assessment of the groundwater potential, reports of the German Namibian exploration project (GNGEP), BGR, Hannover.

Scholz, 1972. The soils of the Central Namib Desert with special consideration of the soils in the vicinity of Gobabeb. Madoqua, 1: 33-51.

Schwartz, U., 2001. Surface and near-surface responses to floods in a large channel (Nahal Zin) in the context of an alluvial aquifer in a hyper-arid environment. PhD Thesis., Hebrew University, Jerusalem.

Shani, Y., 2006. Floodwater percolation and groundwater recharge in arid lands, Arava, Israel. MSc. Thesis, 95 pp.

Sharma, K.D. and Murthy, J.S.R., 1994. Estimating Transmission Losses in an Arid Region. Journal of Arid Environments, 26(3): 209-219.

Shentsis, I., 2003. Increasing transmission losses from flood events due to groundwater extraction. Hydrological Processes, 17: 713-725.

Shentsis, I., Meirovich, L., Ben-Zvi, A. and Rosenthal, E., 1999. Assessment of transmission losses and groundwater recharge from runoff events in a wadi under shortage of data on lateral inflow, Negev, Israel. Hydrological Processes, 13(11): 1649-1663.

Slabbert, A., 1991. Water resource development for Walvis Bay Walvis Bay Workshop. Department of Water Affairs and Forestry, Walvis Bay, pp. 28-63.

Sorman, A.U. and Abdulrazzak, M.J., 1993. Infiltration-Recharge through Wadi Beds in Arid Regions. Hydrological Sciences Journal-Journal Des Sciences Hydrologiques, 38(3): 173-186.

Sorman, A.U., Abdulrazzak, M.J. and Morel-Seytoux, H.J., 1997. Groundwater recharge estimation from ephemeral streams. Case study: Wadi Tabalah, Saudi Arabia. Hydrological Processes, 11(12): 1607-1619.

Stengel, H.W., 1968. The source of drinking water at Gobabeb. Watter Affairs Branch, S.W.A. Administration.

Stephens, D.B., 1995. Vadose Zone Hydrology. CRC Press, 347 pp.

Talby, R., 2006. Water percolation from stream bed channel in wadi Arava, Israel, Ben-Gurion University of the Negev, Beer Sheva.

Tankard, A.J., Jacobson, M.P., Eriksson, K.A., Hobday, D.K., Hunter, D.R. and Minter, W.E.L., 1982. Crustal evolution of South Africa: 3.8 Billion years of earth history. Springer-Verlag, New York.

Theron, G.K., van Rooyen, N. and van Rooyen, M.W., 1985. Vegetation of the Lower Kuiseb River. In: B.J. Huntley (Editor), The Kuiseb environment: the development of a monitoring baseline. South African national scientific programmes, Pretoria, pp. 73-79.

Titus, R., Adams, S., Pietersen, K. and Tredoux, G., 2000. Groundwater flow patterns in fractured rocks of central Namaqualand, South Africa. Journal of Hydrology.

Titus, R., Pietersen, K., Williams, M., Adams, S., Xu, Y., Saayman, I. and Colvin, C., 2002. Groundwater assessment and strategies for sustainable resource supply in arid zones - the Namaqualand case study. 721/1/02, Water Research Commission, Pretoria.

Topp, G.C., Davis, J.L. and Annan, A.P., 1980. Electromagnetic determination of soil water content: measurements in coaxial transmission lines. Water Resources Research, 16(3): 574-582.

Ulaby, F.T., Dubois, P.C. and vanZyl, J., 1996. Radar mapping of surface soil moisture. Journal of Hydrology, 184(1-2): 57-84.

van Genuchten, M.T., 1980. A closed-form equation for predicting the hydraulic conductivity of unsaturated soils. Soil Science Society of America Journal, 44: 892-898.

visser, D., 1989. Explanation of the 1:1,000,000 geological map. Department of Mineral and Energy Affairs- Government Printer.

Visser, D., 2006. Report on a preliminary assessment of the groundwater exploitation potential of the Spektakel Alluvial Aquifer in the Buffels River, SRK consulting SA (Pty) Ltd, Rondebosch.

Walvoord, M.A. and Scanlon, B.R., 2004. Hydrologic processes in deep vadose zones in interdrainage arid environments. In: J.F. Hogan, F.M. Phillips and B.R. Scanlon (Editors), Groundwater recharge in a desert environment: The southwestern United States. AGU, Washington, DC, pp. 15-28.

Wang, X.P., Li, X.R., Xiao, H.L., Berndtsson, R. and Pan, Y.X., 2007. Effects of surface characteristics on infiltration patterns in an and shrub desert. Hydrological Processes, 21(1): 72-79.

Ward, J.D., 1987. The Cenozoic succession in the Kuiseb Valley, Central Namib Desert, Geological Survey of Namibia, Windhoek.

Warrick, A.W., 2002. Soil Physics Companion. CRC Press, 389 pp.

Whalley, W.R., Dean, T.J. and Izzard, P., 1992. Evaluation of the Capacitance Technique as a Method for Dynamically Measuring Soil-Water Content. Journal of Agricultural Engineering Research, 52(2): 147-155.

Wright, C.E., 1980. Surface water and groundwater interaction, UNESCO - Studies and reports in hydrology.

Zimmermann, U., Munnich, K.O. and Roether, W., 1967. Downward movement of soil moisture traced by means of hydrogen isotopes. American Geophysical Union Geoph. Monograph, 11: 28-36.

Appendix 1: FTDR calibration curves

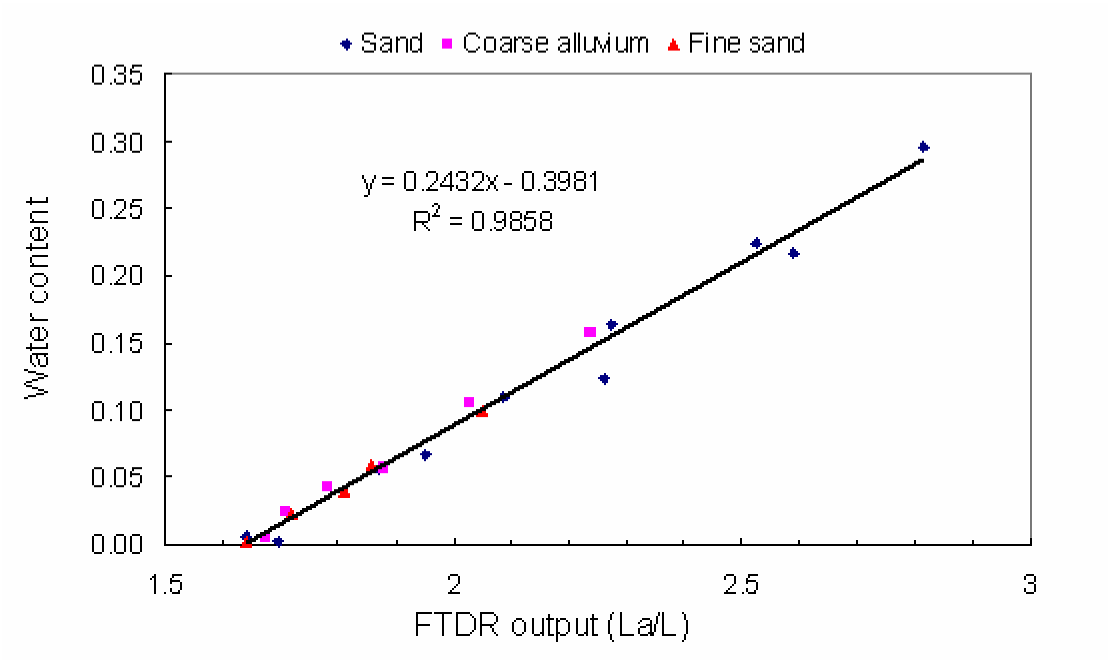

Figure 1.1. *Calibration curve for the flexible TDR probe output (La/L) vs. water content measured by the gravimetric method*

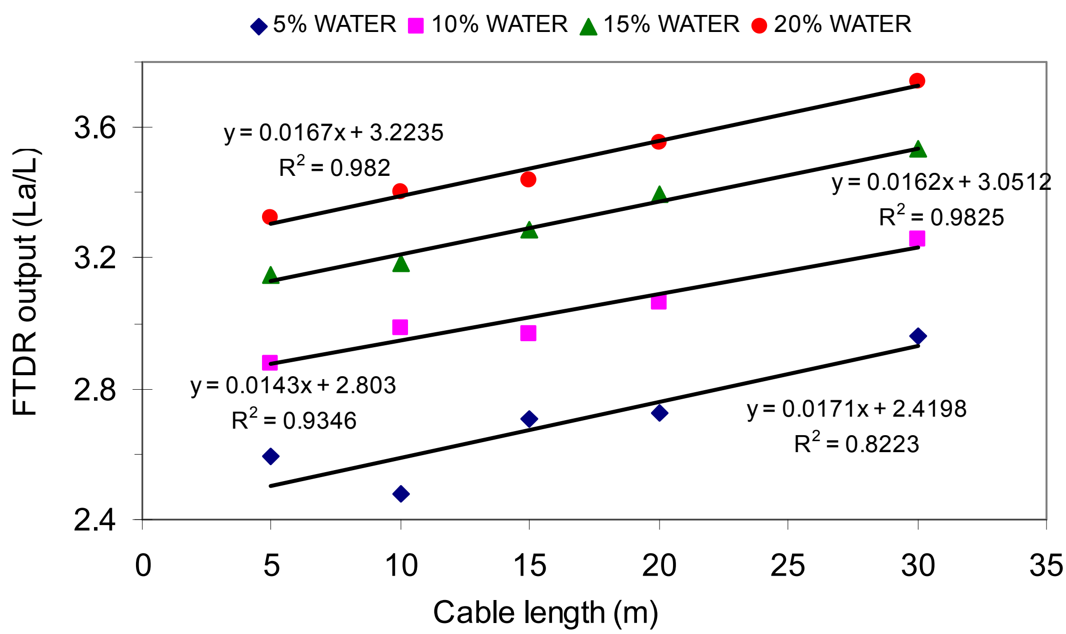

Figure 1.2. *Calibration curves for cable length vs. FTDR output (La/L). Each set of data presents the FTDR outputs achieved by the different cable lengths as measured at a known permittivity of a given dilution ratio of acetic acid solution and water (5%, 10%, 15% and 20% water dilution).*

Appendix 2: Boreholes location and orientation, GOB1 and GOB2

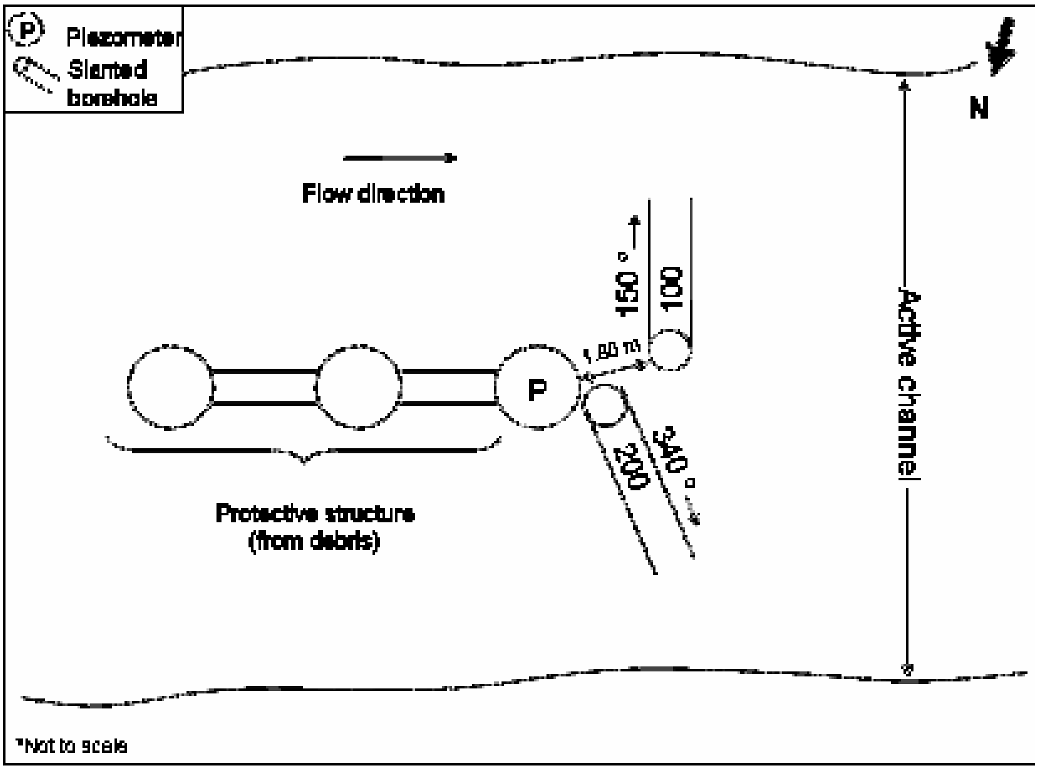

Figure 2.1*. Boreholes (100, 200) location and orientation at the GOB 1 station, Gobabeb, (bird-eye view)*

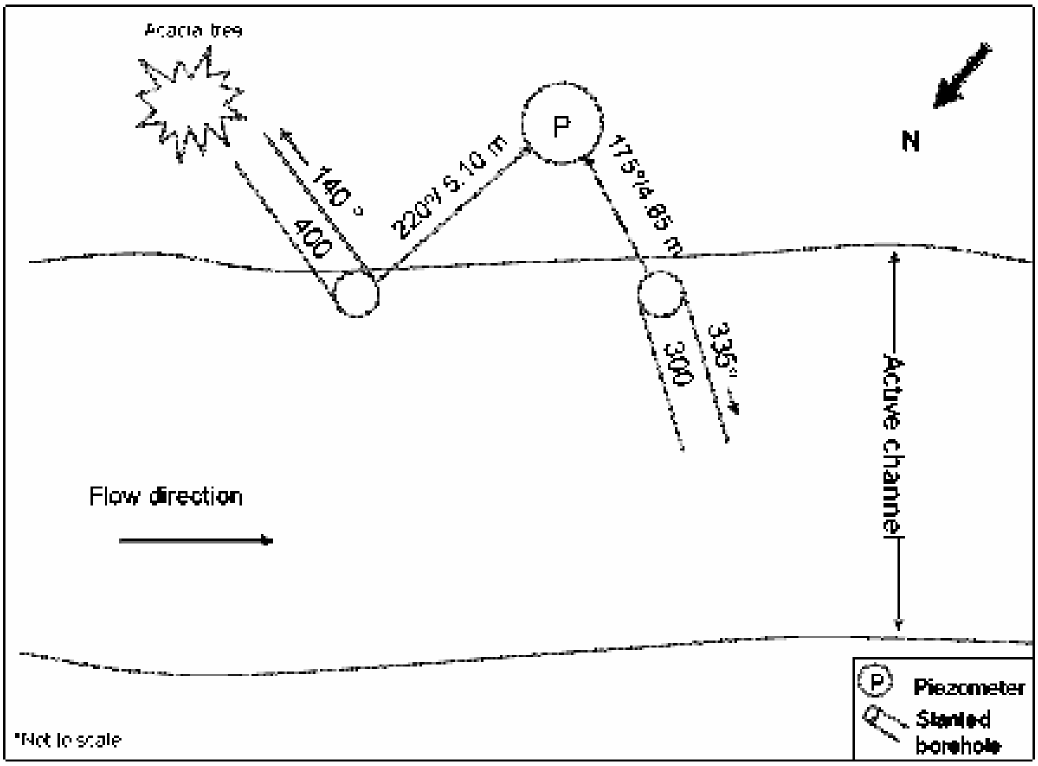

Figure 2.2*. Boreholes (300, 400) location and orientation at the GOB 2 station, Gobabeb, (bird-eye view)*

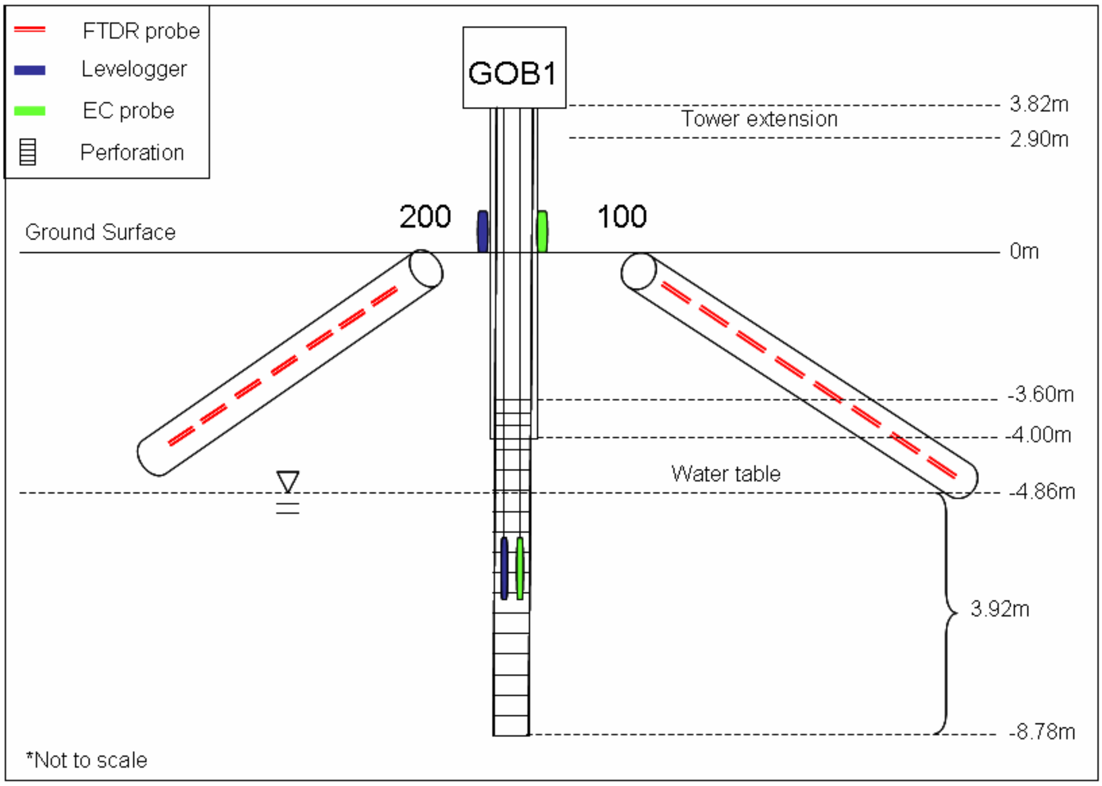

Figure 2.3. *Schematic cross section of the GOB 1 monitoring station set-up (borehole 100 was found to be malfunctioning after installation)*

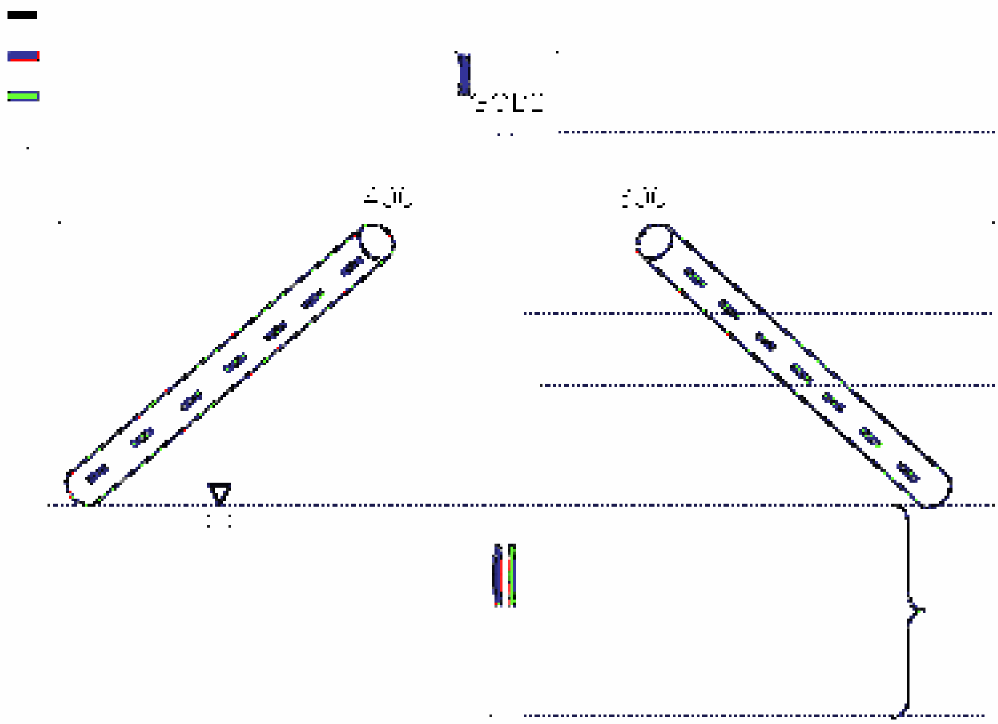

Figure 2.4. *Schematic cross section of the GOB 2 monitoring station set-up*

Appendix 3: Kuiseb River longitude profile and cross section

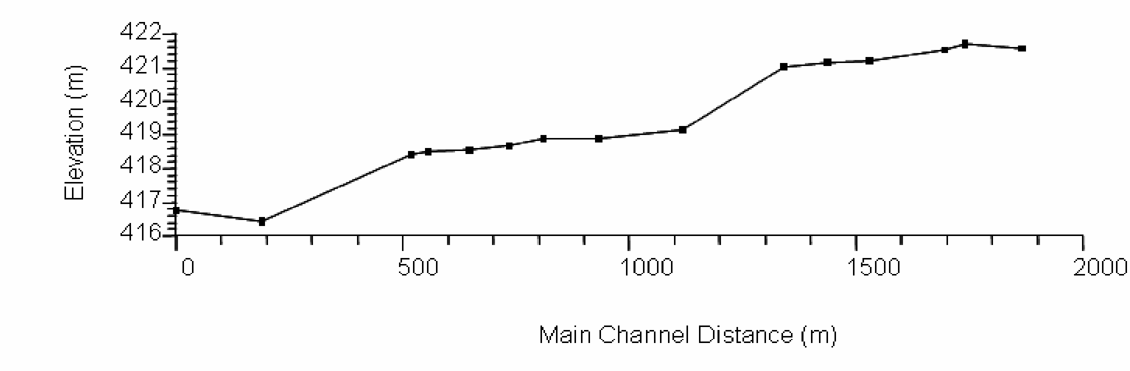

Figure 3.1. *Longitude profile of the Kuiseb channel near Gobabeb*

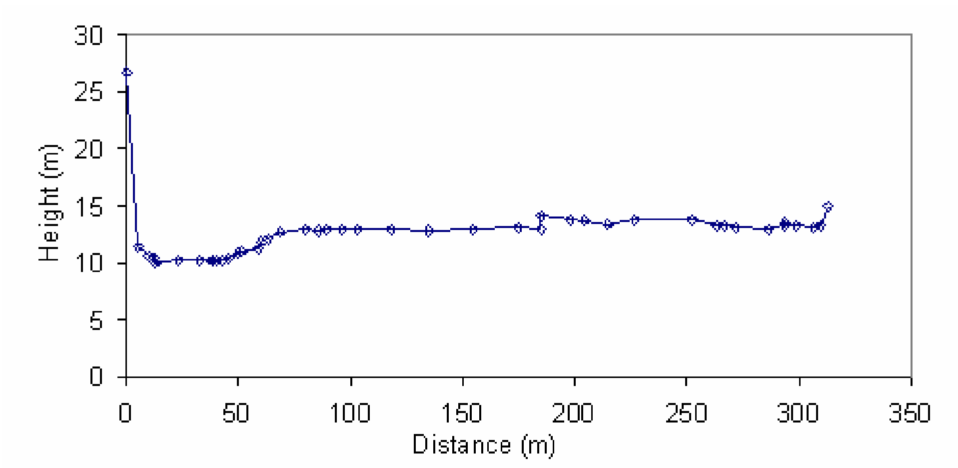

Figure 3.2. *Cross section of the Kuiseb by GOB 1 station*

Appendix 4: Bulk density and porosity at Gobabeb

Location	Depth (cm)	Bulk density (gr/cm^3)	Porosity
Middle of channel	50	1.657	0.389
	100	1.631	0.368
	160	1.546	0.414
	190	1.528	0.440
	230	1.536	0.440
Flood-plains	50	1.327	0.501
	100	1.247	0.531
	150	1.621	0.409
	200	1.592	0.368

Appendix 5: Buffels River catchment name map

Figure 1. *Place name map of the Buffels River study region showing the location of the Spektakel Aquifer and monitoring stations*

Appendix 6: Buffels River longitude profile and cross section

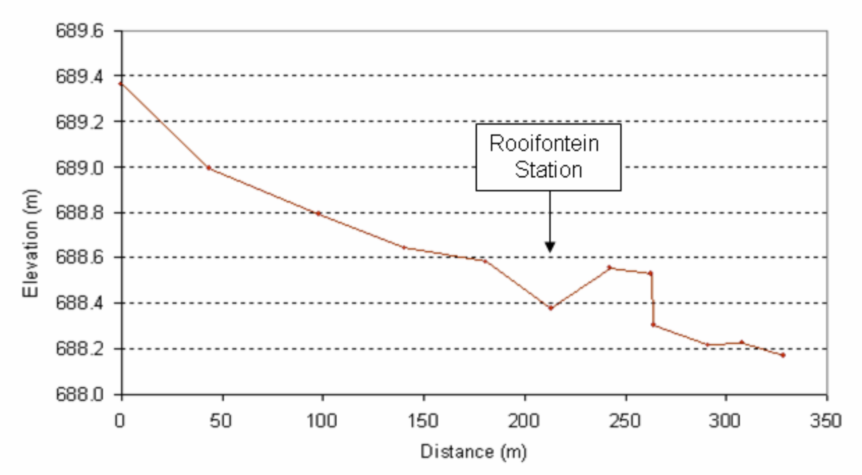

Figure 6.1. *Longitude profile of the Buffels River near the Rooifontein station*

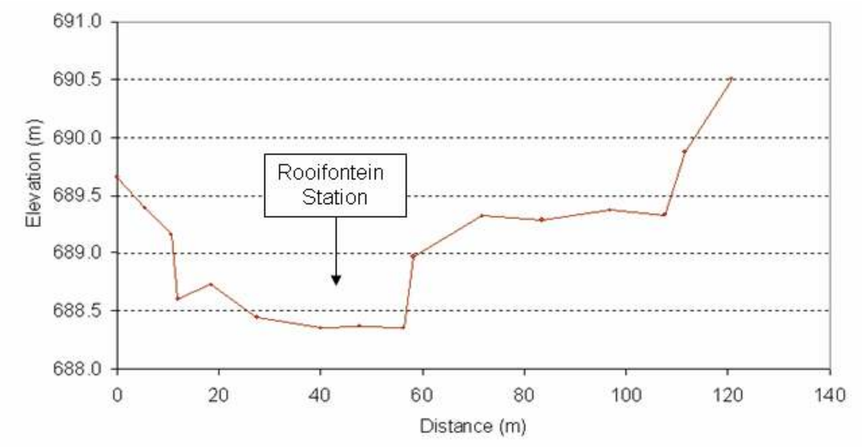

Figure 6.2*. Cross section of the Buffels River at the Rooifontein station*

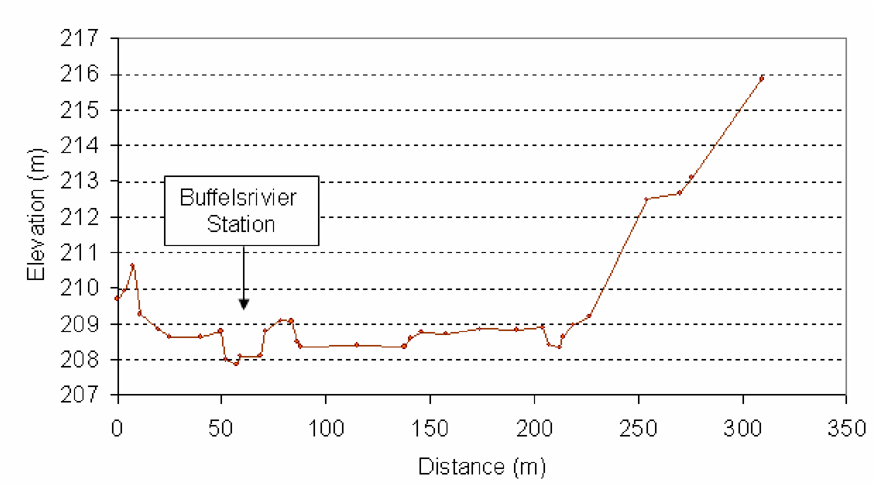

Figure 6.3. *Cross section of the Buffels River at the Buffelsrivier Station*

Appendix 7: Location and orientation of boreholes at Rooifontein

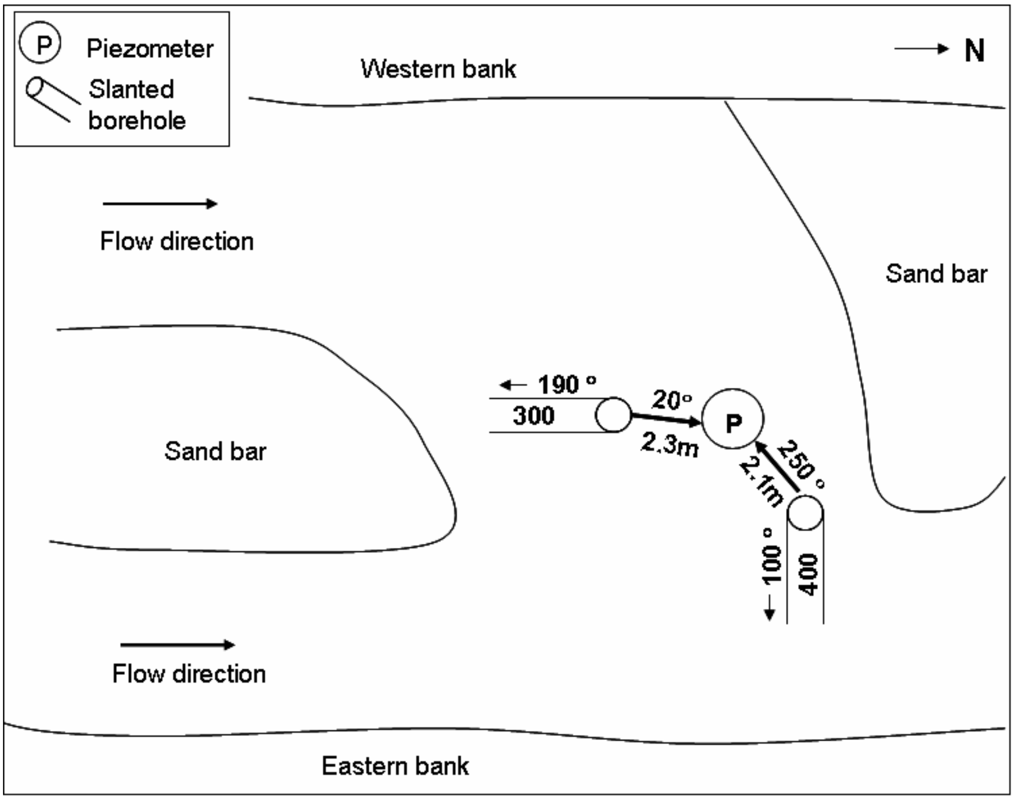

Figure 7.1. *Boreholes (300, 400) location and orientation at the Rooifontein station, Buffels River, (bird-eye view)*

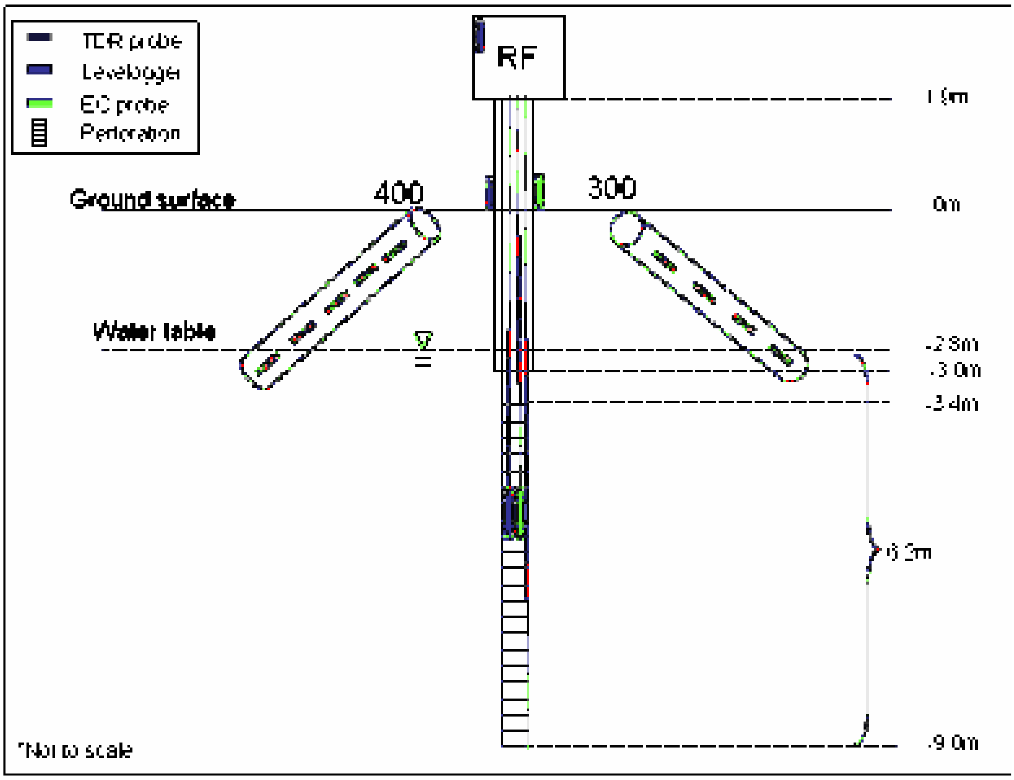

Figure 7.2*. Schematic cross section of the Rooifontein monitoring station set-up*

Figure 7.3. *The Rooifontein Station during a flood event (photograph taken by Simon Todd)*

Appendix 8: Location and orientation of boreholes at Buffelsrivier

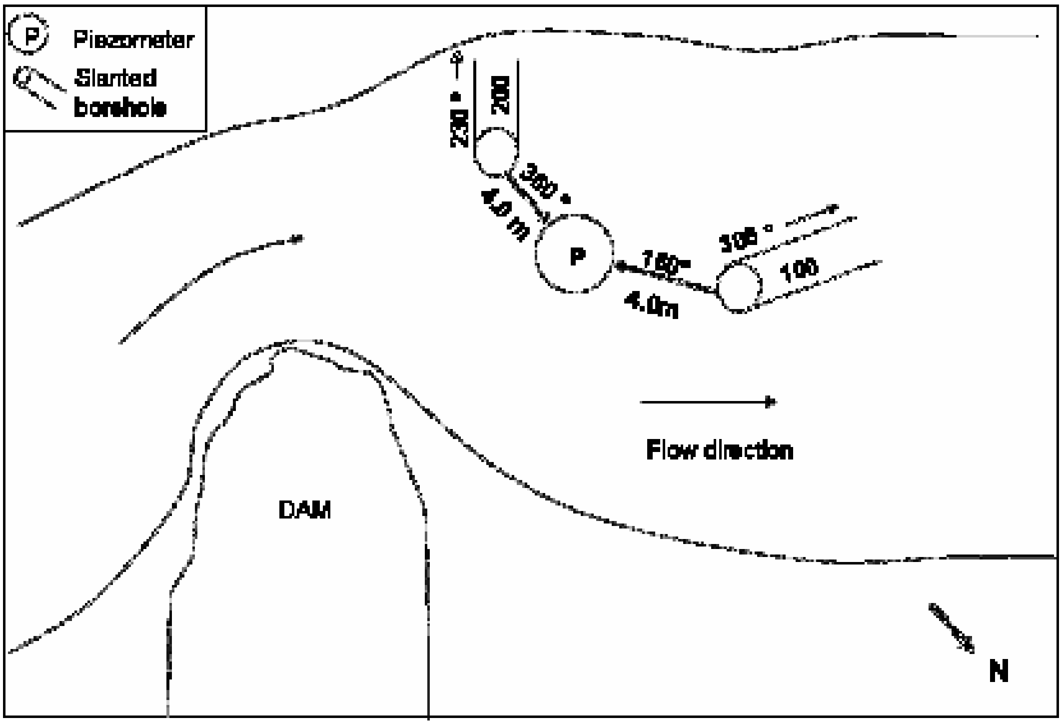

Figure 8.1. *Boreholes (100, 200) location and orientation at the Buffelsrivier station, Buffels River, (bird-eye view)*

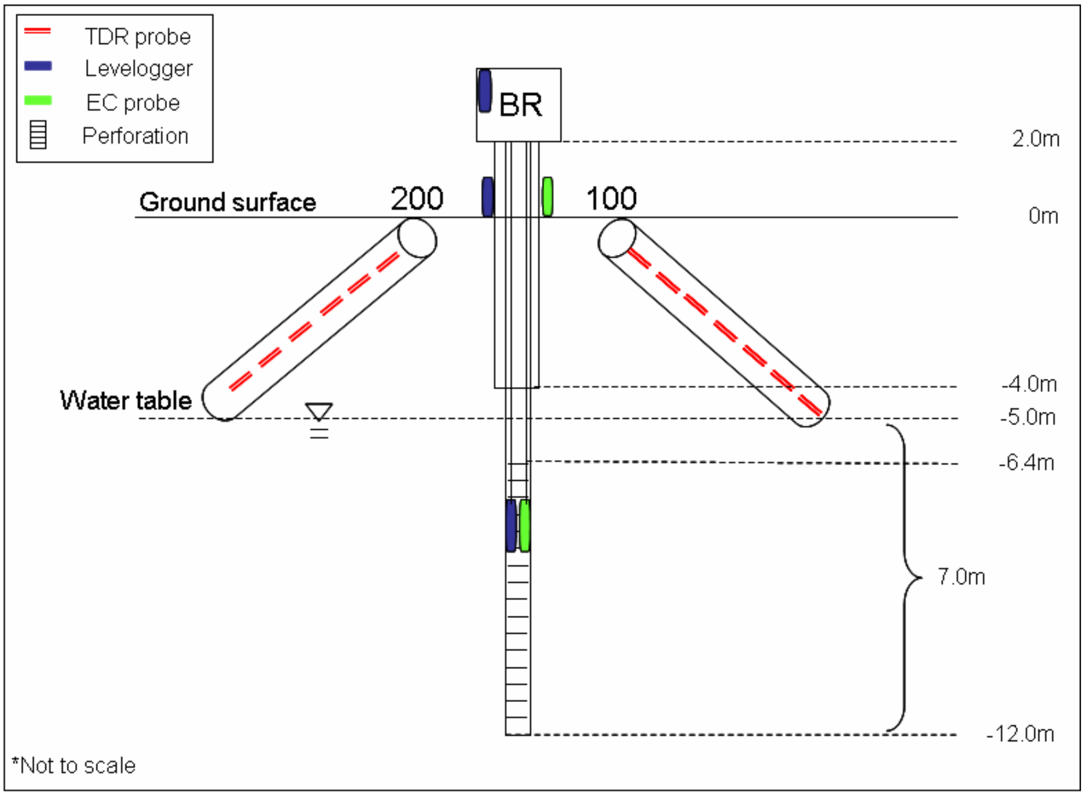

Figure 8.2. *Schematic cross section of the Buffelsrivier monitoring station set-up*

Figure 8.3. *The Buffelsrivier Station during a flood event, August 10th 2007 (photograph taken by Simon Todd)*

Appendix 9: Summary of flood events

Table 9.1. *Gobabeb Station*

Flood no.	Start	End	Duration	Max. stage (cm)	No. of peaks	Time since last flood
1	20/01/2006 20:00	24/01/2006 00:00	76h	150	3	first flood of the season
2	26/01/2006 16:45	31/01/2006 14:00	120h	200	3	~2.5d
3	06/02/2006 04:00	08/02/2006 20:00	67h	80	3	~5.5d
4	11/02/2006 06:00	13/02/2006 03:00	36h	30	1	~2.5d
5	19/02/2006 15:00	04/03/2006 08:00	13.5d	320	8	~6.5d

Table 9.2. *Buffelsrivier Station*

Flood no.	Start	End	Duration	Max. stage (cm)	No. of peaks	Time since last flood
1	17/10/2005 20:15	19/10/2005 3:15	30h	45	1	1st flood
2	29/10/2005 22:15	30/10/2005 7:30	9.5h	14	1	10 days
3	22/04/2006 13:35	23/04/2006 02:35	13h	18.5	1	6 months
4	18/05/2006 17:50	01/06/2006 2:00	12 d	60	2	1 month
5	12/06/2006 21:30	22/06/2006 21:00	10d	50	2	12d
6	14/07/2006 18:40	15/09/2006 05:00	2 months	45	4	1 month
7	06/06/2007 20:30	after 05/07/07	>1 month	60	5	9 months

Table 9.3. *Rooifontein Station*

Flood no.	Start	End	Duration	Max. stage (cm)	No. of peaks	Time since last flood
1	18/10/2005 02:00	19/10/2005 19:15	41h	50	1	1st flood
2	06/02/2006 19:15	07/02/2006 02:15	~7h	?	1?	3.5 months
3	21/05/2006 01:00	25/05/2006 21:00	116h	25	2	7 months
4	14/06/2006 17:30	19/06/2006 15:40	118h	35	1	21d
5	16/07/2006 08:40	11/09/2006 08:10	~2 months	20	4	1 month
6	08/06/2007 23:40	13/06/2007 10:00	108	32	1	10 months
7	27/06/2007 00:00	03/07/2007 08:00	176	24	1	6 weeks

Appendix 10: WFPV and percolation fluxes

Table 10.1 *WFPV and fluxes at boreholes 300 and 400 at the Gobabeb station*

	flood	θi	Δθ	WFPV (cm/h)	Flux (cm/h)			
					WFPR	WTRR		IGWS
						Ave.	Max.	
300	1	3.7	10.6	29.8	2.2	-	-	-
	2	10.8	4	35.8	1.4	0.35	0.38	0.81
	3	9.75	5.8	35.5	1.3	0.2	0.2	0.49
	4	12	2.5	10.3	0.2	0.12	0.12	-
	5	-	-	-	-	0.67	3.43	1.38
	Average	**-**	**-**	**27.83**	**1.28**	**0.34**	**1.03**	**0.90**
400	1	4.5	10.2	5.4	0.6	-	-	-
	2	11.5	6.2	19.9	0.7	0.65	0.7	1.03
	3	10.2	2.8	5.7	0.1	0.19	0.19	0.57
	4	-	-	-	-	0.11	0.11	-
	5	-	-	-	-	0.66	3.37	1.60
	Average	**-**	**-**	**10.3**	**0.47**	**0.40**	**1.09**	**1.07**

Table 10.2 *WFPV and fluxes at borehole 200 at the Buffelsrivier station*

flood	θi	Δθ	WFPV (cm/h)	Flux (cm/h)
			FTDR	WFPR
1	5.5	6	280.8	9.7
2	8.5	8	162.1	2.1
3	4	12	107.4	6.2
4	6.5	7	269.0	10.4
5	8	-	-	-
6	-	-	-	-
7	10	-	-	-
Average	**-**	**-**	**204.83**	**7.1**

Table 10.3 *WFPV and fluxes at borehole 400 at the Rooifontein station*

flood	θi	Δθ	WFPV (cm/h)		Flux (cm/h)	
			FTDR	FTDR-GW	WFPR	FTDR-GW
1	5	5	-	229.3	-	73.4
2	9	12	110.89	-	17.12	-
3	7	5	-	28.7	-	7.5
4	10	-	-	-	-	-
5	-	-	-	-	-	-
6	8.5	-	-	-	-	-
7	-	-	-	-	-	-
Average	**-**	**-**	**110.89**	**129.0**	**17.12**	**40.5**

תקציר

מי תהום באזורים מדבריים עשויים להימצא באקוויפרים מסוגים שונים, בטווח רחב של עומקים ובאיכויות מים משתנות. לרב, המים הנגישים ביותר ובעלי האיכות הטובה ביותר מצויים באקוויפרים אלוביאלים רדודים לאורך ערוצי נחלים. המקור העיקרי להעשרה של מאגרים אלו באזורים מדבריים הינו חלחול מי שיטפונות דרך ערוצי הנחלים.

בעשורים האחרונים חלה עלייה ניכרת בצריכת המים באזורים מדבריים בשל גידול האוכלוסייה, פיתוח אינטנסיבי של תעשיות (בעיקר חקלאיות) ועלייה ברמת החיים. לאור זאת גדלה משמעותית צריכת מי התהום ובעקבותיה חלה ירידה ניכרת במפלסים ובאיכויות המים. ההבנה שכדי למנוע פגיעה במשאבי המים הטבעיים, קצבי השאיבה צריכים להיות מותאמים לקצבי המילוי החוזר הטבעי, הצביעה על צורך בלימוד מעמיק יותר של תהליכי העשרת מי תהום. בנוסף, הערכה של קצבי החלחול וההעשרה עשויים לסייע בהבנת תהליכי הסעה והתפשטות של מזהמים מפני הקרקע אל מי התהום. מידע על קצבים אלו הכרחי בטיפול ושיקום של אתרים מזוהמים ובאיתור ותכנון של אתרי הטמנת פסולת חדשים.

מחקר זה עוסק בחקר תהליכי חלחול מי שיטפונות בערוצי נחלים והעשרה של אקוויפרים אלוביאלים באזורים מדבריים. מטרת המחקר היתה ללמוד על מאפייני החלחול דרך התווך הלא רווי, למדוד את קצבי החידור ובאמצעותם להעריך את כמות המילוי החוזר. במסגרת המחקר הוקמו שלוש תחנות ניטור בשני ערוצי נחלים גדולים באזורים מדבריים בדרום מערב אפריקה: תחנת Gobabeb הוקמה באפיק נהר ה-Kuiseb בנמיביה ואילו על נהר ה-Buffels בדרום אפריקה, הוקמו שתי תחנות: Buffelsrivier ו-Rooifontein במורד הערוץ ובמעלהו, בהתאמה. אירועי השיטפונות והחלחול בכל אחד מהאתרים נמדדו ותועדו באמצעות התחנות במשך כשנתיים. דגש מיוחד ניתן ליחסי הגומלין שבין פני השטח, התווך הבלתי רווי ומי התהום והשפעת התנאים בכל אחד מהאזורים על תהליך החלחול וההעשרה.

בעבודה זו נעשה שימוש במערכת איסוף נתונים שתוכננה ונבנתה במיוחד לצרכי המחקר ובהתאם לתנאים המקומיים בכל אתר ואתר. בכל תחנה נאספו במקביל נתונים משלשת האזורים ההידרולוגיים המעורבים בתהליך ההעשרה: (1) מפלס ומליחות מי השיטפון בפני השטח (2) שינויי תכולת הרטיבות בזמן ובמרחב בתווך הלא רווי (3) מפלס ומליחות מי התהום. תכולת הרטיבות נמדדה במספר בעומקים שונים

מפני השטח ועד למי התהום באמצעות חיישני TDR גמישים (FTDR). טכניקה זו מאפשרת מדידה ישירה ורציפה של תנועת מים בתת הקרקע בזמן אמת וברזולוציה גבוהה.

בתקופת המחקר תועדו 5-7 אירועי שיטפונות בכל אתר. כל שיטפון יצר תהליך הרטבה של התווך הלא רווי ולווה לבסוף בעליה באוגר המים באקוויפר. בכל האתרים נמצא קשר ישיר בין אירועי שיטפון בפני השטח ואירועי העשרה של מי התהום. העשרה התרחשה רק בזמנים בהם התקיימה זרימה בערוץ. הנתונים שנאספו מאפשרים להתחקות בצורה כמעט מלאה אחר תהליכי החלחול והמילוי החוזר של מי התהום שלב אחר שלב: מרגע הגעת השיטפון בערוץ, דרך התקדמות חזית ההרטבה מפני השטח אל פני מי התהום ועד לשלב ההעשרה המאופיין בהיערמות מי התהום ולבסוף התייצבות של מפלס אחיד חדש לרוחב כל האקוויפר.

הנתונים מלמדים כי בכל אירועי החלחול התווך הלא רווי נשאר בלתי רווי על אף שהזרימה באפיק התרחשה במשך מספר ימים ועל פני כל רוחב הערוץ. הרוויה של תת הקרקע התרחשה מלמטה כלפי מעלה ונשלטה ע"י שינויים במפלס מי התהום. בתקופת המחקר, כל האתרים הועשרו בכמויות מים נכבדות עד למילוי מוחלט של כל פוטנציאל האוגר והגעה לקיבול מים מרבי של האקוויפר. עם הגעת מי התהום לפני השטח, פסקו תהליכי החלחול וההעשרה. כתוצאה מכך, נמשך השיטפון זמן רב יותר והתקדם רחוק יותר במורד הערוץ.

מהירויות התקדמות חזית ההרטבה חושבו עבור כל שיטפון בכל אתר. התוצאות מדגימות כי המהירות הממוצעת של התקדמות חזית ההרטבה תלויה ביחס ישר בתכולת הרטיבות ההתחלתית לאורך חתך הקרקע. שטפי החלחול ב-Gobabeb חושבו בשלוש שיטות שונות בלתי תלויות שנתנו כולן תוצאות דומות ביותר. באופן בלתי צפוי, על אף שהשיטפונות ב-Gobabeb נבדלו בגובהם ובמשך הזמן שלהם באופן משמעותי, שטפי החידור בתווך הלא רווי נמצאו דומים ביותר (~1 ס"מ/שעה). ייתכן ותופעה זו מייצגת מנגנון ויסות טבעי של החלחול הנובע מהאופי המשוכב של הסדימנטים האלוביאלים. מאפייני הסדימנטים בתווך הלא רווי (פיזור גודל גרגר, נקבוביות וכו') משפיעים בצורה משמעותית על קצבי החלחול. בנהר ה-Buffels יושמו שתיים מתוך שלוש שיטות החישוב והשטפים המדודים היו גדולים לפחות בסדר גודל אחד מאלו שנמדדו ב-Gobabeb (0.36 עד 52 ס"מ/שעה). הבדל זה נובע מהרכב הסדימנטים בחתך האלוביאלי. בנהר ה Buffels הסדימנטים הינם גסי גרגר ביחס למילוי הסדימנטרי בנהר ה-Kuiseb.

התוצאות מנהר ה Buffels מצביעות על קיומם של נתיבי זרימה מועדפים בתוך המילוי האלוביאלי הפעילים במקביל לתהליך החלחול הדיפוזיבי (matrix flow).

חישוב העשרה כוללת ב-Gobabeb בוצע גם הוא בשלוש שיטות חישוב שונות שתוצאותיהן הראו התאמה גבוהה. הערך הממוצע לתקופת המחקר היה כ- 210,000 מ"ק לקילומטר ערוץ. הערך המינימאלי שחושב ב- Buffelsrivier עמד על כ-200,000 מ"ק לקילומטר ערוץ ואילו ב-Rooifontein חושבה כמות של 41,000 – 81,000 מ"ק לקילומטר ערוץ. חשוב לציין שהערכות אלו מתאימות רק לאזורים בהם המאפיינים המורפולוגיים של הערוץ וממדי האקוויפר דומים לאלו המצויים בתחנות המדידה. בכל האתרים נרשמה ההשפעה החיובית של העשרה ע"י מי שיטפונות על איכות מי האקוויפר בהורדת מליחותו.